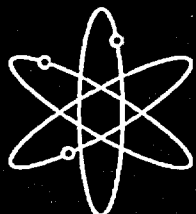
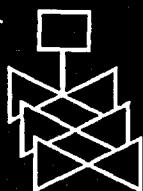




# Strategies for Application of Isotopic Uncertainties in Burnup Credit



**Oak Ridge National Laboratory**



**U.S. Nuclear Regulatory Commission  
Office of Nuclear Regulatory Research  
Washington, DC 20555-0001**



## AVAILABILITY OF REFERENCE MATERIALS IN NRC PUBLICATIONS

### NRC Reference Material

As of November 1999, you may electronically access NUREG-series publications and other NRC records at NRC's Public Electronic Reading Room at <http://www.nrc.gov/reading-rm.html>. Publicly released records include, to name a few, NUREG-series publications; *Federal Register* notices; applicant, licensee, and vendor documents and correspondence; NRC correspondence and internal memoranda; bulletins and information notices; inspection and investigative reports; licensee event reports; and Commission papers and their attachments.

NRC publications in the NUREG series, NRC regulations, and *Title 10, Energy*, in the Code of *Federal Regulations* may also be purchased from one of these two sources.

1. The Superintendent of Documents  
U.S. Government Printing Office  
Mail Stop SSOP  
Washington, DC 20402-0001  
Internet: [bookstore.gpo.gov](http://bookstore.gpo.gov)  
Telephone: 202-512-1800  
Fax: 202-512-2250
2. The National Technical Information Service  
Springfield, VA 22161-0002  
[www.ntis.gov](http://www.ntis.gov)  
1-800-553-6847 or, locally, 703-605-6000

A single copy of each NRC draft report for comment is available free, to the extent of supply, upon written request as follows:

Address: Office of the Chief Information Officer,  
Reproduction and Distribution  
Services Section  
U.S. Nuclear Regulatory Commission  
Washington, DC 20555-0001  
E-mail: [DISTRIBUTION@nrc.gov](mailto:DISTRIBUTION@nrc.gov)  
Facsimile: 301-415-2289

Some publications in the NUREG series that are posted at NRC's Web site address <http://www.nrc.gov/reading-rm/doc-collections/nuregs> are updated periodically and may differ from the last printed version. Although references to material found on a Web site bear the date the material was accessed, the material available on the date cited may subsequently be removed from the site.

### Non-NRC Reference Material

Documents available from public and special technical libraries include all open literature items, such as books, journal articles, and transactions, *Federal Register* notices, Federal and State legislation, and congressional reports. Such documents as theses, dissertations, foreign reports and translations, and non-NRC conference proceedings may be purchased from their sponsoring organization.

Copies of industry codes and standards used in a substantive manner in the NRC regulatory process are maintained at—

The NRC Technical Library  
Two White Flint North  
11545 Rockville Pike  
Rockville, MD 20852-2738

These standards are available in the library for reference use by the public. Codes and standards are usually copyrighted and may be purchased from the originating organization or, if they are American National Standards, from—

American National Standards Institute  
11 West 42<sup>nd</sup> Street  
New York, NY 10036-8002  
[www.ansi.org](http://www.ansi.org)  
212-642-4900

Legally binding regulatory requirements are stated only in laws; NRC regulations; licenses, including technical specifications; or orders, not in NUREG-series publications. The views expressed in contractor-prepared publications in this series are not necessarily those of the NRC.

The NUREG series comprises (1) technical and administrative reports and books prepared by the staff (NUREG-XXXX) or agency contractors (NUREG/CR-XXXX), (2) proceedings of conferences (NUREG/CP-XXXX), (3) reports resulting from international agreements (NUREG/IA-XXXX), (4) brochures (NUREG/BR-XXXX), and (5) compilations of legal decisions and orders of the Commission and Atomic and Safety Licensing Boards and of Directors' decisions under Section 2.206 of NRC's regulations (NUREG-0750).

**DISCLAIMER:** This report was prepared as an account of work sponsored by an agency of the U.S. Government. Neither the U.S. Government nor any agency thereof, nor any employee, makes any warranty, expressed or implied, or assumes any legal liability or responsibility for any third party's use, or the results of such use, of any information, apparatus, product, or process disclosed in this publication, or represents that its use by such third party would not infringe privately owned rights.

NUREG/CR-6811  
ORNL/TM-2001/257

---

---

# Strategies for Application of Isotopic Uncertainties in Burnup Credit

---

---

Manuscript Completed: December 2002  
Date Published: June 2003

Prepared by  
I. C. Gauld

Oak Ridge National Laboratory  
Managed by UT-Battelle, LLC  
Oak Ridge, TN 37831-6370

R. Y. Lee, NRC Project Manager

Prepared for  
Division of Systems Analysis and Regulatory Effectiveness  
Office of Nuclear Regulatory Research  
U.S. Nuclear Regulatory Commission  
Washington, DC 20555-0001  
NRC Job Code W6479



## ABSTRACT

Uncertainties in the predicted isotopic concentrations in spent nuclear fuel represent one of the largest sources of overall uncertainty in criticality calculations that use burnup credit. The methods used to propagate the uncertainties in the calculated nuclide concentrations to the uncertainty in the predicted neutron multiplication factor ( $k_{eff}$ ) of the system can have a significant effect on the uncertainty in the safety margin in criticality calculations and ultimately affect the potential capacity of spent fuel transport and storage casks employing burnup credit. Methods that can provide a more accurate and realistic estimate of the uncertainty may enable increased spent fuel cask capacity and fewer casks needing to be transported, thereby reducing regulatory burden on licensee while maintaining safety for transporting spent fuel. This report surveys several different best-estimate strategies for considering the effects of nuclide uncertainties in burnup-credit analyses. The potential benefits of these strategies are illustrated for a prototypical burnup-credit cask design. The subcritical margin estimated using best-estimate methods is discussed in comparison to the margin estimated using conventional bounding methods of uncertainty propagation. To quantify the comparison, each of the strategies for estimating uncertainty has been performed using a common database of spent fuel isotopic assay measurements for pressurized-light-water reactor fuels and predicted nuclide concentrations obtained using the current version of the SCALE code system. The experimental database applied in this study has been significantly expanded to include new high-enrichment and high-burnup spent fuel assay data recently published for a wide range of important burnup-credit actinides and fission products. Expanded rare earth fission-product measurements performed at the Khlopin Radium Institute in Russia that contain the only known publicly-available measurement for  $^{103}\text{Rh}$  have also been included.

# CONTENTS

	<u>Page</u>
ABSTRACT .....	iii
LIST OF FIGURES .....	vii
LIST OF TABLES .....	ix
FOREWORD .....	xi
ACKNOWLEDGMENTS .....	xiii
1 INTRODUCTION .....	1
2 BIAS AND UNCERTAINTY .....	3
3 METHODS OF UNCERTAINTY PROPAGATION .....	5
3.1 BOUNDING METHOD .....	5
3.2 BEST-ESTIMATE METHODS .....	6
3.2.1 Monte Carlo Uncertainty Sampling .....	6
3.2.2 Sensitivity/Uncertainty .....	7
3.2.3 Direct Difference Method .....	9
4 ANALYSIS OF RADIOCHEMICAL ASSAY DATA .....	11
4.1 REVIEW OF EXPERIMENTAL DATA .....	13
4.2 RADIOCHEMICAL ASSAY BENCHMARK RESULTS .....	19
4.3 APPLICABILITY OF THE EXPERIMENTAL DATABASE .....	22
5 UNCERTAINTY RESULTS .....	25
5.1 ACTINIDE-ONLY BURNUP CREDIT .....	26
5.1.1 Bounding Method .....	26
5.1.2 Monte Carlo Uncertainty Sampling .....	28
5.1.3 Direct Difference Method .....	32
5.1.4 Sensitivity/Uncertainty Method .....	46
5.1.5 Observations .....	47
5.2 ACTINIDE AND FISSION-PRODUCT CREDIT .....	50
6 BIAS RESULTS .....	57
6.1 ACTINIDE-ONLY BURNUP CREDIT .....	57
6.2 ACTINIDE AND FISSION-PRODUCT CREDIT .....	60
7 SUMMARY AND CONCLUSIONS .....	65
8 REFERENCES .....	67

# CONTENTS (continued)

	<u>Page</u>
APPENDIX A: SPENT FUEL ISOTOPIC ASSAY VALIDATION RESULTS .....	71
APPENDIX B: SENSITIVITY AND UNCERTAINTY CALCULATIONS.....	85

# LIST OF FIGURES

<u>Figure</u>	<u>Page</u>
1	Sensitivity coefficients (absolute values) for the major actinides and fission products in burnup-credit criticality calculations. The spent fuel compositions were calculated assuming 3.5 wt % enrichment and a burnup of 20 and 60 GWd/MTU, and a cooling time of 5 years. The nuclides are ranked in order of decreasing importance for the 20 GWd/MTU case. .... 12
2	Enrichment and burnup combinations of discharged spent fuel inventory from pressurized-water reactors in the U.S. prior to 1999. The number of discharged assemblies in each interval is given in the legend ..... 23
3	Relative margin associated with nuclide uncertainty estimated using the Monte Carlo sampling method for actinide-only burnup credit. The margin represents the $2\sigma$ uncertainty interval in the $k_{eff}$ distribution. The results are shown for both a uniform (flat) and an axially-varying (axial) burnup profile. These results have assumed a fixed initial fuel enrichment of 3.5 wt % $^{235}\text{U}$ ..... 31
4	Relative margin for nuclide uncertainties as a function of sample burnup for six major actinides, $^{235}\text{U}$ , $^{236}\text{U}$ , $^{238}\text{U}$ , $^{239}\text{Pu}$ , $^{240}\text{Pu}$ , and $^{241}\text{Pu}$ , for a generic 32-assembly burnup-credit cask. The linear regression fit and the $\pm 2\sigma$ uncertainty interval of the data are also shown. .... 36
5	Relative margin for nuclide uncertainties as a function of sample enrichment based for six major actinides, $^{235}\text{U}$ , $^{236}\text{U}$ , $^{238}\text{U}$ , $^{239}\text{Pu}$ , $^{240}\text{Pu}$ , and $^{241}\text{Pu}$ , for a generic 32-assembly burnup-credit cask. The linear regression fit and the $\pm 2\sigma$ uncertainty interval of the data are also shown. .... 37
6	Standard deviation of the $\Delta k_{eff}$ values from direct difference calculations for different burnup intervals for the actinides in Set 1 (major uranium and plutonium nuclides). The results are illustrated for all spent fuel samples included, and the case with the Yankee Rowe samples removed. .... 39
7	Relative margin for nuclide uncertainties as a function of sample burnup for actinides $^{235}\text{U}$ , $^{236}\text{U}$ , $^{238}\text{U}$ , $^{239}\text{Pu}$ , $^{240}\text{Pu}$ , $^{241}\text{Pu}$ , $^{242}\text{Pu}$ , and $^{241}\text{Am}$ in actinide Set 2, for a generic 32-assembly burnup-credit cask. The linear regression fit and the $\pm 2\sigma$ uncertainty interval of the data are also shown..... 43
8	Relative margin for nuclide uncertainties as a function of sample burnup for actinides $^{235}\text{U}$ , $^{236}\text{U}$ , $^{238}\text{U}$ , $^{239}\text{Pu}$ , $^{240}\text{Pu}$ , $^{241}\text{Pu}$ , $^{242}\text{Pu}$ , $^{241}\text{Am}$ , and $^{243}\text{Am}$ in actinide Set 3, for a generic 32-assembly burnup-credit cask. The linear regression fit and the $\pm 2\sigma$ uncertainty interval of the data are also shown..... 44
9	Relative margin for nuclide uncertainties as a function of sample burnup for all important burnup-credit actinides, except $^{243}\text{Am}$ , in actinide Set 4, for a generic 32-assembly burnup-credit cask. The linear regression fit and the $\pm 2\sigma$ uncertainty interval of the data are also shown. .... 45

## LIST OF FIGURES (continued)

<u>Figure</u>	<u>Page</u>
10	Relative margins for nuclide uncertainties estimated using sensitivity methods for actinide-only burnup credit. The margins represent the net effect of a $2\sigma$ variability in the computed nuclide concentrations. The results are shown for both a uniform (flat) and an axially-varying burnup profile, and a fixed initial fuel enrichment of 3.5 wt % $^{235}\text{U}$ .....48
11	Relative margins for nuclide variability estimated using the limiting bounding method, and best-estimate methods for actinide-only burnup credit and a uniform (flat) axial burnup. The bounding, Monte Carlo (MC) and sensitivity/uncertainty (S/U) margins were all generated assuming a fixed initial enrichment of 3.5 wt % $^{235}\text{U}$ .....49
12	Relative margins for nuclide variability estimated using the limiting bounding method, and best-estimate Monte Carlo (MC) sampling, and sensitivity/uncertainty (S/U) methods for actinide and fission-product burnup credit and a uniform (flat) axial burnup. The criticality calculations were performed using a generic burnup-credit cask and assumed a fixed initial enrichment of 3.5 wt % $^{235}\text{U}$ .....54
13	Relative margins for nuclide variability estimated using the limiting bounding method, and best-estimate Monte Carlo (MC) sampling, and sensitivity/uncertainty (S/U) methods for actinide and fission-product burnup credit and an axially-varying burnup profile. The criticality calculations were performed using a generic burnup-credit cask and assumed a fixed initial enrichment of 3.5 wt % $^{235}\text{U}$ . .....55
14	Relative margins for nuclide bias for actinide-only burnup credit. The results were based on bias-adjusted nuclide concentrations that conservatively did not credit positive bias. ....59
15	Relative margins for nuclide bias for actinide and fission-product burnup credit. The results were based on bias-adjusted nuclide concentrations that conservatively did not credit positive bias.....62

# LIST OF TABLES

<u>Table</u>	<u>Page</u>
1 Major isotopes in criticality calculations .....	11
2 Summary of selected PWR spent fuel radiochemical assay data .....	14
3 Summary of actinide measurements .....	15
4 Summary of available fission-product measurements .....	18
5 Nuclide validation results used in bias and uncertainty analyses .....	21
6 Results of actinide-only bounding criticality calculations .....	27
7 Results of Monte Carlo actinide-only $k_{eff}$ uncertainty calculations .....	30
8 Burnup-credit actinide sets .....	33
9 Summary of $k_{eff}$ calculations for actinide Set 1 .....	34
10 Summary of $k_{eff}$ calculations for actinide Set 2 .....	40
11 Summary of $k_{eff}$ calculations for actinide Set 3 .....	41
12 Summary of $k_{eff}$ calculations for actinide Set 4 .....	42
13 Results of actinide plus fission product bounding criticality calculations .....	52
14 Results of Monte Carlo actinide plus fission-product uncertainty calculations .....	53
15 Results of nuclide bias calculations for actinide-only burnup credit .....	58
16 Effect of nuclide bias for actinide and fission-product burnup credit .....	61
A.1 Experimental actinide assay results .....	73
A.2 Actinide validation results .....	77
A.3 Experimental fission-product assay results .....	81
A.4 Fission product validation results .....	82
B.1 Tabulated actinide-only sensitivity coefficients and estimated uncertainties (uniform axial burnup) .....	87

## LIST OF TABLES (continued)

<u>Table</u>	<u>Page</u>
B.2 Tabulated actinide-only sensitivity coefficients and estimated uncertainties (with axial-burnup profile) .....	88
B.3 Tabulated actinide plus fission product sensitivity coefficients and estimated uncertainties (uniform axial burnup) .....	89
B.4 Tabulated actinide plus fission product sensitivity coefficients and estimated uncertainties (with axial-burnup profile) .....	91

## FOREWORD

In 1999, the United States Nuclear Regulatory Commission (U.S. NRC) issued initial recommended guidance for using negative reactivity credit due to fuel irradiation (i.e., burnup credit) in the criticality safety analysis of spent pressurized-water-reactor (PWR) fuel in storage and transportation packages. This guidance was issued by the NRC Spent Fuel Project Office (SFPO) as Revision 1 to Interim Staff Guidance 8 (ISG-8 Rev. 1) and published in the *Standard Review Plan for Transportation Packages for Spent Nuclear Fuel*, NUREG-1617 (March 2000). With this initial guidance as a basis, the NRC Office of Nuclear Regulatory Research initiated a program to provide the SFPO with technical information that would:

- enable realistic estimates of the subcritical margin for systems with spent nuclear fuel (SNF) and an increased understanding of the phenomena and parameters that impact the margin, and
- support the development of technical bases and recommendations for effective implementation of burnup credit and provide realistic SNF acceptance criteria while maintaining an adequate margin of safety.

ISG-8 Rev. 1 recommends that the bias and uncertainty associated with predicting the actinide compositions should be determined from benchmarks of applicable fuel assay measurements. However, there currently is no guidance or consensus on how the nuclide bias and uncertainty should be propagated to the criticality calculation. The methods used to propagate the uncertainties can have a significant effect on the predicted subcritical margin. Conventional bounding approaches to treating nuclide uncertainty lead to considerable conservatism in the criticality calculation and underestimate the real subcritical margin for the system. This report examines several best-estimate strategies for propagating nuclide uncertainties to provide more realistic estimates of the uncertainty and the subcritical margin. The best-estimate methods are compared to conventional bounding methods to illustrate the potential benefits these strategies may provide in burnup-credit analyses. The uncertainty studies presented in this report were performed using a recently expanded radiochemical isotopic assay database that includes new measurements on spent fuel samples that achieved higher burnup and involved higher enrichments than were previously available. The nuclide benchmark results and related discussion provide an important technical basis for expanding the recommendations and guidance in ISG-8 Rev. 1 to enable increased utilization of burnup credit and for removal of the loading offset. The use of burnup-credit results in fewer casks needing to be transported, thereby reducing regulatory burden on licensees while maintaining safety for transporting SNF.



Farouk Eltawila, Director  
Division of Systems Analysis and Regulatory Effectiveness

## ACKNOWLEDGMENTS

This work was performed under contract with the Office of Nuclear Regulatory Research, U.S. Nuclear Regulatory Commission (NRC). The author acknowledges the review and helpful comments by C. V. Parks, M. D. DeHart, B. D. Murphy, and L. M. Petrie, of Oak Ridge National Laboratory (ORNL), and N. Gulliford of British Nuclear Fuels Limited (BNFL). The technical assistance of M. D. DeHart on the use of the KRONOS stochastic uncertainty analysis methods, and B. T. Rearden on the use of the SEN35 sensitivity sequence of SCALE is greatly appreciated. C. K. Bayne also provided a valuable review of the statistical concepts and terminology used in the report. Finally, the author is thankful to W. C. Carter for the careful attention to the formatting and preparation of the final report.

# 1 INTRODUCTION

Over the past decade, there has been a concerted effort in the United States and other countries to use more accurate and realistic estimates of the reactivity worth of spent fuel in licensing of spent fuel storage and transportation systems by applying burnup credit. Burnup credit is an approach that credits the reduction in reactivity in spent fuel due to irradiation. Criticality safety analyses have traditionally assumed that the fuel is unirradiated, which clearly leads to considerable safety margins. The reduction in reactivity that occurs with burnup is due to the change in concentration (net reduction) of fissile nuclides and the production of actinide and fission-product neutron absorbers. The U.S. Nuclear Regulatory Commission (NRC) issued Revision 1 of the Interim Staff Guidance 8 (ISG-8) in July 1999, to provide guidance on the application of limited burnup credit in criticality safety analyses for pressurized-water-reactor (PWR) spent fuel in transportation and storage casks.<sup>1</sup>

The process for performing criticality calculations in a burnup-credit model requires two distinct steps — the first to predict the spent fuel nuclide concentrations using burnup calculations; the second, to perform a criticality calculation using the nuclide concentrations estimated in the first step. Consideration of the burnup phenomena in the criticality assessment significantly increases the overall complexity of a criticality safety analysis, placing increased demands and reliance on the computational tools and methods, and necessitating consideration of many additional sources of uncertainty associated with fuel depletion that are not encountered in analyses that assume the fuel to be unirradiated. ISG-8 recommends that

“The applicant should ensure that the analysis methodologies used for predicting the actinide compositions and determining the neutron multiplication factor ( $k_{eff}$ ) are properly validated. Bias and uncertainties associated with predicting the actinide compositions should be determined from benchmarks of applicable fuel assay measurements.”

Uncertainties in the predicted nuclide concentrations in spent nuclear fuel (SNF) represent one of the largest potential sources of overall uncertainty in criticality calculations that use burnup credit. Radiochemical assay data provide a basis for determining bias and uncertainty in the predicted nuclide concentrations. However, the analyst is ultimately required to assess the impact of the nuclide bias and uncertainty on the predicted neutron multiplication factor ( $k_{eff}$ ) for the system. Unfortunately, there currently is no guidance or consensus on how the bias and uncertainties associated with the spent fuel concentrations should be propagated to the  $k_{eff}$  in a burnup-credit analysis. The different approaches to considering nuclide uncertainties can have a significant effect on the predicted margin of subcriticality and ultimately impact the number and types of spent fuel assemblies that may be acceptable for loading in casks or storage systems that use burnup credit.

This report reviews and illustrates several different strategies for considering the effects of nuclide uncertainties in burnup credit. These strategies include a conventional bounding approach whereby the concentration of each nuclide used in the criticality calculation is conservatively adjusted to account for bias and uncertainty. Several alternative best-estimate strategies are also evaluated. Best-estimate strategies attempt to provide a more accurate estimate of the effect of nuclide uncertainty on the  $k_{eff}$  (subcritical margin for uncertainty) by combining the effects of individual nuclide uncertainties in a more realistic manner. The margin resulting from nuclide uncertainties, as estimated using each strategy, is illustrated for PWR spent fuel stored in a prototype burnup-credit cask. The nuclide uncertainties used in these illustrative studies are derived from a recently revised and expanded set of common radiochemical assay benchmarks. Recent publication of assay measurements for Japanese Takahama-3 reactor spent

fuel has significantly expanded the database that is publicly available in the United States, in terms of both the number of measurements and the enrichment and burnup range covered by the database. These new measurements include data for high-enrichment and high-burnup samples and include extensive actinide and fission-product measurements. Recently-published fission-product measurements performed at the V. G. Khlopin Radium Institute (KRI) in Russia for rare earth fission products are also included. The KRI measurements include the only known publicly-available measurement for the major fission-product absorber  $^{103}\text{Rh}$ .

Although the effect of nuclide uncertainties is illustrated for PWR fuel, the methodologies described in this report are equally applicable to the analysis of boiling-water-reactor (BWR) spent fuel.

## 2 BIAS AND UNCERTAINTY

Implementation of burnup credit requires the computational prediction of the nuclide inventories (compositions) for the dominant fissile and absorbing nuclide species in spent fuel. This task introduces sources of bias and uncertainty in the criticality calculation that are not present in analyses that assume the fuel to be unirradiated. This section defines the terms bias and uncertainty, and briefly discusses the potential sources of bias and uncertainty in burnup calculations used to predict nuclide compositions.

The American National Standard ANSI/ANS-8.1 for nuclear criticality safety in operations outside reactors<sup>2</sup> identifies the key requirements for the validation of computational methods used to determine the subcritical state of a system. The ANS Standard requires that the computer codes and methods used in a criticality evaluation are validated and the bias and uncertainty in these predictions are well characterized and quantified. The Standard defines the term "bias" as a measure of the systematic differences between calculational method results and experimental data. The term "uncertainty" is a measure of both the accuracy of the calculations and the uncertainty in the experimental data used in the validation process.

There are a variety of potential sources of bias and uncertainty that can influence the accuracy and precision of computer codes used to predict spent fuel compositions. These sources can be generally categorized as follows:

- **Computational methods.** The bias and uncertainty attributed to the computational algorithms, methods and numerical approximations.
- **Nuclear cross-section and decay data.** The bias and uncertainty in the nuclear data used in the burnup calculations. These may include errors in the evaluated neutron cross sections, fission-product yields, branching fractions, and decay constants, etc., that are used by the code in computing the spent fuel compositions.
- **Input parameters.** The uncertainty in the values of the input data used in the code predictions. Examples include the declared burnup of the spent fuel, and reactor-operating parameters (e.g., fission power, fuel temperatures, and moderator density).
- **Modeling.** The bias and uncertainty introduced by modeling approximations. For example, the time-dependent fission power may be well known, but may be approximated using a series of discrete steps that simulate the average power for each irradiation interval. Other sources of uncertainty may be introduced by approximations in modeling the fuel assembly geometry, control rod (CR) exposure, and other difficult-to-simulate phenomena (e.g., the effects from adjacent reactor fuel assemblies).
- **Experimental data.** The bias and uncertainty associated with the experimental data. This source of error can represent a potentially large source of the overall uncertainty in isotopic validation. Radiochemical analysis of spent fuel is complex and difficult, and the uncertainties associated with the nuclide measurements can be significant. When computer code predictions are benchmarked against experimental data, the differences between calculations and observation are often incorrectly attributed to the bias and uncertainty of the code, because it is usually not possible to differentiate between code errors and experimental errors.

All of the results presented in this report are based strictly on the analysis of nuclide bias and uncertainties as determined by comparison of calculated and measured nuclide concentrations for well-documented and

well-characterized spent fuel samples. That is, the calculated concentrations were obtained using as-published operating history data, reactor conditions, and detailed assembly design information. This report does not address the potential use of conservative input parameters and/or modeling assumptions to bound the uncertainties in these types of parameters. For example, conservative reactor operating conditions (e.g., fuel temperatures, moderator density, etc.) may be used to account for uncertainties in these input parameters when detailed information is not available. Similarly, a conservative assembly model may be used to bound the effects for assemblies that were potentially exposed to CRs or burnable poison rods (BPRs). These types of modeling assumptions may be used to provide additional conservative bias to the calculation, but are not addressed in this report.

## 3 METHODS OF UNCERTAINTY PROPAGATION

The different approaches used for treating uncertainties in complex calculational models are generally grouped as either “bounding” methods or “best-estimate” techniques. The former methods conservatively account for individual parameter uncertainty. The latter techniques use best-estimate parameter values in the analysis and then use Monte Carlo (probabilistic) methods or other techniques, such as sensitivity analysis, in an attempt to realistically quantify the uncertainty in the final results caused by parameter uncertainties.

This section describes several different methods of estimating the uncertainty in the subcritical margin in a burnup-credit analysis due to uncertainty in the predicted nuclide inventories used in the criticality calculation. Although this discussion covers a variety of different techniques that have either been used or proposed for use in burnup credit or other applications, the methods described do not represent all of the potential methods available to treat nuclide uncertainties in burnup credit.

The sources of bias and uncertainty discussed in this report are restricted to those associated with the nuclide concentrations only, and do not include sources associated with other aspects of the criticality calculation. Similarly, as discussed in the previous section, this report does not address the use of conservative input parameters or models to bound the effects of other uncertainties in the analysis. Such uncertainty contributions must be addressed, and may be included as separate biases that are based on bounding parameter values.

The term “margin” is used throughout this report to define the margin of subcriticality for safety to conservatively account for the effect of nuclide uncertainties on the calculated  $k_{eff}$  for the system.

### 3.1 BOUNDING METHOD

In a conventional bounding approach to treating uncertainty, the analysis assumptions and input parameters are simultaneously set to their limiting values (maximum or minimum) to produce the most conservative result. As applied to nuclide uncertainties in burnup credit, this approach uses conservatively-adjusted values for the predicted concentration of each nuclide used in the criticality calculation. This requires that the bias and uncertainty in the predicted concentration of all nuclides used in the analysis be established by comparisons of calculated and measured radiochemical assay data.

In the bounding approach, the calculated nuclide concentrations are adjusted in a way that always leads to a more reactive system. In other words, the concentration of fissile nuclides is always increased, while the concentration of absorbing nuclides is always decreased, in order to maximize the  $k_{eff}$  of the system. This approach ensures that the predicted margin of subcriticality due to the bias and uncertainties will be a limiting, or bounding value. The U.S. Department of Energy (DOE) proposed such an approach in support of transportation and storage burnup credit.<sup>3</sup>

The bounding approach, whereby individual nuclides are simultaneously adjusted to their limiting values, is conservative, but the predicted margin will be unrealistically large. The variability in the calculated nuclide concentrations will not always be in a direction that results in a more reactive system – the concentration of some nuclides will be underpredicted, while other nuclides will be overpredicted. However, such an approach is simple, easy to justify as conservative, and yields concentrations that, when used in a criticality calculation, will provide an upper-bounding estimate of the  $k_{eff}$  for the system.

The margin predicted using bounding methods is not a conventional uncertainty in the sense that it is a one-sided limiting margin that does not have an associated variance. The bounding margin represents the maximum contribution of nuclide variability to the subcritical margin. Because bounding methods lead to an unrealistically large estimate of the effects of nuclide variability, the  $k_{eff}$  tends to be overestimated, and as a result, the actual criticality safety margin is underestimated.

Several published benchmark studies have analyzed available experimental isotopic assay data using the depletion methods of the SCALE code system in order to determine average isotopic correction factors that are applied to the predicted nuclide concentration to account for nuclide bias and uncertainty. Such factors are appropriate for use in a bounding-type analysis approach. A description of the statistical concepts and methods in this approach is given in Refs. 4, 5, and 6.

## 3.2 BEST-ESTIMATE METHODS

Best-estimate methods are expected to provide a more realistic and accurate estimate of effects of nuclide uncertainty in a burnup-credit spent fuel system by combining the effects of nuclide uncertainty in a more realistic and rational manner. The best-estimate methods enable more accurate estimates by attempting to realistically simulate the random nature of uncertainty, and thus, the methods partially credit compensating random uncertainties in the calculated nuclide concentrations.

Current recommended practice in nuclear criticality safety does not credit positive bias. In this report uncertainty is addressed separately from the bias component, which is a non-random systematic error. This approach allows the practice of not crediting positive bias to be preserved in the best-estimate methods described.

Several best-estimate methods can be used to propagate individual nuclide uncertainties to a global estimate of the margin for uncertainty. Three best-estimate methods are explored in this report:

- Monte Carlo (MC) uncertainty sampling method,
- Sensitivity/uncertainty (S/U) method, and
- a “direct difference” method.

### 3.2.1 Monte Carlo Uncertainty Sampling

The total uncertainty in a computed quantity may be estimated using a technique that involves Monte Carlo (probabilistic) sampling of the uncertainty distributions for the different parameters used in a calculation. Unlike a bounding calculation that is performed using a single set of conservative parameter values and leads to a single bounding estimate of the margin, the Monte Carlo approach undertakes multiple calculations with changes to the input parameters that reflect the random uncertainty variation for each parameter. The multiple calculations yield a distribution of results from which the expected mean is obtained, and probability of exceeding a particular value, or threshold, can be determined. Any potential correlation between different parameters must be considered and accounted for in the sampling scheme.

For burnup-credit nuclide uncertainty calculations, the technique involves stochastically varying the nuclide concentrations according to the uncertainty in the predicted concentration of each burnup-credit

nuclide (e.g., a normal distribution defined by a mean and variance). The mean and variance for each burnup-credit nuclide are established from comparisons of measured and computed nuclide concentrations. By sampling the nuclide concentrations independently, this technique inherently assumes that the uncertainties in individual nuclide concentrations are independent. This assumption is investigated later in Section 5, by comparing the results obtained by Monte Carlo sampling with independent methods that do not presume independent uncertainties. Although the nuclides **uncertainties** are assumed to be independent in the Monte Carlo approach, the nuclide **biases** are known to be strongly correlated. The analysis of nuclide bias is discussed in Section 6.

The practical implementation of the Monte Carlo method requires automation of the statistical sampling to determine the nuclide concentrations that are applied in the criticality analysis model. To illustrate this approach, a Monte Carlo sampling method was implemented at Oak Ridge National Laboratory (ORNL) in a computer code called KRONOS,<sup>7</sup> designed to function within the SCALE code system. The KRONOS program provides a realistic estimate of the uncertainty in the neutron multiplication factor due to nuclide uncertainties by randomly sampling from the probability distributions for the individual nuclides as determined from nuclide benchmark studies. The mean and variance for each nuclide (used to define the sampling distribution) are input directly to the code. KRONOS will perform either a SCALE CSAS1X one-dimensional (1-D) XSDRNPM calculation or a CSAS25 three-dimensional (3-D) KENO V.a criticality calculation for the system. The calculations are repeated, automatically, until the mean  $k_{eff}$  and variance of  $k_{eff}$  are converged. Because of the large number of criticality calculations required by this method to provide statistically reliable results, the code was developed for parallel processing on a distributed network environment.

### 3.2.2 Sensitivity/Uncertainty

Sensitivity methods have been widely used as a means of quantifying the effect of input data and other data parameters on computer model predictions. These methods are generally used to develop sensitivity coefficients for a system. Sensitivity coefficients are defined physically such that they represent the change in a calculated response with respect to a change in the input or data parameter. A sensitivity coefficient of 1.0 means that a 1% change in the parameter will cause a 1% change in the result. The sensitivity coefficients provide a direct measure of parameter importance by quantifying the effect of changes in the system response due to variations in the parameter values. Combined with parameter uncertainty information, S/U techniques can provide a powerful tool to estimate the global system uncertainty caused by uncertainties in multiple parameters.

As applied to the analysis of nuclide uncertainty in burnup-credit calculations, sensitivity coefficients are proportional to the derivative of the neutron multiplication factor of the system,  $k_{eff}$ , with respect to the nuclide concentrations evaluated at some reference value. With this approach the relative change in  $k_{eff}$  due to a change in the concentration of nuclide  $N$  is expressed to first-order accuracy by the linear relationship

$$\frac{dk}{k} = S_N \frac{dN}{N},$$

where the proportionality constant  $S_N$  is the sensitivity coefficient of  $k$  to the nuclide concentration  $N$ . This technique provides a straightforward method of predicting the change in the  $k_{eff}$  given a variability in the nuclide concentration attributed to the nuclide uncertainty. The uncertainty, expressed as a relative change in the concentration,  $dN/N$ , may be obtained for the important burnup-credit nuclides by comparing predicted and measured nuclide concentrations in SNF. The uncertainty from multiple nuclides may be combined to provide a measure of total uncertainty. If the uncertainties for each nuclide

are assumed to be independent, the total uncertainty can be estimated as the root sum square of the individual nuclide effects, such that

$$\frac{dk}{k} = \sqrt{\sum_{i=1}^n \left( \frac{dN}{N} \{S_N\} \right)^2},$$

where the sum is performed over all  $n$  burnup-credit nuclides in the criticality analysis. If the uncertainties from each nuclide are combined additively (using the absolute values of the sensitivity coefficients  $S_N$ ), such that

$$\frac{dk}{k} = \sum_{i=1}^n \frac{dN}{N} \{S_N\},$$

then the uncertainty is equivalent to that predicted using the bounding approach discussed in Section 3.1.

Several methods are available to obtain sensitivity coefficients. Traditionally, many sensitivity analyses have relied on direct parameter perturbations (i.e., slightly altering the value of a parameter and recalculating the response). However, for large systems involving many different parameters, this approach is extremely inefficient. Another technique involves the use of automatic differentiation methods to provide partial derivatives (which are directly related to the sensitivity coefficients) of the response to any of the input parameters. Other techniques have applied the widely used perturbation theory approach. This technique involves solution of the forward and adjoint neutron fluxes to provide sensitivity coefficients for the system.

Sensitivity coefficients used in this report were generated for a generic burnup-credit cask using SEN35, a prototypic SCALE code sequence that implements sensitivity analysis techniques for 3-D Monte Carlo criticality calculations.<sup>8</sup> The methods used to generate the sensitivity information are based on the widely-used perturbation theory approach.<sup>9</sup> SEN35 calculates forward and adjoint neutron fluxes using an enhanced version of the KENO V.a Monte Carlo criticality code. Once the fluxes are obtained, the SAMS module (Sensitivity Analysis Module of SCALE) produces flux moments and calculates the sensitivity coefficients from these data and the cross-section data. The SAMS module also calculates the uncertainty in the sensitivity coefficients resulting from Monte Carlo uncertainties. The principal motivation behind the development of the SEN35 sequence has been the need for modern computational tools that can generate the sensitivity data necessary to gauge the applicability of validation experiments used for criticality studies.<sup>10</sup>

SEN35 generates sensitivity coefficients for the various partial and total macroscopic cross sections for each nuclide in the criticality calculation. Since the macroscopic cross section is the product of the atomic number density and the microscopic cross section, the sensitivity coefficient for the nuclide concentration is exactly equal to the sensitivity coefficient of the total (energy-integrated) nuclide cross section calculated by SEN35. To generate sensitivity coefficients representative of spent fuel compositions, multiple SEN35 calculations were undertaken at discrete burnup values, with each calculation using a different fuel composition representative of each burnup level. Sensitivity coefficients were generated for spent fuel assemblies with a uniform axial burnup and a varying axial-burnup profile.

### 3.2.3 Direct Difference Method

Another best-estimate technique, called the direct difference method in this report, has been explored at ORNL. Instead of evaluating the bias and uncertainty in the individual nuclides used in burnup-credit calculations, the measured nuclide concentrations from radiochemical assays are applied directly in a criticality calculation for a spent fuel configuration representative of the intended burnup-credit application. The  $k_{eff}$  calculated for the system is then compared to the value predicted using calculated nuclide concentrations for the same set of burnup-credit nuclides. The difference ( $\Delta k_{eff}$ ) is a direct measure of the net bias and uncertainty in the  $k_{eff}$  calculation due to the variability in the predicted nuclide concentrations.

Unlike the other methods described in this report, this approach evaluates the aggregate effect of the nuclide uncertainties on  $k_{eff}$  directly, and does not require a statistical analysis of bias and uncertainty for any individual nuclide. Rather, the net effect of bias and uncertainty from all nuclides is determined directly from analysis of the mean and variance of the distribution of  $\Delta k_{eff}$  values obtained using the predicted and measured nuclide concentrations from many experiments. Like the other best-estimate methods described, the direct difference method inherently credits compensating uncertainties in the nuclide concentrations. This method requires a comprehensive database of measured isotopic validation data for a common set of burnup-credit nuclides. That is, an experimental data set must contain measurements for all nuclides selected for the burnup-credit analysis in order to be used by this method. Consequently, as the number of nuclides used in a burnup-credit analysis increases, the number of experiments containing all of the required nuclides tends to decrease. A sufficient number of measurements is needed to allow statistically reliable observations to be made about the uncertainty and trends in the predicted  $k_{eff}$ . Another limitation of the method is that only spent fuel with a uniform axial burnup can be simulated since assay data are not available for all of the burnup values required to simulate an axial profile.

The Monte Carlo uncertainty sampling, S/U, and direct difference best-estimate approaches are expected to yield similar results since all methods have applied a common set of nuclide uncertainties. The direct difference method of using measured nuclide assay data directly in criticality calculations has the potential to require far less computational effort than either the Monte Carlo or S/U techniques. Moreover, the direct difference method does not assume that the nuclide uncertainties are independent, and makes no assumptions about nuclide uncertainty distribution (e.g., normal distribution, etc.); particularly for nuclides with too few measurements to obtain a reliable estimate of the distribution.

The effect of nuclide uncertainties on the subcritical margin predicted using the Monte Carlo, S/U, and direct difference approaches is demonstrated for a typical burnup-credit cask in Section 5. The experimental assay data currently available that were applied to the different methods are described in Section 4.

## 4 ANALYSIS OF RADIOCHEMICAL ASSAY DATA

The net effect of nuclide uncertainties on the predicted effective neutron multiplication factor,  $k_{eff}$ , was evaluated using best-estimate methods and compared to the results using a bounding approach. These methods are summarized in Section 3. To establish a common basis for the comparisons, values of the bias and uncertainty for each burnup-credit nuclide were required. The bias and uncertainties were estimated from radiochemical isotopic assay data and applied to each of the respective uncertainty analysis methodologies. This section reviews the nuclides that are important in burnup-credit calculations, describes the publicly-available radiochemical assay data selected and evaluated for this study, and summarizes the results of the benchmark studies to predict the isotopic compositions in spent fuel using the SCALE code system.

The actinides and fission products that are most neutronically important in burnup-credit criticality calculations are listed in Table 1. These nuclides are considered to be important to dry storage and transport cask criticality safety analyses.<sup>11</sup> The relative importance of these nuclides will vary to some degree, depending on the enrichment, burnup, cooling time, assembly design, and configuration, but the important nuclides remain largely the same. The sensitivity coefficients of the major burnup-credit nuclides are illustrated in Figure 1 for low- and high-burnup fuel, following a 5-year-cooling time. The sensitivity coefficients were calculated by the SEN35 sequence of SCALE assuming uniformly-distributed nuclide concentrations. The values of the coefficients are listed in Appendix B. The sensitivity coefficients (unitless) represent the change in the neutron multiplication factor with respect to a change in the concentration of each nuclide. The coefficients are therefore a direct measure of the relative importance of each nuclide to the predicted neutron multiplication factor.

Table 1 Major isotopes in criticality calculations (from Ref. 11)

Actinides					
<sup>234</sup> U	<sup>235</sup> U	<sup>236</sup> U	<sup>238</sup> U	<sup>238</sup> Pu	<sup>239</sup> Pu
<sup>240</sup> Pu	<sup>241</sup> Pu	<sup>242</sup> Pu	<sup>241</sup> Am	<sup>243</sup> Am	<sup>237</sup> Np
Fission products					
<sup>95</sup> Mo	<sup>99</sup> Tc	<sup>101</sup> Ru	<sup>103</sup> Rh	<sup>109</sup> Ag	<sup>133</sup> Cs
<sup>143</sup> Nd	<sup>145</sup> Nd	<sup>147</sup> Sm	<sup>149</sup> Sm	<sup>150</sup> Sm	<sup>151</sup> Sm
<sup>151</sup> Eu	<sup>152</sup> Sm	<sup>153</sup> Eu	<sup>155</sup> Gd		

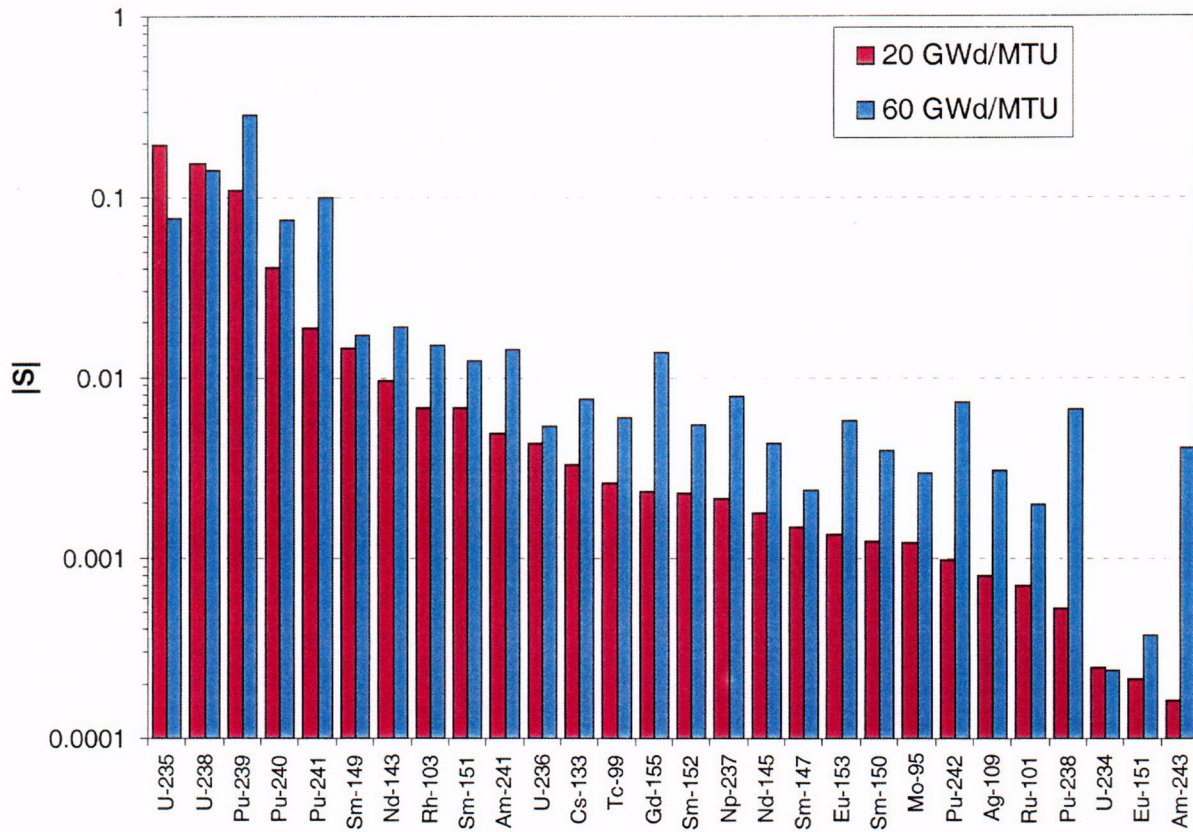


Figure 1 Sensitivity coefficients (absolute values) for the major actinides and fission products in burnup-credit criticality calculations. The spent fuel compositions were calculated assuming 3.5 wt % enrichment and a burnup of 20 and 60 GWd/MTU, and a cooling time of 5 years. The nuclides are ranked in order of decreasing importance for the 20 GWd/MTU case.

## 4.1 REVIEW OF EXPERIMENTAL DATA

A comprehensive review of available PWR radiochemical assay data was undertaken for this study. This included a review of previous validation studies performed at ORNL<sup>12,5</sup> and by the U.S. DOE Office of Civilian Radioactive Waste Management (OCRWM),<sup>6</sup> and new assay data published more recently. The data sets selected for this study include all PWR assays used previously in ORNL benchmark studies (Calvert Cliffs, H. B. Robinson, Obrigheim, Trino Vercellese, and Turkey Point reactor fuel) and the Yankee Rowe reactor assay data previously used only in the OCRWM studies. Details of the reactor descriptions, fuel descriptions, laboratories, and experimental methods can be found in the citations to the original works in Refs. 12, 5, and 6.

In addition to these previous studies, recently published assay data for spent fuel from the Japanese PWR Takahama-3 reactor,<sup>13</sup> which include samples with the highest enrichment and burnup publicly available, have also been evaluated at ORNL<sup>14</sup> and added to the database. The updated database includes a total of 56 individual spent fuel assay samples from seven different reactors. Table 2 summarizes the reactors, assembly designs, and fuel parameters. Table 3 lists the important burnup-credit actinides measured in each sample. Note that measurements are available for all of the major actinides listed in Table 1. There are additional spent fuel samples available from some of these programs that have not been analyzed in the previous studies. The assay samples were selected to provide a reasonable number of data comparisons for validation and provide a representative sample of the available data.

Spent fuel assay data for the Mihama reactor, used previously in the OCRWM study,<sup>6</sup> were not selected for the present study. A review of the Mihama data by ORNL<sup>15</sup> indicated there was a high variation in the measurements for fuel having similar burnups and fuel assembly locations. Erratic behavior was also observed for fuel samples taken from different axial positions of the same rod. Since the enrichment and burnup range of the Mihama measurements did not extend beyond the range provided by other data sets, these data were not added to the present study.

The availability of experimental fission-product data is currently very limited. A summary of the measured fission-product data used in this study is given in Table 4. Measurements for fission products important to burnup credit (see Table 1) are available in only a small subset of the fuel samples. The majority of fission-product data available previously for burnup-credit nuclides come from measurements of the Calvert Cliffs Approved Testing Material (ATM) samples performed at the Pacific Northwest Laboratory (PNL) Materials Characterization Center. The Calvert Cliffs measurements, designated ATM-103, ATM-104, and ATM-106, included nine samples with measurements for <sup>99</sup>Tc. However, only the three samples in the ATM-104 series included measurements for the burnup-credit fission-product nuclides <sup>133</sup>Cs, and the Nd, Sm, Eu, and Gd isotopes. A limitation of the ATM-104 fission-product measurements, described in Ref. 16, is that the mass spectrometry measurements for nuclides with mass numbers 147 (Pm, Sm), 150 (Nd, Sm), 151 (Sm, Eu), and 155 (Eu, Gd) included the parent and daughter nuclides of more than one element. In other words, the combined concentrations of the parent-daughter pairs in the mass chains (e.g., <sup>147</sup>Pm + <sup>147</sup>Sm) were measured, rather than the concentrations of the individual isotopes. The reported concentrations for the isotopes <sup>147</sup>Sm, <sup>150</sup>Sm, <sup>151</sup>Eu, <sup>151</sup>Eu, and <sup>155</sup>Gd were estimated from the measurements and fractional element distributions obtained from burnup calculations.

Table 2 Summary of selected PWR spent fuel radiochemical assay data

Reactor	Lattice type	Enrichment (wt %)	Burnup (GWd/t)	Absorbers	No. of samples
Trino Vercellese	WE 15 × 15	3.13	11.5 – 24.5	CR <sup>a</sup>	13
		3.897	12.0		1
Turkey Point	WE 15 × 15	2.556	30.5 – 31.5		5
Obrigheim	CE 14 × 14	3.13	25.9 – 29.5		6
H. B. Robinson-2	WE 15 × 15	2.561	16.0 – 31.7	BPR <sup>b</sup>	4
Yankee Rowe	WE 17 × 18	3.4	16.0 – 36.0	CR	8
Calvert Cliffs	CE 14 × 14	3.038	27.4 – 44.3		3
		2.72	18.7 – 33.2		3
		2.453	31.4 – 46.5	BPR	3
Takahama-3	WE 17 × 17	4.11	14.3 – 47.3	BPR	10
Range		2.56 – 4.11	11.5 – 47.3		Total 56

<sup>a</sup> CR = Assemblies exposed to control rods.

<sup>b</sup> BPR = Assemblies with burnable poison rods.

Table 3 Summary of actinide measurements

Set	Reactor	Assembly	Sample	Enrichment (wt %)	Burnup (GWd/MTU)	Available actinide measurements											
						<sup>234</sup> U	<sup>235</sup> U	<sup>236</sup> U	<sup>238</sup> U	<sup>237</sup> Np	<sup>238</sup> Pu	<sup>239</sup> Pu	<sup>240</sup> Pu	<sup>241</sup> Pu	<sup>242</sup> Pu	<sup>241</sup> Am	<sup>243</sup> Am
1	Trino Vercellese	509-104	M11-7	3.90	12.0		○	○	○			○	○	○	○		
2	Trino Vercellese	509-032	E11-4	3.13	15.4		○	○	○			○	○	○	○		
3	Trino Vercellese	509-032	E11-7	3.13	15.9		○	○	○			○	○	○	○		
4	Trino Vercellese	509-032	E11-9	3.13	11.5		○	○	○			○	○	○	○		
5	Trino Vercellese	509-069	E11-1	3.13	12.9		○	○	○		○	○	○	○	○	○	
6	Trino Vercellese	509-069	E11-2	3.13	20.6		○	○	○		○	○	○	○	○	○	○
7	Trino Vercellese	509-069	E11-4	3.13	23.7		○	○	○		○	○	○	○	○	○	○
8	Trino Vercellese	509-069	E11-7	3.13	24.3		○	○	○		○	○	○	○	○	○	○
9	Trino Vercellese	509-069	E5-4	3.13	23.9		○	○	○		○	○	○	○	○	○	○
10	Trino Vercellese	509-069	E5-7	3.13	24.5		○	○	○		○	○	○	○	○	○	○
11	Trino Vercellese	509-069	L11-4	3.13	23.9		○	○	○		○	○	○	○	○	○	○
12	Trino Vercellese	509-069	L11-7	3.13	24.4		○	○	○		○	○	○	○	○	○	○
13	Trino Vercellese	509-069	L5-4	3.13	24.3		○	○	○		○	○	○	○	○	○	○
14	Trino Vercellese	509-069	L5-7	3.13	24.3		○	○	○		○	○	○	○	○	○	○
15	Turkey Point	D01	G9	2.56	30.7	○	○	○	○		○	○	○	○	○	○	○
16	Turkey Point	D01	G10	2.56	30.5	○	○	○	○		○	○	○	○	○	○	○
17	Turkey Point	D01	H9	2.56	31.6	○	○	○	○		○	○	○	○	○	○	○
18	Turkey Point	D04	G9	2.56	31.3	○	○	○	○		○	○	○	○	○	○	○
19	Turkey Point	D04	G10	2.56	31.3	○	○	○	○		○	○	○	○	○	○	○

Table 3 (continued)

Set	Reactor	Assembly	Sample	Enrichment (wt %)	Burnup (GWd/MTU)	Available actinide measurements											
						<sup>234</sup> U	<sup>235</sup> U	<sup>236</sup> U	<sup>238</sup> U	<sup>237</sup> Np	<sup>238</sup> Pu	<sup>239</sup> Pu	<sup>240</sup> Pu	<sup>241</sup> Pu	<sup>242</sup> Pu	<sup>241</sup> Am	<sup>243</sup> Am
20	Calvert Cliffs ATM-104	D047	MKP109-P	3.04	44.3	○	○	○	○	○	○	○	○	○	○	○	○
21	Calvert Cliffs ATM-104	D047	MKP109-LL	3.04	27.4	○	○	○	○	○	○	○	○	○	○	○	○
22	Calvert Cliffs ATM-104	D047	MKP109-CC	3.04	37.1	○	○	○	○	○	○	○	○	○	○	○	○
23	Calvert Cliffs ATM-103	D101	MLA098-P	2.72	33.2	○	○	○	○	○	○	○	○	○	○	○	○
24	Calvert Cliffs ATM-103	D101	MLA098-JJ	2.72	18.7	○	○	○	○	○	○	○	○	○	○	○	○
25	Calvert Cliffs ATM-103	D101	MLA098-BB	2.72	26.6	○	○	○	○	○	○	○	○	○	○	○	○
26	Calvert Cliffs ATM-106	BT03	NBD107-Q	2.45	46.5	○	○	○	○	○	○	○	○	○	○	○	○
27	Calvert Cliffs ATM-106	BT03	NBD107-MM	2.45	31.4	○	○	○	○	○	○	○	○	○	○	○	○
28	Calvert Cliffs ATM-106	BT03	NBD107-GG	2.45	37.3	○	○	○	○	○	○	○	○	○	○	○	○
29	H. B. Robinson	B05	N-9C-D	2.56	31.7		○	○	○	○	○	○	○	○			
30	H. B. Robinson	B05	N-9C-J	2.56	28.5		○	○	○	○	○	○	○	○			
31	H. B. Robinson	B05	N-9B-N	2.56	23.8		○	○	○	○	○	○	○	○			
32	H. B. Robinson	B05	N-9B-S	2.56	16.0		○	○	○	○	○	○	○	○			
33	Obrigheim	170	94	3.13	25.9		○	○	○	○	○	○	○	○	○		
34	Obrigheim	172	92	3.13	26.5		○	○	○	○	○	○	○	○	○		
35	Obrigheim	176	91	3.13	28.0		○	○	○	○	○	○	○	○	○		
36	Obrigheim	168	86	3.13	28.4		○	○	○	○	○	○	○	○	○		
37	Obrigheim	171	89	3.13	29.0		○	○	○	○	○	○	○	○	○		
38	Obrigheim	176	90	3.13	29.5		○	○	○	○	○	○	○	○	○		
39	Takahama-3	NT3G23	SF95-1	4.11	14.3	○	○	○	○	○	○	○	○	○	○	○	○

Table 3 (continued)

Set	Reactor	Assembly	Sample	Enrichment (wt %)	Burnup (GWd/MTU)	Available actinide measurements											
						<sup>234</sup> U	<sup>235</sup> U	<sup>236</sup> U	<sup>238</sup> U	<sup>237</sup> Np	<sup>238</sup> Pu	<sup>239</sup> Pu	<sup>240</sup> Pu	<sup>241</sup> Pu	<sup>242</sup> Pu	<sup>241</sup> Am	<sup>243</sup> Am
40	Takahama-3	NT3G23	SF95-2	4.11	24.4	○	○	○	○		○	○	○	○	○	○	○
41	Takahama-3	NT3G23	SF95-3	4.11	35.4	○	○	○	○		○	○	○	○	○	○	○
42	Takahama-3	NT3G23	SF95-4	4.11	36.7	○	○	○	○		○	○	○	○	○	○	○
43	Takahama-3	NT3G23	SF95-5	4.11	30.4	○	○	○	○		○	○	○	○	○	○	○
44	Takahama-3	NT3G24	SF97-2	4.11	30.7	○	○	○	○	○	○	○	○	○	○	○	○
45	Takahama-3	NT3G24	SF97-3	4.11	42.2	○	○	○	○	○	○	○	○	○	○	○	○
46	Takahama-3	NT3G24	SF97-4	4.11	47.0	○	○	○	○	○	○	○	○	○	○	○	○
47	Takahama-3	NT3G24	SF97-5	4.11	47.3	○	○	○	○	○	○	○	○	○	○	○	○
48	Takahama-3	NT3G24	SF97-6	4.11	40.8	○	○	○	○	○	○	○	○	○	○	○	○
49	Yankee Rowe	E6-C-F6	T-175	3.4	15.9	○	○	○	○		○	○	○	○	○	○	○
50	Yankee Rowe	E6-C-F6	T-177 <sup>a</sup>	3.4	30.4	○	○	○	○		○	○	○	○	○	○	○
51	Yankee Rowe	E6-C-F6	T-179 <sup>b</sup>	3.4	31.3	○	○	○	○		○	○	○	○	○	○	○
52	Yankee Rowe	E6-C-F6	T-180	3.4	20.2	○	○	○	○		○	○	○	○	○	○	○
53	Yankee Rowe	E6-SE-C2	T-187	3.4	32.0	○	○	○	○		○	○	○	○	○	○	○
54	Yankee Rowe	E6-SE-C2	T-188	3.4	31.4	○	○	○	○		○	○	○	○	○	○	○
55	Yankee Rowe	E6-SE-E4	T-185	3.4	36.0	○	○	○	○		○	○	○	○	○	○	○
56	Yankee Rowe	E6-SE-E4	T-186	3.4	35.3	○	○	○	○		○	○	○	○	○	○	○

<sup>a</sup> Measured isotopes based on the average of samples T-177, N-26, and G-126.

<sup>b</sup> Measured isotopic results based on the average of samples T-179 and N-27.

Table 4 Summary of available fission-product measurements

Set	Reactor	Assembly	Sample	Enrichment (wt %)	Burnup (GWd/MTU)	Available fission-product measurements														
						<sup>95</sup> Mo	<sup>99</sup> Tc	<sup>101</sup> Ru	<sup>103</sup> Rh	<sup>109</sup> Ag	<sup>133</sup> Cs	<sup>143</sup> Nd	<sup>145</sup> Nd	<sup>147</sup> Sm	<sup>150</sup> Sm	<sup>151</sup> Sm	<sup>152</sup> Sm	<sup>151</sup> Eu	<sup>153</sup> Eu	<sup>155</sup> Gd
20	Calvert Cliffs	D047	MKP109-P	3.04	44.3		○				○	●	○	●	●	●	●	●	●	●
21	Calvert Cliffs	D047	MKP109-LL	3.04	27.3		○				○	●	○	●	●	●	●	●	●	●
22	Calvert Cliffs	D047	MKP109-CC	3.04	37.1		○				○	●	○	●	●	●	●	●	●	●
23	Calvert Cliffs	D101	MLA098-P	2.72	33.2		○													
24	Calvert Cliffs	D101	MLA098-JJ	2.72	18.7		○													
25	Calvert Cliffs	D101	MLA098-BB	2.72	26.6		○													
26	Calvert Cliffs	BT03	NBD107-Q	2.45	46.5		○													
27	Calvert Cliffs	BT03	NBD107-MM	2.45	31.4		○													
28	Calvert Cliffs	BT03	NBD107-GG	2.45	37.3		○		○			○	○	○	○	○	○	○	○	○
39	Takahama-3	NT3G23	SF95-1	4.11	14.3							○	○							
40	Takahama-3	NT3G23	SF95-2	4.11	24.4							○	○							
41	Takahama-3	NT3G23	SF95-3	4.11	35.4							○	○							
42	Takahama-3	NT3G23	SF95-4	4.11	36.7							○	○							
43	Takahama-3	NT3G23	SF95-5	4.11	30.4							○	○							
44	Takahama-3	NT3G24	SF97-2	4.11	30.7							○	○	○	○	○	○	○	○	○
45	Takahama-3	NT3G24	SF97-3	4.11	42.2							○	○	○	○	○	○	○	○	○
46	Takahama-3	NT3G24	SF97-4	4.11	47.0							○	○	○	○	○	○	○	○	○
47	Takahama-3	NT3G24	SF97-5	4.11	47.3							○	○	○	○	○	○	○	○	○
48	Takahama-3	NT3G24	SF97-6	4.11	40.8							○	○	○	○	○	○	○	○	○

(○) Indicates nuclides and samples measured at a single laboratory.

(●) Indicates nuclides and samples with independent measurements from both the ATM Program and from KRI (Russia). In this study the KRI results were used preferentially. Note: Assembly D047 was analyzed as ATM-104, assembly D101 was analyzed as ATM-103, and assembly BT03 was analyzed as ATM-106.

Subsequent to the original ATM-series fission-product measurements made at PNL, an independent analysis of the three ATM-104 samples, and one sample from ATM-106, was performed at the V. G. Khlopin Radium Institute (KRI) in Russia using samples partitioned from the original archived samples. The isotopic measurements included Nd, Sm, Eu, and Gd for all samples. In addition, the  $^{103}\text{Rh}$  content of the ATM-106 sample was measured. This represents the only known publicly-available measurement of Rh in spent fuel. In addition, the KRI results also include measurements for several rare earth fission products not available previously for ATM-106 sample NBD107-GG. The KRI results were only recently published in Ref. 17, an effort supported by the NRC for burnup-credit validation studies. The results from the analysis by KRI were normalized to  $^{145}\text{Nd}$  concentration instead of the more usual basis of uranium mass or fuel mass. However, absolute  $^{145}\text{Nd}$  concentrations, normalized to the fuel mass, were measured as part of the ATM-series of experiments and are reported in Ref. 17. The PNL results for  $^{145}\text{Nd}$  were used in this study to renormalize the KRI results to an absolute basis of fuel mass for use in the isotopic benchmark calculations. For this study the KRI results for the Nd, Sm, Eu, and Gd isotopes were used (with the noted exception of  $^{145}\text{Nd}$ ). The calculated results for these nuclides were adjusted to the cooling time of the KRI measurements, performed about 8 years after the ATM-series measurements.

Results for the important burnup-credit isotopes of Nd and Sm were also available from the Takahama-3 samples, significantly augmenting the number of measurements for these isotopes. The relative importance of the fission-product nuclides in criticality calculations using burnup credit is illustrated in Figure 1. Note that  $^{103}\text{Rh}$ , one of the dominant fission products in high-burnup spent fuel, currently has only one measurement. To date, no published assay results have been identified for  $^{95}\text{Mo}$ ,  $^{101}\text{Ru}$ , and  $^{109}\text{Ag}$ .

## 4.2 RADIOCHEMICAL ASSAY BENCHMARK RESULTS

In order to evaluate the various methods for propagating nuclide uncertainties, comparisons of calculated and measured nuclide compositions are needed to estimate the code bias and uncertainty for each nuclide. For this study, the depletion analysis sequence SAS2H<sup>18</sup> of the SCALE code system was used to predict the nuclide compositions for each spent fuel sample. Cross sections for the ORIGEN-S depletion analysis<sup>19</sup> performed by SAS2H were obtained from the SCALE 44-group ENDF/B-V-based cross-section library.<sup>20</sup> The spent fuel nuclide compositions were recalculated for this work using the most recent version of SCALE 4.4a and cross-section data and improved models of the fuel assemblies.

Several improvements were made to the models used in early isotopic validation studies from Ref. 15. Most notably, the models for the three Calvert Cliffs assembly BT03 samples were revised to include 12 burnable-poison shim rods and four non-fuel steel rods present in the assembly. The presence of these non-fuel rods was not documented in the Approved Testing Material (ATM-106) report<sup>21</sup> for these samples (the assemblies are incorrectly described as standard Combustion Engineering (CE)  $14 \times 14$  assemblies containing 176 fuel rods) and thus they were not included in the original models. Information on the non-fuel rods and the updated assembly models was obtained from Ref. 6.

Measurements for  $^{241}\text{Am}$  and  $^{238}\text{Pu}$  were available for several Trino Vercellese samples from assembly 509-069 but were not included in previous benchmark studies. Results for these nuclides were included in the present study. The  $^{241}\text{Am}$  results were reported for a 4-year-cooling time.

The measured actinide concentrations for all spent fuel samples used in this study, converted to standardized units of mg/g U initial, are listed in Appendix Table A.1. The results of the actinide benchmark calculations obtained using SCALE are given in Table A.2 as the ratio of the calculated-to-experimental (C/E) nuclide compositions. Table A.2 also provides a statistical summary of the results

and lists the average C/E ratio and the relative standard deviation (percent of C/E) for each nuclide. The average experiment-to-measured ratio is also listed. Experimental results for the major burnup-credit fission products are listed in Table A.3, and the C/E ratios are given in Table A.4. The actinide results are observed to be generally consistent with previous studies,<sup>5</sup> although the uncertainty associated with several major uranium and plutonium isotopes is somewhat improved. This is due in part from the improved data and models used in the present calculations, and the addition of the Takahama-3 data that were generally found to be in very good agreement with the calculations. These improvements are negated to some extent by the addition of the Yankee Rowe data (not included in previous ORNL studies), which exhibited consistently large deviations with the calculations.

The fission-product database has been expanded with the addition of the Takahama-3 results. The use of the fission-product results from KRI also enhances the database by providing the first <sup>103</sup>Rh measurement, and direct measurements of the <sup>147</sup>Sm, <sup>151</sup>Sm, <sup>151</sup>Eu, and <sup>155</sup>Gd isotopes. In addition, the KRI results included measurements for rare earth fission products in Calvert Cliffs sample NBD107-GG that were not previously available. The C/E results for the fission products are again generally consistent with previous studies.<sup>5</sup> Overall, however, there is a paucity of fission-product data, with three nuclides having no measurements and one nuclide (<sup>103</sup>Rh) having only one measurement. The uncertainty for several fission products is also seen to be relatively large (e.g., <sup>149</sup>Sm, <sup>152</sup>Sm, <sup>151</sup>Eu, <sup>155</sup>Gd).

A summary of the nuclide validation results is given in Table 5. The table lists the number of measured samples analyzed for each nuclide ( $n$ ), the average experiment-to-measured ratio ( $\bar{X}$ ) and the relative standard deviation ( $s$ ) of  $\bar{X}$  for each burnup-credit nuclide,  $i$ . The value of  $\bar{X}_i$  is calculated as:

$$\bar{X}_i = \sum_{j=1}^n (M_{i,j} / C_{i,j}) / n ,$$

where  $M_i$  are the measured and  $C_i$  are the computed concentrations for nuclide  $i$ , and the summation is performed over all  $n$  samples. The standard deviation  $s_i$  associated with  $\bar{X}_i$ , is computed as:

$$s_i = \sqrt{\frac{1}{(n-1)} \sum_{j=1}^n (X_{i,j} - \bar{X}_i)^2} .$$

The value of  $\bar{X}_i$  represents the factor, that when multiplied by the predicted nuclide concentration, will correct for the average bias in the predicted concentration.

The current recommended practice in criticality safety evaluations involving transportation packages<sup>22</sup> does not credit biases that result in an overprediction in the neutron multiplication factor, i.e., positive biases. As applied to burnup credit, this practice would lead to modified values of  $\bar{X}$ , depending on whether the nuclide was a net neutron absorber or a fissile nuclide. In other words, no credit would be applied for the overprediction of fissile nuclides or the underprediction of absorbing nuclides. For fissile nuclides, the modified factor  $\bar{X}'$  can be expressed as

$$\bar{X}' = \begin{cases} \bar{X}, & \text{if } \bar{X} > 1 \\ 1, & \text{if } \bar{X} \leq 1 \end{cases} .$$

and for net neutron absorbing nuclides,

$$\bar{X}' = \begin{cases} \bar{X}, & \text{if } \bar{X} < 1 \\ 1, & \text{if } \bar{X} \geq 1. \end{cases}$$

The values of  $\bar{X}$  and  $\bar{X}'$  are given in Table 5. The effect of using either  $\bar{X}$  or  $\bar{X}'$  in a criticality calculation is evaluated in Section 6.

Table 5 Nuclide validation results used in bias and uncertainty analyses

Nuclide	n	$\bar{X}$	$\bar{X}'$	$s^a$	Nuclide	n	$\bar{X}$	$\bar{X}'$	s
U-234	32	0.962	0.962	0.113	Ru-101	0	N/A <sup>c</sup>	N/A	N/A
U-235 <sup>b</sup>	56	1.018	1.018	0.030	Rh-103	1	1.269	1.000	N/A
U-236	56	1.008	1.000	0.037	Ag-109	0	N/A	N/A	N/A
U-238	56	1.000	1.000	0.005	Cs-133	3	0.976	0.976	0.009
Np-237	18	0.952	0.952	0.086	Nd-143	14	1.012	1.000	0.013
Pu-238	52	1.068	1.000	0.100	Nd-145	14	0.996	0.996	0.009
Pu-239 <sup>b</sup>	56	1.008	1.008	0.042	Sm-147	9	1.001	1.000	0.039
Pu-240	56	1.008	1.000	0.028	Sm-149	9	1.002	1.000	0.221
Pu-241 <sup>b</sup>	56	1.045	1.045	0.048	Sm-150	9	0.934	0.934	0.018
Pu-242	52	0.987	0.987	0.051	Sm-151	9	0.777	0.777	0.059
Am-241	28	0.919	0.919	0.204	Sm-152	9	0.751	0.751	0.142
Am-243	16	0.934	0.934	0.105	Eu-151	4	0.926	0.926	0.532
Mo-95	0	N/A <sup>c</sup>	N/A	N/A	Eu-153	4	0.966	0.966	0.048
Tc-99	9	0.844	0.844	0.194	Gd-155	4	1.287	1.000	0.124

<sup>a</sup> Standard deviation of  $\bar{X}$ .

<sup>b</sup> Fissile nuclides.

<sup>c</sup> Insufficient experimental data available to determine mean or standard deviation.

### 4.3 APPLICABILITY OF THE EXPERIMENTAL DATABASE

A potential concern when applying measured isotopic assay data to evaluate nuclide uncertainties in computational predictions is whether the experimental database is representative of modern fuel characteristics. The issue of applicability is important since a large number of the currently-available measurements were obtained from fuel assemblies irradiated in the 1970s. There are currently no rigorous criteria against which the applicability of the isotopic database can be gauged, and engineering judgement is required. The database may be characterized in terms of the obvious enrichment and burnup range, fuel assembly design, and BPR exposure (integral and non-integral). Other more subtle factors (e.g., the effects of adjacent assemblies in complex core loading patterns and fuel management schemes) may be more difficult to evaluate.

The enrichment and burnup combinations of the 56 PWR spent fuel samples used in this study were summarized in Table 2. The enrichment and burnup combinations of the actual inventory of spent fuel assemblies discharged from PWRs in the U.S. through 1998, are illustrated in Figure 2. The radiochemical assay data appear, qualitatively, to provide reasonable coverage of the spent fuel inventory. The fuel assembly designs (Table 2) also represent a wide range of assembly classes. Assembly designs with large water holes (e.g., CE 14 × 14 design) are included. The experimental database also has a reasonable number of assemblies that incorporate guide tubes and assemblies operated with BPRs. The H. B. Robinson assembly included steel-borosilicate glass rods, and the Calvert Cliffs assembly BT03 operated with Al<sub>2</sub>O<sub>3</sub>-B<sub>4</sub>C rods. The Takahama-3 assemblies were the only assemblies incorporating gadolinia (Gd<sub>2</sub>O<sub>3</sub>) integral burnable poison rods, commonly used in many modern assembly designs.

Although assemblies with BPRs are represented in the database, the number of these samples compared to the total database is relatively low. Given that many of the assemblies now being discharged have been exposed to BPRs during their irradiation history, the database may be deemed marginal for these designs.

The Yankee Rowe Westinghouse (WE) 17 × 18 and Trino Vercellese 15 × 15 assembly designs are somewhat of an anomaly in the database, both in terms of the assembly design and reactor operation. These reactors operated with control rods (Ag-In-Gd and Ag-In-Cd), which is not typical of modern U.S. PWR nuclear plants. Detailed information on the use of the control rods (locations, percent insertion, etc.) were not available for the assemblies, which resulted in additional uncertainty in the depletion analysis models. The assembly models for the Trino Vercellese calculations used reactor-average control rod information. The models for the Yankee Rowe calculations excluded the control rods altogether since insufficient design and operating information was available.

The Yankee Rowe and Trino Vercellese samples were included in the database since they add to the diversity of the assembly database. Also, the Yankee Rowe samples represent some of the higher-enrichment samples in the database and span a relatively wide burnup range. However, the inclusion of the validation results for these assemblies means that additional uncertainty from the poorly-documented exposure to control rods implicitly contributes to the estimated nuclide uncertainties. This is particularly true for the Yankee Rowe results, since the effects of the control rods were entirely excluded in the calculations. Consequently, any analysis assumptions that may be employed to conservatively account for uncertainty due to control rod exposure may lead to double accounting of the control rod effects in a burnup-credit calculation. For this reason, it may be argued that inclusion of these data sets to evaluate nuclide uncertainties for the analysis of modern PWR fuels is not reasonable. The Yankee Rowe results exhibit the largest consistent deviations between calculations and measurements of all results in the database. The impact of excluding the Yankee Rowe fuel samples is evaluated in Section 5.

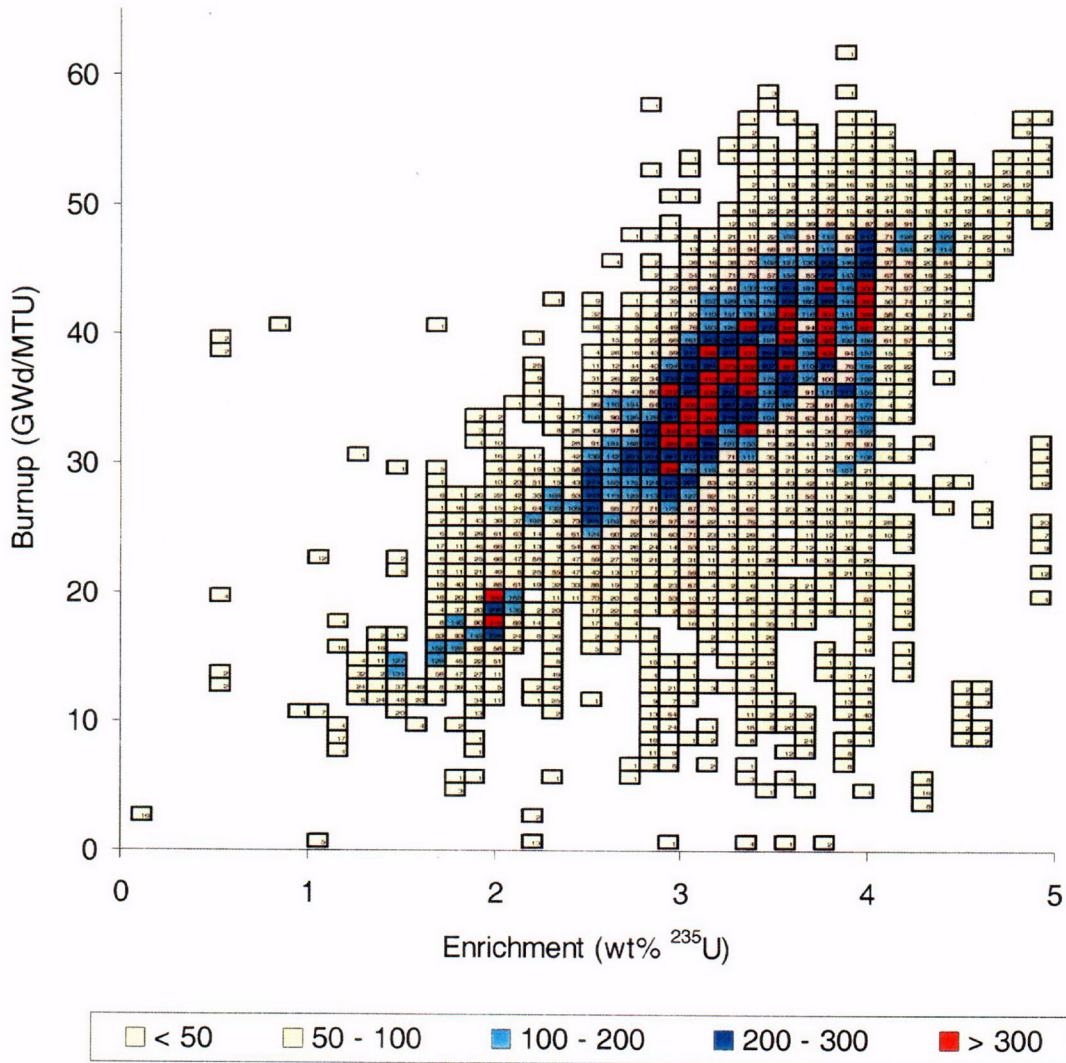


Figure 2 Enrichment and burnup combinations of discharged spent fuel inventory from pressurized-water reactors in the U.S. prior to 1999. The number of discharged assemblies in each interval is given in the legend (data obtained from Ref. 23).

Another potential consideration is the degree to which the experimental data represent fuel near the ends of the assembly. The end regions of the assembly become more important in burnup credit because of the lower burnup in these regions due to the axial-burnup profile. This phenomenon is discussed in more detail in Section 5.1. A number of the spent fuel samples in the database were obtained from axial locations very near the end of the assembly. For example, the Calvert Cliffs samples included six samples obtained from locations within 30 cm of the assembly end. The Takahama-3 samples also included several samples located near the end of the assembly. Notably, the Takahama-3 sample identified as SF97-1, was located approximately 4 mm from the end of the active fuel length. This sample was not evaluated in this study, but was evaluated previously in Ref. 14. The results indicate that the predicted actinide concentrations in SF97-1 exhibit larger deviations than other sample locations. The concentration of the fissile plutonium isotopes  $^{239}\text{Pu}$  and  $^{241}\text{Pu}$  are significantly overpredicted compared to measurement, suggesting that the reactivity associated with the samples located extremely close to the end of the fuel will also be overpredicted. Therefore, the calculated nuclide concentrations are expected to lead to slightly conservative reactivity effects for the region of the fuel at the very ends of the assembly.

With the notable exception of the Takahama-3 results, the publicly-available radiochemical assay data are obtained from relatively old experiments, and therefore involved older assembly designs. The present direction in the commercial nuclear power industry is towards the use of higher initial enrichments and burnups, more complex assembly designs, increased use of burnable poisons, and more complex fuel management schemes. Although the characteristics of the fuels in the database are deemed to be reasonably representative of modern fuel types, there is a continuing need to obtain additional assay data for modern fuel designs and modern reactor operations.

## 5 UNCERTAINTY RESULTS

The nuclide bias and uncertainty values calculated from the PWR isotopic validation results presented in Appendix A, and summarized in Table 5, were used as a common basis to estimate the overall effect of the nuclide uncertainties on the calculated  $k_{eff}$  for a spent fuel cask. A margin associated with the nuclide variability was predicted using the bounding methodology and compared to the margins obtained using the different best-estimate strategies of uncertainty propagation: (1) Monte Carlo uncertainty sampling, (2) direct difference, and (3) S/U methods. The margin associated with the nuclide uncertainties is one component that contributes to the overall margin of subcriticality.

This section evaluates the effects of nuclide uncertainty only. The effects associated with nuclide bias are addressed separately in Section 6.

Again, it is emphasized that the analyses presented in this report address only the variability associated with the predicted spent fuel nuclide compositions used in a burnup-credit criticality calculation. Additional uncertainties associated with the actual criticality calculation itself (e.g., cross-section uncertainties, etc.) are not considered. Also, the effects of conservative modeling assumptions or additional margins to bound other depletion uncertainties (e.g., fission power, irradiation history, soluble boron concentration, fuel temperatures, exposure to control rods, etc.) must be addressed separately.

All criticality calculations were performed using a common fuel and cask design. The spent fuel assembly was assumed to be a WE  $17 \times 17$  OFA design, and the cask design was based on a conceptual generic rail-type burnup-credit cask that would accommodate 32 fuel assemblies. The cask and fuel assembly descriptions and specifications are given in Ref. 24. Burnup-credit calculations were performed to address the effect of using both a flat (uniform) burnup distribution and a bounding axial-burnup profile. The calculations performed with an axial profile assumed a fixed profile for all burnups, based on an 18-axial-zone profile derived for assemblies with an average burnup greater than 30 GWd/MTU.<sup>3</sup>

The results presented in this section are intended to illustrate the typical margins predicted using different uncertainty propagation methods and a common set of nuclide validation results, so that informed judgements on the benefits of, and required effort for, the various approaches can be made. Section 5.1 presents results for actinide-only burnup credit, and Section 5.2 presents results for actinide plus fission-product credit. These results are based on a generic burnup-credit cask and the burnup and criticality calculations were performed using the SCALE code system. The results for specific fuel and cask-design configurations and other code systems must be assessed individually.

## 5.1 ACTINIDE-ONLY BURNUP CREDIT

The recommendations within the ISG-8 Rev. 1 guidance<sup>1</sup> limit the amount of burnup credit to that available in the actinides only (i.e., fission products are conservatively excluded). The burnup-credit calculations presented in this section were performed assuming actinide credit only. Therefore, the  $k_{eff}$  uncertainties predicted using the different methodologies reflect only the uncertainties in the predicted actinide concentrations.

### 5.1.1 Bounding Method

An upper limit on the effect of nuclide uncertainty in a criticality calculation was first estimated using a bounding approach, whereby the concentrations of the individual burnup-credit nuclides were conservatively adjusted to reflect the bias and uncertainty in the predicted concentration of each nuclide. The concentrations for all fissile isotopes were always increased, and all neutron-absorbing isotopes were simultaneously decreased. In this study, the calculated concentrations ( $C_i$ ) were conservatively adjusted such that the value applied in the criticality calculation ( $M_i$ ) was

$$M_i = C_i (\overline{X}_i \pm 2s_i)$$

where  $\overline{X}_i$  is the average experiment-to-measured ratio for nuclide  $i$ , and  $s_i$  is the standard deviation associated with  $\overline{X}_i$ . Adjusting the concentrations by two standard deviations ( $2s_i$ ) is sufficient to ensure an adjusted concentration will indeed be conservative with a probability that exceeds 0.97 (for a one-sided Gaussian distribution). The sign of the standard deviation term is determined such that the adjusted concentration will yield a more reactive system. This approach will lead to a highly conservative, bounding estimate of  $k_{eff}$  for the system. The results presented in this section applied values of  $\overline{X}_i$  from Table 5 instead of the  $\overline{X}_i'$  values that do not credit positive bias. The effect of bias is addressed separately in Section 6 using both the  $\overline{X}_i$  and the conservative  $\overline{X}_i'$  values.

All of the important burnup-credit actinides listed in Table 1 were applied in the criticality analysis. Additional tolerance factors that account for uncertainty due to the limited sample size may also be applied in such analyses. Tolerance factors were not applied in this study since the sample population for the important actinides was sufficiently large that this uncertainty contribution was considered small. A more detailed discussion of statistical methods and the use of tolerance factors is given in Ref. 4.

The bounding criticality calculations were performed using the STARBUCS<sup>25</sup> (Standardized Analysis of Reactivity Using Burnup Credit in SCALE) burnup-credit code sequence to be released with SCALE 5. STARBUCS couples the burnup and decay calculations and the criticality calculations within a single integrated sequence. The burnup calculations within STARBUCS are performed using the ARP and ORIGEN-S depletion modules of SCALE.<sup>26</sup> STARBUCS will perform the criticality calculation using either the KENO V.a or KENO-VI 3-D Monte Carlo criticality codes.<sup>27</sup> All criticality calculations in this study were performed using KENO V.a and the SCALE 44-group ENDF/B-V-based cross-section library.

The results of the bounding criticality calculations are listed in Table 6 for spent fuel with a fixed initial enrichment of 3.5 wt % and burnup values extending to 60 GWd/MTU. Criticality calculations using a uniform axial-burnup profile and a conservative axial-burnup profile are compared. The  $k_{eff}$  values calculated using the predicted nuclide concentrations, without any adjustment, are listed as nominal  $k_{eff}$

Table 6 Results of actinide-only bounding criticality calculations

Case	Burnup <sup>b</sup> (GWd/MTU)	Axial profile included	Neutron multiplication factor ( $k_{eff}$ ) <sup>a</sup>			Bounding margin	
			Nominal	Best- estimate	Bounding <sup>c</sup>	$\Delta k_{eff}$ <sup>d</sup>	$\Delta k_{eff}/k_{eff}$ <sup>e</sup>
1	10	No	1.0561	1.0609	1.0813	0.0204	1.92%
2	20	No	0.9956	0.9991	1.0239	0.0248	2.48%
3	30	No	0.9316	0.9384	0.9681	0.0297	3.16%
4	40	No	0.8774	0.8832	0.9157	0.0325	3.68%
5	50	No	0.8258	0.8340	0.8698	0.0358	4.29%
6	60	No	0.7970	0.8028	0.8410	0.0382	4.76%
7	10	Yes	1.0527	1.0573	1.0765	0.0192	1.82%
8	20	Yes	0.9924	0.9996	1.0213	0.0217	2.17%
9	30	Yes	0.9447	0.9489	0.9738	0.0249	2.62%
10	40	Yes	0.9013	0.9078	0.9352	0.0274	3.02%
11	50	Yes	0.8647	0.8706	0.9003	0.0297	3.41%
12	60	Yes	0.8383	0.8431	0.8753	0.0322	3.82%

<sup>a</sup> Standard deviation of all KENO V.a  $k_{eff}$  calculations  $< 10^{-3}$ .

<sup>b</sup> Initial enrichment of 3.5 wt % <sup>235</sup>U.

<sup>c</sup> Calculated using bias and uncertainty adjusted concentrations.

<sup>d</sup> Bounding – best-estimate  $k_{eff}$  values.

<sup>e</sup>  $\Delta k_{eff} / k_{eff} \times 100\%$ , where  $k_{eff}$  is the best-estimate  $k_{eff}$  value.

values in the table. The  $k_{eff}$  values obtained using the calculated nuclide concentrations, corrected only for the average bias (e.g.,  $C_i \bar{X}_i$ ) are listed in the table as the best-estimate values. The bounding  $k_{eff}$  values in Table 6 were calculated using the limiting values for the actinide concentrations. The bounding margins, calculated as the differences between the bounding and best-estimate  $k_{eff}$  values, are expressed as the  $\Delta k_{eff}$  and as the relative margin,  $\Delta k_{eff} / k_{eff}$ . These margins represent a limiting single-valued estimate of the maximum possible effect of the nuclide variability on the  $k_{eff}$  values. It is important to note that the bounding margins presented in Table 6 include only the effects of nuclide uncertainty, and not bias.

The results indicate that the margin associated with nuclide variability increases with burnup, assuming a fixed initial enrichment. This is attributed to larger nuclide uncertainties associated with some of the transuranic actinides (see  $s$  values in Table 5) that increase in concentration with burnup. For uniform axial burnup, the maximum relative margin is about 4.8% for an enrichment of 3.5 wt % and a burnup of 60 GWd/MTU. Note that this burnup is significantly greater than that experienced by typical discharged commercial fuel with an enrichment of 3.5 wt % (see Figure 2). The results in Table 6 indicate that the bounding relative margin associated with the actinide uncertainties for a burnup of 40 GWd/MTU, an average burnup for an initial enrichment of 3.5 wt %, is about 3.4%.

The effect of the nuclide uncertainties simulated with an axial-burnup profile is observed to be somewhat less than that for uniform axial burnup. The lower burnup near the ends of a fuel assembly, and the concomitant increase in the flux and fission density near the ends, leads to a strong sensitivity of the neutron multiplication factor to the compositions near the end of the fuel assembly. Since the effect of nuclide uncertainties on the neutron multiplication factor is observed to decrease as the burnup decreases, the effect is also expected to decrease when an axial-burnup profile is applied since the burnup near the neutronically-important fuel ends will decrease. Based on this observation, the axial profiles that are most reactive (i.e., those that have large burnup gradients near the ends) are also anticipated to exhibit a smaller bounding margin. Conversely, the margins derived assuming an assembly-averaged burnup (uniform distribution) are expected to bound those with a variable axial profile because the average assembly burnup is always greater than that near the ends of the assembly.

The importance of the actual axial-burnup profile used to calculate a bounding margin is expected to be small, since the differences observed between the calculations performed using a uniform assembly-average burnup and a conservative axial-burnup profile are seen to be relatively minor.

### 5.1.2 Monte Carlo Uncertainty Sampling

In the Monte Carlo method the nuclide concentrations are randomly varied according to their measured variance, as determined from the nuclide validation results, to simulate the random nature of uncertainty in the criticality calculation. In this procedure, nominal calculated nuclide concentrations and their estimated bias and uncertainty (obtained from Table 5) are required input. Nuclide concentrations are randomly sampled, according to the measured variance, about the best-estimate (bias-corrected) concentration for each nuclide and applied in a criticality calculation to determine the  $k_{eff}$ . The criticality calculations are repeated, randomly sampling new values for the nuclide concentrations used in each calculation, until a sufficient number of criticality calculations have been run to provide a reliable estimate of the mean and variance of the distribution of  $k_{eff}$  results.

The distribution of the expected concentration of given nuclide  $M_i$  can be estimated as follows:

$$M_i = C_i (\overline{X}_i + R_\sigma s_i)$$

where  $R_\sigma$  is a random number selected from a normal distribution, i.e., the distribution of  $R_\sigma$  is not uniform but has a mean of 0 and a standard distribution of 1. In other words, given adequate sampling, the mean value of  $M_i$  would converge toward the best-estimate value of  $C_i \overline{X}_i$ , and the distribution of  $M_i$  values would have a standard deviation of  $s_i$ .

The criticality calculations were performed using the KRONOS code.<sup>7</sup> Several important modifications to the code (as described in Ref. 7) were made for this study: (1) the bias and uncertainty values for the burnup-credit nuclides used in the KRONOS calculations were updated using the revised evaluations of 56 radiochemical assay experiments (Table 5), (2) tolerance factors to account for uncertainty due to the sample size were not implemented, (3) all isotopes were sampled assuming a normal probability distribution, and (4) the method of random sampling for problems involving multiple fissionable regions applied when simulating variable axial-burnup distributions was corrected. For calculations involving an axial-burnup profile modeled with many axial zones, the original KRONOS uncertainty sampling scheme underpredicted the  $k_{eff}$  uncertainty.

KRONOS calculations were performed using the generic burnup-credit cask model and all burnup-credit actinides from Table 1. The KENO V.a criticality code and the 44-group ENDF/B-V cross-section library of SCALE were used for the calculations. In this study, 100 separate criticality simulations were used to determine the uncertainty associated with a  $k_{eff}$  value. The nuclide bias and standard deviations input to KRONOS were the values listed in Table 5. These values are assumed to be independent of enrichment and burnup.

The KRONOS results are listed in Table 7. The table lists the nominal  $k_{eff}$  value calculated using unadjusted nuclide concentrations calculated using SCALE, the best-estimate results obtained using predicted nuclide concentrations corrected for bias only, and the mean  $k_{eff}$  value and its associated uncertainty as derived from the multiple KENO V.a criticality calculations run by KRONOS using the randomly-varied nuclide concentrations. The  $k_{eff}$  uncertainty is listed as the  $\pm 2\sigma$  uncertainty interval of the  $k_{eff}$  distribution. The relative uncertainty in the  $k_{eff}$  is also listed. Clearly, the mean of the  $k_{eff}$  distribution and the best-estimate results should yield the same  $k_{eff}$  value, and indeed the results are statistically the same. The  $2\sigma$  uncertainty margin in the  $k_{eff}$  values is plotted in Figure 3 for calculations performed with a uniform and a variable axial-burnup profile.

The nominal and best-estimate  $k_{eff}$  results are observed to be statistically the same as the values calculated using the bounding approach presented in Table 6. This result is expected since both methods are based on the same nuclide validation data. The results are not exactly equal because of different random number sequences used in the KENO V.a Monte Carlo calculations. The  $2\sigma$  uncertainty margin estimated using the Monte Carlo method is significantly smaller than the limiting margins predicted using the bounding method. The maximum uncertainty margin obtained using the best-estimate method for an enrichment of 3.5 wt % and burnup of 60 GWd/MTU and a uniform axial burnup is  $\pm 0.0188$ . Expressed in relative terms, the margin is  $\pm 2.3\%$ . This is compared to the relative margin estimated using the bounding method of  $\pm 4.8\%$  for the same enrichment and burnup. The additional margin imposed by the bounding method is a result of the highly conservative, but unrealistic method of combining the effects of individual nuclide variability using a limiting and worst-case approach.

Table 7 Results of Monte Carlo actinide-only  $k_{eff}$  uncertainty calculations

Case	Burnup <sup>a</sup> (GWd/MTU)	Axial profile included	Neutron multiplication factor ( $k_{eff}$ ) <sup>b</sup>		
			Nominal	Best-estimate	KRONOS <sup>c</sup> mean $k_{eff} \pm 2\sigma$ (%)
1	10	No	1.0572	1.0607	1.0608 $\pm$ 0.0136 (1.28%)
2	20	No	0.9960	0.9982	0.9987 $\pm$ 0.0130 (1.30%)
3	30	No	0.9334	0.9374	0.9381 $\pm$ 0.0136 (1.45%)
4	40	No	0.8763	0.8810	0.8818 $\pm$ 0.0146 (1.65%)
5	50	No	0.8283	0.8344	0.8332 $\pm$ 0.0158 (1.90%)
6	60	No	0.7965	0.8030	0.8023 $\pm$ 0.0188 (2.34%)
7	10	Yes	1.0537	1.0581	1.0573 $\pm$ 0.0134 (1.27%)
8	20	Yes	0.9935	0.9982	0.9978 $\pm$ 0.0130 (1.30%)
9	30	Yes	0.9448	0.9471	0.9491 $\pm$ 0.0126 (1.33%)
10	40	Yes	0.9021	0.9065	0.9066 $\pm$ 0.0130 (1.43%)
11	50	Yes	0.8644	0.8679	0.8692 $\pm$ 0.0134 (1.54%)
12	60	Yes	0.8400	0.8442	0.8451 $\pm$ 0.0138 (1.63%)

<sup>a</sup> Initial enrichment of 3.5 wt % <sup>235</sup>U.

<sup>b</sup> Standard deviation of all KENO V.a  $k_{eff}$  calculations  $< 10^{-3}$ .

<sup>c</sup> Uncertainty estimated from  $2\sigma$  in the distribution of  $k_{eff}$  values calculated using KRONOS.

An assumption inherent in random sampling is that the uncertainties for the different nuclides are independent. That is, the uncertainty for any particular nuclide is independent of the uncertainty in another nuclide. Although the biases are known to be highly dependent, the uncertainties are expected to be random and independent. The basis for this assumption is explored in more detail in the following section.

The relative margin (see Figure 3) calculated with an axial-burnup profile are observed to be less than for a uniform (flat) burnup distribution for burnups exceeding 30 GWd/MTU. Again, this reduction is attributed to the lower burnup at the end regions of the assembly, which become increasingly important as the assembly burnup increases. The results indicate that the effect of the nuclide uncertainties derived using a flat burnup distribution will bound those derived with a variable axial profile.

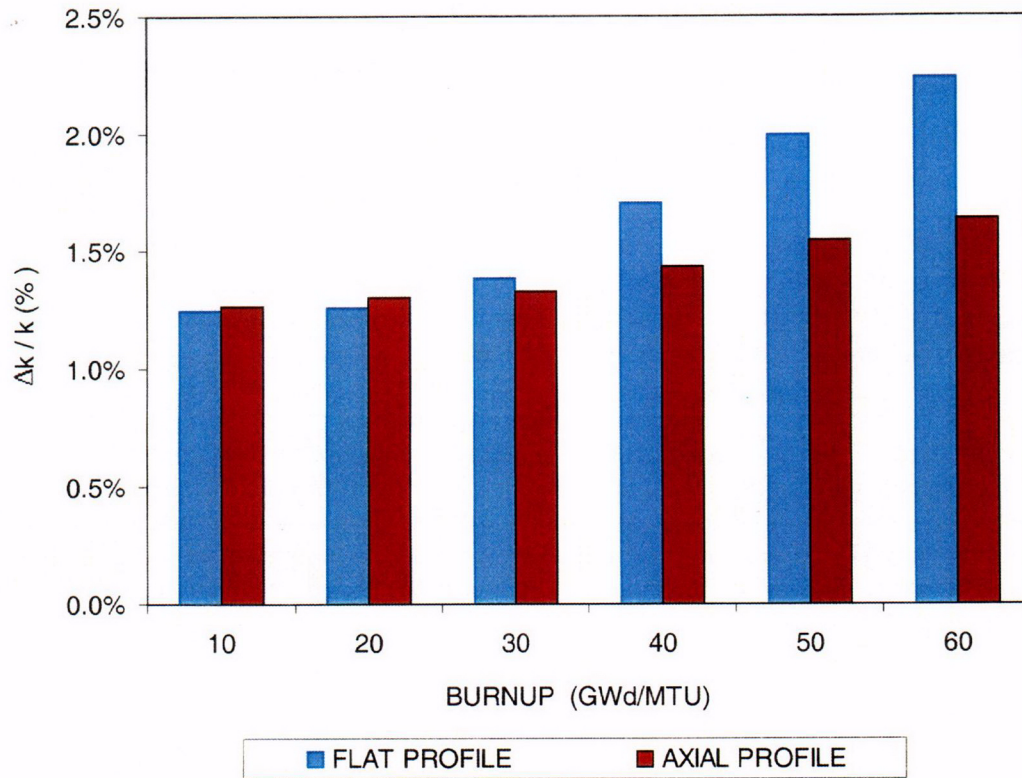


Figure 3 Relative margin associated with nuclide uncertainty estimated using the Monte Carlo sampling method for actinide-only burnup credit. The margin represents the  $2\sigma$  uncertainty interval in the  $k_{eff}$  distribution. The results are shown for both a uniform (flat) and an axially-varying (axial) burnup profile. These results have assumed a fixed initial fuel enrichment of 3.5 wt %  $^{235}\text{U}$ .

### 5.1.3 Direct Difference Method

The direct difference method applies measured spent fuel nuclide compositions directly in a criticality calculation and compares the  $k_{eff}$  results with those obtained using computed nuclide compositions. For each set of measured burnup-credit actinide compositions, two criticality calculations are performed; one using the measured concentrations, the other using predicted concentrations. The difference in the  $k_{eff}$  results ( $\Delta k_{eff}$ ) yields a direct measure of the aggregate effect of nuclide bias and uncertainty in the criticality calculation. The method requires an adequate number of diverse experiments with measurements for a common set of the major actinides. Provided a sufficient number of such comparisons can be made, the bias can be estimated from the mean of the  $\Delta k_{eff}$  distribution, and the variance can be derived from the distribution of the  $\Delta k_{eff}$  values about the mean.

The direct difference method does not require any evaluation of the bias or uncertainty in the predicted concentrations for individual burnup-credit nuclide. Therefore, the method makes no *a priori* assumptions about the potential trends in the nuclide bias and uncertainty with enrichment or burnup. Similarly, there are no required assumptions that the nuclide uncertainties are independent, or that the probability distributions of the uncertainties are normally distributed. This method allows the net trends in the  $k_{eff}$  bias and the uncertainty to be determined directly from the experimental data.

A practical limitation of this method is that few experiments contain measurements for all of the important burnup-credit nuclides. However, most sets contain measurements for the important uranium and plutonium isotopes in Table 1. In this study, several different actinide subsets were considered, each set consisting of a unique set of burnup-credit actinides. The different actinide sets evaluated in this report are listed in Table 8. The first subset (Set 1) included only the major uranium and plutonium isotopes  $^{235}\text{U}$ ,  $^{236}\text{U}$ ,  $^{238}\text{U}$ ,  $^{239}\text{Pu}$ ,  $^{240}\text{Pu}$ , and  $^{241}\text{Pu}$  for which measurements (see Table 3) were available for all 56 spent fuel samples. Combined, these nuclides represent > 90% of the reactivity worth from all actinides in spent fuel 5 years after discharge. Subsets with additional actinides (minor U and Pu, and Np and Am) were also evaluated. However, as the number of actinides increases, the number of available experiments that report measurements for all of the actinides decreases. A judicious selection of the burnup-credit actinides used in the criticality calculation is required to ensure an adequate number of comparisons are available to enable a statistically-reliable interpretation of the results. Note that some actinides considered here may not be recommended for use in burnup credit based on insufficient reactivity-worth (cross-section) validation. Therefore, availability of radiochemical assay data is not the only consideration in selecting the burnup-credit actinides used in the criticality calculation.

The measured data for the Obrigheim reactor spent fuel samples do not include  $^{238}\text{U}$ , effectively precluding use of the Obrigheim data by the direct difference method. However, the amount of  $^{238}\text{U}$  depletion in commercial LWR fuel is low (typically < 3%) and consequently the relative uncertainty in code predictions is small. Therefore, calculated  $^{238}\text{U}$  concentrations were used in place of measured concentrations for the Obrigheim data.

All criticality calculations were performed using the generic 32-assembly burnup-credit cask and fuel assembly configuration described previously. The measured and calculated nuclide concentrations were assumed to be uniformly distributed axially and radially in the fuel region (i.e., no axial-burnup profile was applied). Analyses using an axial-burnup profile are not possible using the direct difference method because measurements provide data for only a single burnup value. Thus, measurements are not available for the range of axial-burnup values necessary to simulate an axial profile. As described in Section 5.1.1, the assumption of a uniform (flat) burnup results in a larger uncertainty margin compared to an axially-varying burnup profile, and is therefore conservative.

Table 8 Burnup-credit actinide sets

Actinide Set	n <sup>a</sup>	Actinides included in the criticality calculations											
		<sup>234</sup> U	<sup>235</sup> U	<sup>236</sup> U	<sup>238</sup> U	<sup>238</sup> Pu	<sup>239</sup> Pu	<sup>240</sup> Pu	<sup>241</sup> Pu	<sup>242</sup> Pu	<sup>241</sup> Am	<sup>243</sup> Am	<sup>237</sup> Np
1	56		X <sup>b</sup>	X	X		X	X	X				
2	28		X	X	X	X	X	X	X	X	X		
3	16		X	X	X	X	X	X	X	X	X	X	
4	14	X	X	X	X	X	X	X	X	X	X		X

<sup>a</sup> Total number of samples available in each set.

<sup>b</sup> X indicates nuclide included in the set.

The  $k_{eff}$  results for the major burnup-credit actinides in Set 1 (<sup>235</sup>U, <sup>236</sup>U, <sup>238</sup>U, <sup>239</sup>Pu, <sup>240</sup>Pu, <sup>241</sup>Pu) are listed in Table 9. The table listed the  $k_{eff}$  values obtained using the measured concentrations for each sample, and the values obtained using the concentrations as obtained directly from the burnup calculations. The  $\Delta k_{eff}$  values are the difference between the  $k_{eff}$  values using computed and measured actinide concentrations. The relative difference is also listed for each sample. Negative  $\Delta k_{eff}$  values indicate that the  $k_{eff}$  value obtained using the computed actinide concentrations was underpredicted with respect to the value obtained using measured concentrations. The mean bias was determined from a linear regression fit of the data, and the  $\pm 2\sigma$  uncertainty interval derived from the distribution of  $\Delta k_{eff}$  values and  $\Delta k_{eff}/k_{eff}$  values about the linear regression fit are listed at the bottom of the table. The relative uncertainty margin is plotted as a function of sample burnup in Figure 4. The figure shows the linear regression fit and the  $\pm 2\sigma$  uncertainty interval of the data. The trends in the bias and the uncertainty level were found to be similar for the analysis of both the  $\Delta k_{eff}$  and  $\Delta k_{eff}/k_{eff}$  results.

The linear regression fit of the data shown in Figure 4 is constrained to intercept the origin since the measured and calculated nuclide concentrations approach the same values as the burnup approaches zero. However, performing the least-squares fit with no intercept constraint still yields an intercept of zero, within the fit uncertainty, indicating that the data are consistent with this assumption. The fit indicates an increasingly negative bias in the calculated  $k_{eff}$  (i.e., a trend to underpredict  $k_{eff}$ ) with burnup. The slope of the line is small but is statistically significant. The maximum negative bias ( $\Delta k_{eff}$ ) is  $< 0.01$  over the range of the data. The  $\pm 2\sigma$  relative uncertainty interval of the data is about  $\pm 1.8\%$ .

The same data, plotted as a function of initial sample enrichment instead of burnup, are shown in Figure 5. The results indicate a negative bias trend with increasing enrichment, similar to that seen with burnup. Note that the deviations for the high-burnup and high-enrichment fuel samples are observed to be similar to those for the other lower-enrichment samples.

A review of Figures 4 and 5 suggests that two data sets, namely Yankee Rowe and H. B. Robinson 2, yield erratic results that contribute a large part of the total uncertainty. A review of these experiments indicates that the H. B. Robinson data were obtained for a fuel rod that was adjacent to both a BPR and a water hole. Since the SCALE calculations are designed to predict the assembly-averaged neutronic environment and hence assembly-averaged nuclide compositions, it is perhaps not surprising that larger deviations are seen for these samples. The Yankee Rowe results exhibit some of the largest

Table 9 Summary of  $k_{eff}$  calculations for actinide Set 1

Reactor	Enrichment (wt %)	Burnup (GWd/MTU)	$k_{eff}^a$		$\Delta k_{eff}$	$\Delta k_{eff}/k_{eff}^b$
			Measured isotopics	Calculated isotopics		
Calvert Cliffs	3.04	44.3	0.7862	0.7850	-0.0012	-0.153%
Calvert Cliffs	3.04	27.4	0.8771	0.8688	-0.0083	-0.946%
Calvert Cliffs	3.04	37.1	0.8236	0.8108	-0.0128	-1.554%
Calvert Cliffs	2.72	33.1	0.8037	0.8061	0.0024	0.299%
Calvert Cliffs	2.72	18.7	0.8949	0.8922	-0.0027	-0.302%
Calvert Cliffs	2.72	26.6	0.8481	0.8390	-0.0091	-1.073%
Calvert Cliffs	2.45	46.5	0.6983	0.7017	0.0034	0.487%
Calvert Cliffs	2.45	31.4	0.7663	0.7616	-0.0047	-0.613%
Calvert Cliffs	2.45	37.3	0.7364	0.7327	-0.0037	-0.502%
H. B. Robinson	2.56	31.7	0.7975	0.8160	0.0185	2.320%
H. B. Robinson	2.56	28.5	0.8376	0.8272	-0.0104	-1.242%
H. B. Robinson	2.56	23.8	0.8378	0.8487	0.0109	1.301%
H. B. Robinson	2.56	16.0	0.8984	0.8998	0.0014	0.156%
Obrigheim	3.13	25.9	0.9016	0.8966	-0.0050	-0.555%
Obrigheim	3.13	26.5	0.8930	0.8941	0.0011	0.123%
Obrigheim	3.13	28.0	0.8919	0.8836	-0.0083	-0.931%
Obrigheim	3.13	28.4	0.8863	0.8819	-0.0044	-0.496%
Obrigheim	3.13	29.0	0.8874	0.8789	-0.0085	-0.958%
Obrigheim	3.13	29.5	0.8793	0.8755	-0.0038	-0.432%
Takahama-3	4.11	14.3	1.0515	1.0527	0.0012	0.114%
Takahama-3	4.11	24.4	1.0063	1.0072	0.0009	0.089%
Takahama-3	4.11	35.4	0.9667	0.9598	-0.0069	-0.714%
Takahama-3	4.11	36.7	0.9537	0.9437	-0.0100	-1.049%
Takahama-3	4.11	30.4	0.9742	0.9707	-0.0035	-0.359%
Takahama-3	4.11	30.7	0.9811	0.9783	-0.0028	-0.285%
Takahama-3	4.11	42.2	0.9365	0.9303	-0.0062	-0.662%
Takahama-3	4.11	47.0	0.9115	0.9027	-0.0088	-0.965%
Takahama-3	4.11	47.3	0.9066	0.8923	-0.0143	-1.577%
Takahama-3	4.11	40.8	0.9222	0.9193	-0.0029	-0.314%
Trino Vercellese	3.90	12.0	1.0519	1.0520	0.0001	0.010%

Table 9 (continued)

Reactor	Enrichment (wt %)	Burnup (GWd/MTU)	$k_{eff}^a$		$\Delta k_{eff}$	$\Delta k_{eff}/k_{eff}^b$
			Measured isotopics	Calculated isotopics		
Trino Vercellese	3.13	15.4	0.9851	0.9815	-0.0036	-0.365%
Trino Vercellese	3.13	15.9	0.9766	0.9801	0.0035	0.358%
Trino Vercellese	3.13	11.5	0.9989	0.9993	0.0004	0.040%
Trino Vercellese	3.13	12.9	0.9972	0.9926	-0.0046	-0.461%
Trino Vercellese	3.13	20.6	0.9623	0.9561	-0.0062	-0.644%
Trino Vercellese	3.13	23.7	0.9448	0.9428	-0.0020	-0.212%
Trino Vercellese	3.13	24.3	0.9451	0.9381	-0.0070	-0.741%
Trino Vercellese	3.13	23.9	0.9483	0.9429	-0.0054	-0.569%
Trino Vercellese	3.13	24.6	0.9431	0.9358	-0.0073	-0.774%
Trino Vercellese	3.13	23.9	0.9529	0.9414	-0.0115	-1.207%
Trino Vercellese	3.13	24.4	0.9423	0.9341	-0.0082	-0.870%
Trino Vercellese	3.13	24.3	0.9534	0.9405	-0.0129	-1.353%
Trino Vercellese	3.13	24.3	0.9464	0.9366	-0.0098	-1.036%
Turkey Point	2.56	30.7	0.8283	0.8289	0.0006	0.072%
Turkey Point	2.56	30.5	0.8232	0.8277	0.0045	0.547%
Turkey Point	2.56	31.6	0.8256	0.8255	-0.0001	-0.012%
Turkey Point	2.56	31.3	0.8257	0.8262	0.0005	0.061%
Turkey Point	2.56	31.3	0.8208	0.8237	0.0029	0.353%
Yankee Rowe	3.40	16.0	1.0236	1.0143	-0.0093	-0.909%
Yankee Rowe	3.40	30.4	0.9891	0.9633	-0.0258	-2.608%
Yankee Rowe	3.40	31.3	0.9827	0.9606	-0.0221	-2.249%
Yankee Rowe	3.40	20.2	1.0097	0.9966	-0.0131	-1.297%
Yankee Rowe	3.40	32.0	0.9798	0.9621	-0.0177	-1.806%
Yankee Rowe	3.40	31.4	0.9759	0.9598	-0.0161	-1.650%
Yankee Rowe	3.40	36.0	0.9421	0.9526	0.0105	1.115%
Yankee Rowe	3.40	35.3	0.9385	0.9514	0.0129	1.375%
2 Std deviations ( $\pm 2 \sigma$ )					$\pm 0.0161$	$\pm 1.76\%$

<sup>a</sup> Standard deviation of all KENO V.a  $k_{eff}$  calculations  $< 10^{-3}$ .

<sup>b</sup> Defined as  $(k_c - k_m)/k_m \times 100\%$ , where  $k_m$  and  $k_c$  are the  $k_{eff}$  values based on measured and calculated nuclide concentrations.

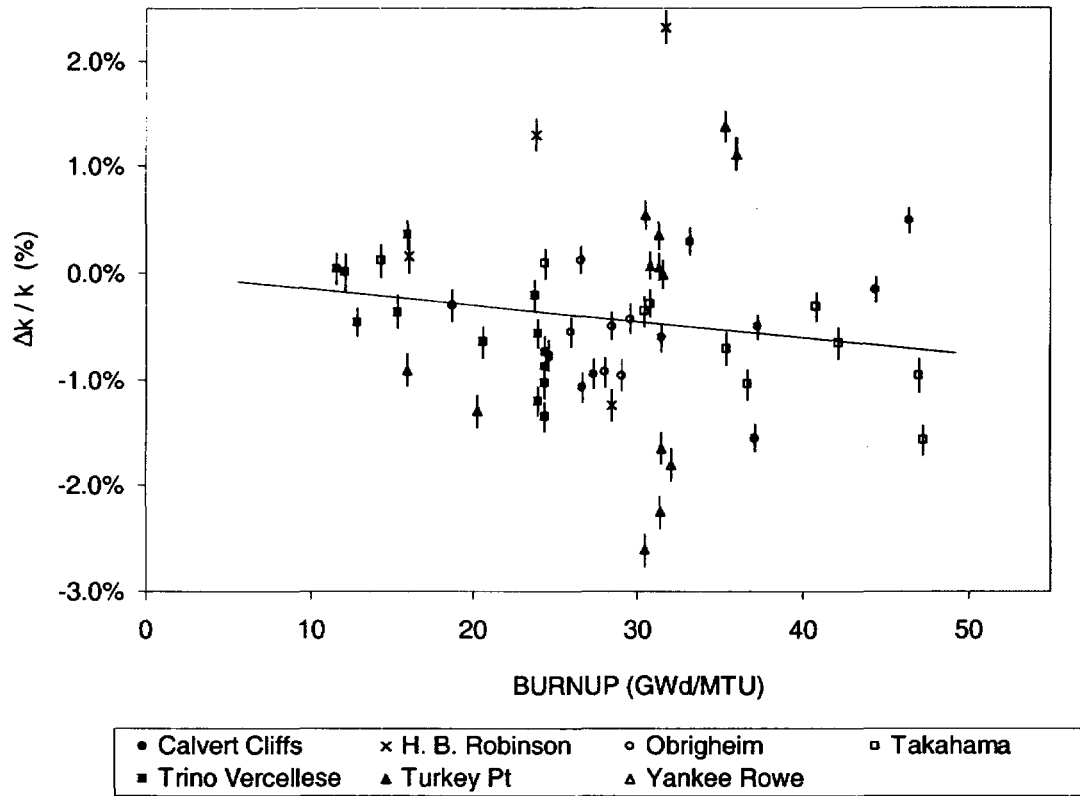


Figure 4 Relative margin for nuclide uncertainties as a function of sample burnup for six major actinides,  $^{235}\text{U}$ ,  $^{236}\text{U}$ ,  $^{238}\text{U}$ ,  $^{239}\text{Pu}$ ,  $^{240}\text{Pu}$ , and  $^{241}\text{Pu}$ , for a generic 32-assembly burnup-credit cask. The linear regression fit and the  $\pm 2\sigma$  uncertainty interval of the data are also shown.



deviations of any data set. The Yankee Rowe reactor used Ag-In-Gd cruciform-type control rods, which is not typical of modern U.S. PWR nuclear plant operation. Insufficient data were available in the specifications to accurately model the control rods and therefore they were excluded from the assembly models. Yankee Rowe assay rod E6-SE-E4 resided in close proximity to the control rods and was considered to be in a “highly perturbed” flux region. Similarly rod E6-SE-C2 also resided close to a control rod. However, other samples from assay rod E6-C-F6 residing near the center of the assembly exhibited equally poor agreement.

The  $\pm 2\sigma$  uncertainty interval of the data, illustrated in Figure 4, has assumed that the uncertainty is uniform over the range of the data. In other words, the uncertainty has been estimated based on the deviation of all data points from the mean, regardless of the burnup or enrichment of the spent fuel samples. Potential trends in the uncertainty were evaluated by plotting the deviation as a function of burnup. The data were binned into burnup intervals to obtain a sufficient number of data points in each group to calculate the standard deviation. The results are illustrated in Figure 6. The standard deviation in each interval is illustrated with all samples included and for a case with the Yankee Rowe samples excluded because of their large deviations. The standard deviation does not show a strong dependence on the burnup of the samples. Therefore, the assumption that the uncertainty is uniform over the range of the data was deemed to be appropriate.

Additional analyses were performed using the direct difference method for different subsets of the burnup-credit actinides. As the number of actinides included in the criticality analysis increases, the number of available experiments containing all the desired nuclides decreases. The  $k_{eff}$  results for actinide Sets 2, 3, and 4 (see Table 8) are listed in Tables 10–12 and are illustrated in Figures 7–9. These sets include all of the major uranium and plutonium isotopes from Set 1 plus combinations of other minor actinides. Only five samples from the Takahama-3 reactor included all of the burnup-credit actinides listed in Table 1.

The results illustrate that the different minor actinide sets do not significantly alter the bias in the predicted  $k_{eff}$  compared to the value obtained using only the major uranium and plutonium isotopes. As seen in Figure 1, the relative importance of the actinides not included in Set 1 is low, typically more than an order of magnitude smaller than the major uranium and plutonium isotopes. An exception is that for longer cooling times of up to about 100 years, the relative importance of  $^{241}\text{Am}$  (a neutron absorber) increases significantly.

Actinide sets that excluded the Yankee Rowe or H. B. Robinson results (due to missing actinide measurements in these sets) yielded smaller variances due to the large variability associated with these particular experiments. If the Yankee Rowe data are excluded from Set 1 (because of inadequate control rod information) the bias is unchanged but the relative uncertainty margin decreases from  $\pm 1.8\%$  to about  $\pm 1.3\%$ . If the H. B. Robinson results are also excluded (due to poor sample location) the margin is reduced further to  $\pm 1.0\%$ .

It is interesting to note that the negative trends in the bias and the uncertainties observed using the direct difference method are similar to those seen in the evaluation of calculational bias and uncertainty determined using critical state point data for 45 commercial reactor critical configurations (CRCs).<sup>28</sup> However, the analysis of the CRCs includes uncertainty components from both the nuclide concentrations and the criticality calculation, and the results are therefore not directly comparable to the results in this study. The CRC results exhibit smaller variability, possibly because the CRC measurements do not include the potentially large experimental uncertainties associated with the measurement of the nuclide concentrations.

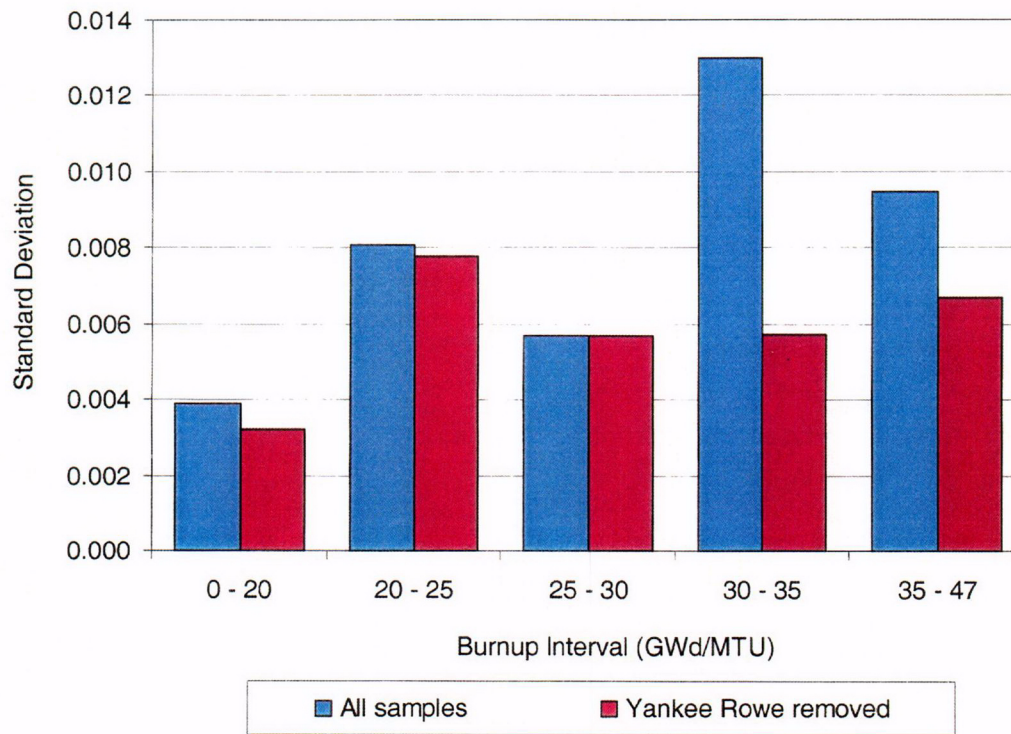


Figure 6 Standard deviation of the  $\Delta k_{eff}$  values from direct difference calculations for different burnup intervals for the actinides in Set 1 (major uranium and plutonium nuclides). The results are illustrated for all spent fuel samples included, and the case with the Yankee Rowe samples removed.

Table 10 Summary of  $k_{eff}$  calculations for actinide Set 2

Reactor	Enrichment (wt %)	Burnup (GWd/MTU)	$k_{eff}^a$		$\Delta k_{eff}$	$\Delta k_{eff}/k_{eff}^b$
			Measured isotopics	Calculated isotopics		
Calvert Cliffs	3.04	37.1	0.8007	0.7914	-0.0093	-1.161%
Calvert Cliffs	3.04	44.3	0.7665	0.7620	-0.0045	-0.587%
Calvert Cliffs	3.04	27.4	0.8647	0.8569	-0.0078	-0.902%
Calvert Cliffs	2.72	26.6	0.8318	0.8249	-0.0069	-0.830%
Calvert Cliffs	2.72	33.1	0.7843	0.7880	0.0037	0.472%
Calvert Cliffs	2.72	18.7	0.8876	0.8826	-0.0050	-0.563%
Calvert Cliffs	2.45	37.3	0.7131	0.7108	-0.0023	-0.323%
Calvert Cliffs	2.45	46.5	0.6660	0.6790	0.0130	1.952%
Calvert Cliffs	2.45	31.4	0.7458	0.7452	-0.0006	-0.080%
Takahama-3	4.11	14.3	1.0516	1.0514	-0.0002	-0.019%
Takahama-3	4.11	24.4	1.0043	1.0048	0.0005	0.050%
Takahama-3	4.11	35.4	0.9578	0.9517	-0.0061	-0.637%
Takahama-3	4.11	36.7	0.9460	0.9391	-0.0069	-0.729%
Takahama-3	4.11	30.4	0.9694	0.9619	-0.0075	-0.774%
Takahama-3	4.11	30.7	0.9788	0.9718	-0.0070	-0.715%
Takahama-3	4.11	42.2	0.9283	0.9209	-0.0074	-0.797%
Takahama-3	4.11	47.0	0.8987	0.8913	-0.0074	-0.823%
Takahama-3	4.11	47.2	0.8939	0.8809	-0.0130	-1.454%
Takahama-3	4.11	40.8	0.9151	0.9118	-0.0033	-0.361%
Trino Vercellese	3.13	12.9	0.9923	0.9895	-0.0028	-0.282%
Trino Vercellese	3.13	20.6	0.9550	0.9502	-0.0048	-0.503%
Trino Vercellese	3.13	23.7	0.9354	0.9387	0.0033	0.353%
Trino Vercellese	3.13	24.3	0.9318	0.9309	-0.0009	-0.097%
Trino Vercellese	3.13	23.9	0.9404	0.9355	-0.0049	-0.521%
Trino Vercellese	3.13	24.5	0.9325	0.9295	-0.0030	-0.322%
Trino Vercellese	3.13	24.4	0.9353	0.9334	-0.0019	-0.203%
Trino Vercellese	3.13	24.3	0.9424	0.9347	-0.0077	-0.817%
Trino Vercellese	3.13	24.3	0.9337	0.9307	-0.0030	-0.321%
2 Std deviations ( $\pm 2\sigma$ )					$\pm 0.0100$	$\pm 1.26\%$

<sup>a</sup> Standard deviation of all KENO V.a  $k_{eff}$  calculations  $< 10^{-3}$ .

<sup>b</sup> Defined as  $(k_c - k_m)/k_m \times 100\%$ , where  $k_m$  and  $k_c$  are the  $k_{eff}$  values based on measured and calculated nuclide concentrations.

Table 11 Summary of  $k_{eff}$  calculations for actinide Set 3

Reactor	Enrichment (wt %)	Burnup (GWd/MTU)	$k_{eff}^a$		$\Delta k_{eff}$	$\Delta k_{eff}/k_{eff}^b$
			Measured isotopics	Calculated isotopics		
Takahama-3	4.11	14.3	1.0512	1.0508	-0.0004	-0.04%
Takahama-3	4.11	24.4	1.0034	1.0020	-0.0014	-0.14%
Takahama-3	4.11	35.4	0.9572	0.9523	-0.0049	-0.51%
Takahama-3	4.11	36.7	0.9470	0.9374	-0.0096	-1.01%
Takahama-3	4.11	30.4	0.9681	0.9637	-0.0044	-0.45%
Takahama-3	4.11	30.7	0.9797	0.9710	-0.0087	-0.89%
Takahama-3	4.11	42.2	0.9281	0.9204	-0.0077	-0.83%
Takahama-3	4.11	47.0	0.8969	0.8895	-0.0074	-0.83%
Takahama-3	4.11	47.3	0.8952	0.8784	-0.0168	-1.88%
Takahama-3	4.11	40.8	0.9124	0.9069	-0.0055	-0.60%
Trino Vercellese	3.13	20.6	0.9541	0.9531	-0.0010	-0.10%
Trino Vercellese	3.13	23.7	0.9341	0.9365	0.0024	0.26%
Trino Vercellese	3.13	24.3	0.9340	0.9319	-0.0021	-0.22%
Trino Vercellese	3.13	23.9	0.9397	0.9374	-0.0023	-0.24%
Trino Vercellese	3.13	24.5	0.9296	0.9300	0.0004	0.04%
Trino Vercellese	3.13	24.4	0.9325	0.9301	-0.0024	-0.26%
2 Std deviations ( $\pm 2\sigma$ )					$\pm 0.0072$	$\pm 0.79\%$

<sup>a</sup> Standard deviation of all KENO V.a  $k_{eff}$  calculations  $< 10^{-3}$ .

<sup>b</sup> Defined as  $(k_c - k_m)/k_m \times 100\%$ , where  $k_m$  and  $k_c$  are the  $k_{eff}$  values based on measured and calculated nuclide concentrations.

Table 12 Summary of  $k_{eff}$  calculations for actinide Set 4

Reactor	Enrichment (wt %)	Burnup (GWd/MTU)	$k_{eff}^a$		$\Delta k_{eff}$	$\Delta k_{eff}/k_{eff}^b$
			Measured isotopics	Calculated isotopics		
Calvert Cliffs	3.04	44.3	0.7959	0.7865	-0.0094	-1.181%
Calvert Cliffs	3.04	27.4	0.7599	0.7548	-0.0051	-0.671%
Calvert Cliffs	3.04	37.1	0.8596	0.8498	-0.0098	-1.140%
Calvert Cliffs	2.72	33.2	0.8253	0.8191	-0.0062	-0.751%
Calvert Cliffs	2.72	18.7	0.7813	0.7847	0.0034	0.435%
Calvert Cliffs	2.72	26.6	0.8847	0.8818	-0.0029	-0.328%
Calvert Cliffs	2.45	46.5	0.7072	0.7051	-0.0021	-0.297%
Calvert Cliffs	2.45	31.4	0.6620	0.6734	0.0114	1.722%
Calvert Cliffs	2.45	37.3	0.7433	0.7427	-0.0006	-0.081%
Takahama-3	4.11	30.7	0.9729	0.9652	-0.0077	-0.791%
Takahama-3	4.11	42.2	0.9205	0.9145	-0.0060	-0.652%
Takahama-3	4.11	47.0	0.8888	0.8837	-0.0051	-0.574%
Takahama-3	4.11	47.3	0.8866	0.8736	-0.0130	-1.466%
Takahama-3	4.11	40.8	0.9064	0.9039	-0.0025	-0.276%
2 Std deviations ( $\pm 2\sigma$ )					$\pm 0.0117$	$\pm 1.49\%$

<sup>a</sup> Standard deviation of all KENO V.a  $k_{eff}$  calculations  $< 10^{-3}$ .

<sup>b</sup> Defined as  $(k_c - k_m)/k_m \times 100\%$ , where  $k_m$  and  $k_c$  are the  $k_{eff}$  values based on measured and calculated nuclide concentrations.

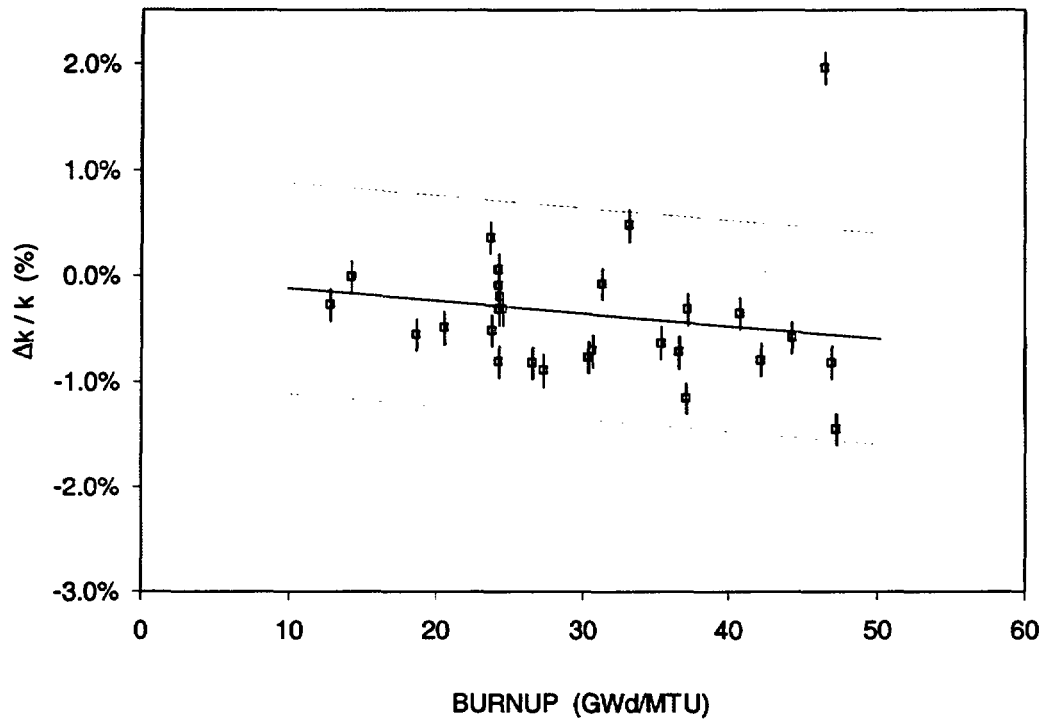


Figure 7 Relative margin for nuclide uncertainties as a function of sample burnup for actinides  $^{235}\text{U}$ ,  $^{236}\text{U}$ ,  $^{238}\text{U}$ ,  $^{239}\text{Pu}$ ,  $^{240}\text{Pu}$ ,  $^{241}\text{Pu}$ ,  $^{242}\text{Pu}$ , and  $^{241}\text{Am}$  in actinide Set 2, for a generic 32-assembly burnup-credit cask. The linear regression fit and the  $\pm 2\sigma$  uncertainty interval of the data are also shown.

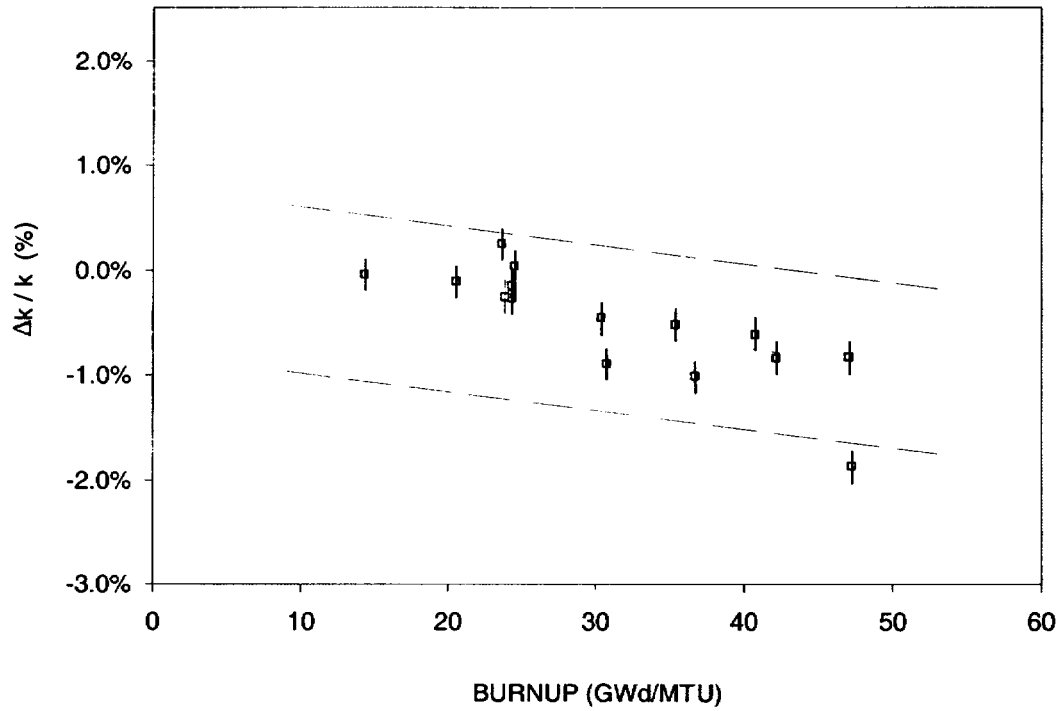


Figure 8 Relative margin for nuclide uncertainties as a function of sample burnup for actinides  $^{235}\text{U}$ ,  $^{236}\text{U}$ ,  $^{238}\text{U}$ ,  $^{239}\text{Pu}$ ,  $^{240}\text{Pu}$ ,  $^{241}\text{Pu}$ ,  $^{242}\text{Pu}$ ,  $^{241}\text{Am}$ , and  $^{243}\text{Am}$  in actinide Set 3, for a generic 32-assembly burnup-credit cask. The linear regression fit and the  $\pm 2\sigma$  uncertainty interval of the data are also shown.

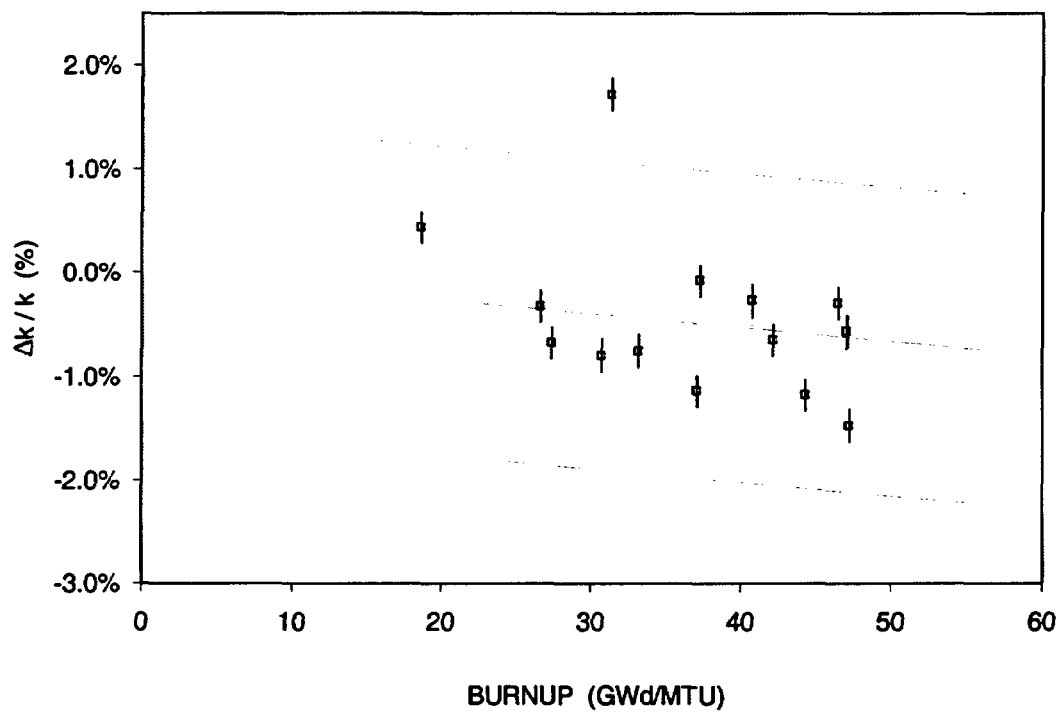


Figure 9 Relative margin for nuclide uncertainties as a function of sample burnup for all important burnup-credit actinides, except  $^{243}\text{Am}$ , in actinide Set 4, for a generic 32-assembly burnup-credit cask. The linear regression fit and the  $\pm 2\sigma$  uncertainty interval of the data are also shown.

The margin to account for nuclide uncertainty predicted using the direct difference results are based on experimental data with a relatively wide range of enrichments and burnup values. In most cases (but not all) the sample burnup was commensurate with the initial enrichment. That is, as the enrichments increase, so do the discharge burnup values. The measured data, and therefore the nuclide bias and uncertainties, reflect a proportionality between the enrichment and burnup. The uncertainties estimated previously using the Monte Carlo sampling method in Section 5.1.2 assumed a variable burnup but used a **fixed** initial enrichment of 3.5 wt %. Therefore, the enrichment and burnup combinations used in the Monte Carlo methods are not representative of typical variation in discharged fuel. The margin determined using the Monte Carlo approach for a burnup of 40 GWd/MTU, and burnup level typical for an enrichment of 3.5 wt %, is about 1.7%. Note that this value is in good agreement with direct difference results of about 1.8% over the range of all experimental data. The agreement in the margins estimated using these independent methods provides strong evidence supporting the assumption that uncertainties in nuclides concentrations used in burnup-credit calculations can be treated independently.

### 5.1.4 Sensitivity/Uncertainty Method

The S/U method provides an alternate approach for obtaining estimates of subcritical margin to account for the variability in the nuclide concentrations. The sensitivity-based method was introduced, and sensitivity terms were previously defined in Section 3.2. The method is similar to the Monte Carlo sampling method in that the bias and uncertainty of each nuclide on the  $k_{eff}$  value are evaluated on a nuclide-by-nuclide basis. The combined uncertainty from all nuclides is estimated by assuming the uncertainty associated with each nuclide is independent of the other nuclides. The validity of this assumption is supported by the good agreement observed between the margin estimated using the direct difference method, and that obtained with the Monte Carlo uncertainty sampling method, described in the previous sections.

The SEN35 sequence was used to calculate relative sensitivity coefficients for the nuclide concentrations applied in the KENO V.a 3-D cask criticality model for the generic 32-assembly burnup-credit cask. The sensitivity coefficients calculated for the important burnup-credit actinides in spent fuel with a fixed initial enrichment of 3.5 wt % and burnup values from 10 to 60 GWd/MTU are listed in Appendix B. A cooling time of 5 years was assumed (i.e., actinide compositions associated with a 5-year cooling time were applied in the SEN35 sensitivity calculations). Nuclides with a positive sensitivity coefficient indicate net neutron production (i.e., an increase in the concentration increases the neutron multiplication factor), while negative coefficients indicate net neutron absorption. Sensitivity coefficients were calculated for both a uniform (Table B.1) and for an axially-varying (Table B.2) burnup profile. Given a nuclide  $i$  with a standard deviation,  $s_i$ , (obtained from Table 5), the relative effect of the uncertainty on the neutron multiplication factor is given by

$$\frac{\Delta k_i}{k} = \left( \frac{s_i}{X_i} \right) S_i,$$

where  $S_i$  is the sensitivity coefficient for nuclide  $i$ . The total uncertainty from all nuclides is estimated by combining the individual contributions such that

$$\frac{\Delta k}{k} = \sqrt{\sum_i \left\{ \left( \frac{s_i}{X_i} \right) S_i \right\}^2}.$$

The margin predicted using the sensitivity method for actinide-only calculations, with and without an axial-burnup profile, is plotted in Figure 10. The margins are very similar to those obtained using the Monte Carlo methods presented in Section 5.1.2. Combining the reactivity effect for individual nuclides using an additive approach (results presented in Appendix B) yields subcritical margins for nuclide uncertainty that are very close to the values obtained using the bounding approach as presented in Section 5.1.1.

The sensitivity method combines the uncertainty contributions from individual nuclide to obtain an overall subcritical margin. The sensitivity coefficients, combined with nuclide uncertainty data, can be used to readily identify the nuclides making the largest contributions to the total nuclide uncertainty in a criticality calculation. This information may also be used to rank the nuclides in terms of where additional research effort is needed to reduce the overall level of nuclide uncertainty in burnup-credit calculations.

### 5.1.5 Observations

Figure 11 compares the limiting margin from the bounding analysis results with the margins predicted using the different best-estimate techniques for the uniform-axial-burnup case. The results from the Monte Carlo and sensitivity methods are very similar. The  $2\sigma$  relative margin for nuclide variability is about 1.2% at 10 GWd/MTU, increasing to 2.3% at 60 GWd/MTU. Similar agreement between the best-estimate methods was also found for calculations with an axial-burnup profile. The margins predicted with an axial-burnup profile are smaller than those without a profile for burnups greater than about 30 GWd/MTU. The margin predicted using best-estimate methods for a burnup of 60 GWd/MTU is 1.6% with an axial-burnup profile, compared to 2.3% with a flat axial profile (e.g., see Table 7).

The best-estimate uncertainty margins, determined using a  $2\sigma$  criteria, ensure a likelihood greater than 0.97 that the combined effects of nuclide uncertainty will not exceed the margin. The limiting margins predicted using a bounding approach are approximately two times larger than the margins predicted by the best-estimate methods. Thus, the bounding margin is equivalent to the best-estimate uncertainty determined using about a  $4\sigma$  confidence interval. The likelihood that a given set of computed nuclide concentrations will not exceed the bounding margin is roughly 0.99996, illustrating the degree to which the bounding method is conservative.

The direct difference results, simulated for a uniform axial-burnup distribution only, exhibit a relatively uniform standard deviation (margin for uncertainty) over the range of all experimental data. The increase in the margin with increasing burnup found in the Monte Carlo and the sensitivity results is not evident in the direct difference results. However, there is an important distinction between the direct difference method and the other analysis methods. The direct difference results are derived from experimental data for a wide range of enrichments and burnup values. In most cases (but not all) the sample burnup is commensurate with the initial enrichment. That is, as the enrichment increases, so does the discharge burnup. The results, therefore, reflect a proportionality between the enrichment and burnup. However, the Monte Carlo and sensitivity calculations were illustrated for cases with variable burnup and a *fixed* initial enrichment. Therefore, the results in the low-burnup regime reflect the uncertainty for fuel that has not achieved a typical burnup, while the results in the high-burnup regime reflect fuel that is overburned with respect to the initial enrichment, as compared to typical discharged fuel. The margins determined from the  $\pm 2\sigma$  uncertainty interval of the Monte Carlo uncertainty method for a burnup of 40 GWd/MTU, a value commensurate with the initial enrichment of 3.5 wt %  $^{235}\text{U}$  used in the analysis, is about  $\pm 1.7\%$ . This value is in good agreement with the value of  $\pm 1.8\%$  derived using the direct difference method.

The bounding method yields upper limit margins that are significantly larger than those predicted using the best-estimate methods. Although all methods used the same nuclide uncertainty data, the bounding method yielded a larger margin because of the highly-conservative method of combining the uncertainties of individual nuclides. The bounding approach leads to a limiting margin that is typically a factor of two times larger than the best-estimate methods for actinide-only burnup-credit calculations.

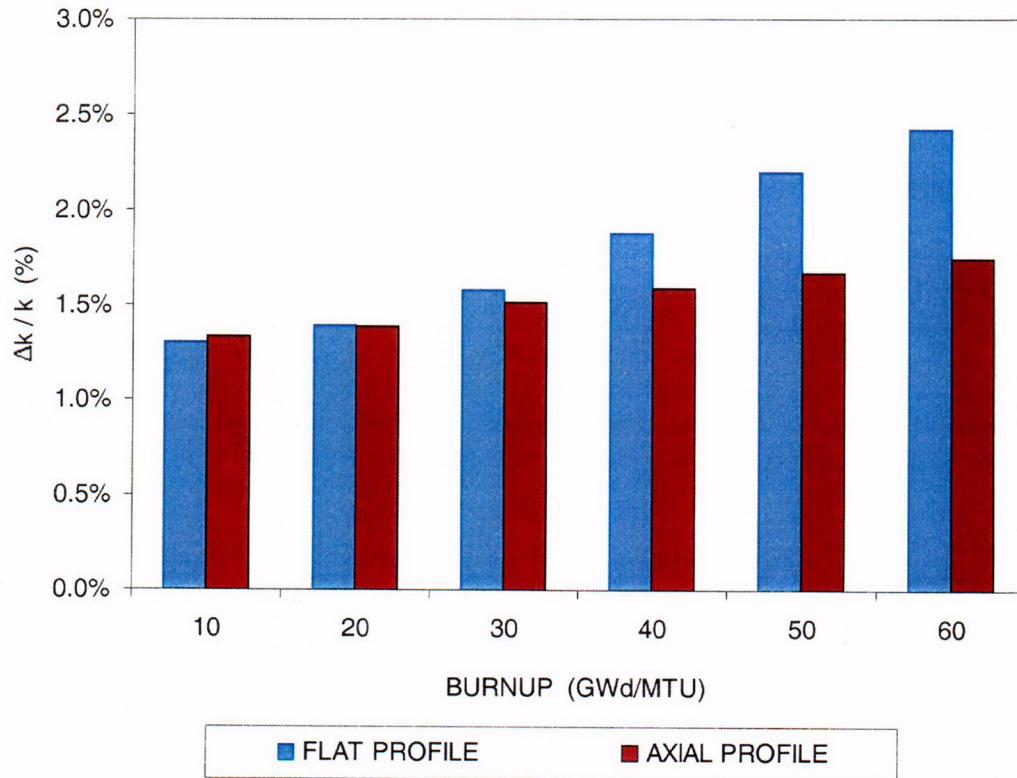


Figure 10 Relative margins for nuclide uncertainties estimated using sensitivity methods for actinide-only burnup credit. The margins represent the net effect of a  $2\sigma$  variability in the computed nuclide concentrations. The results are shown for both a uniform (flat) and an axially-varying burnup profile, and a fixed initial fuel enrichment of 3.5 wt %  $^{235}\text{U}$ .

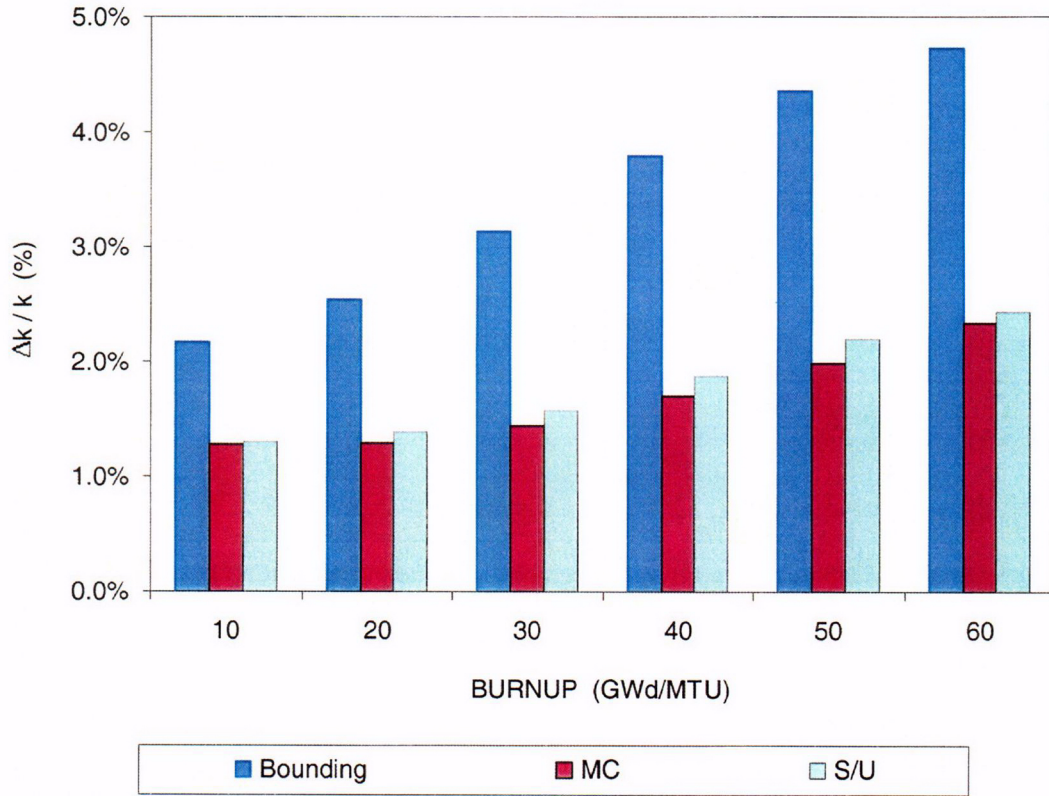


Figure 11 Relative margins for nuclide variability estimated using the limiting bounding method, and best-estimate methods for actinide-only burnup credit and a uniform (flat) axial burnup. The bounding, Monte Carlo (MC) and sensitivity/uncertainty (S/U) margins were all generated assuming a fixed initial enrichment of 3.5 wt % <sup>235</sup>U.

## 5.2 ACTINIDE AND FISSION-PRODUCT CREDIT

The ISG-8 Rev. 1 guidance on burnup credit excludes credit for fission products. However, an estimate of the additional reactivity margin available from the fission products by the applicant is recommended. The fission products, individually, have a small effect on the neutron multiplication factor than the actinides. Collectively, fission products represent about 25% of the total reactivity of SNF in a cask configuration. The most important fission products in criticality calculations are listed in Table 1 (also see Figure 1). These nuclides are considered to be most important to dry storage and transport cask criticality safety analyses. The relative importance of these nuclides will vary to some degree, depending on the enrichment, burnup, and cooling time. This section briefly examines some of the difficulties associated with implementing fission-product credit, and estimates the margin associated with uncertainties in the nuclide concentrations for actinide and fission-product burnup credit calculations.

The quantity of measured isotopic assay data for the fission products is considerably less than that available for the actinides, and for some important fission products (e.g.,  $^{95}\text{Mo}$ ,  $^{109}\text{Ag}$ , and  $^{101}\text{Ru}$ ) there are no known sources of publicly-available assay data. The limited quantity of data makes validation of the fission products difficult, and ultimately will lead to an increased uncertainty in the predicted nuclide concentrations. Consequently, the amount of negative reactivity that can ultimately be credited from fission products is likely to be limited until additional measured data are acquired.

The nuclide uncertainties derived in this report are based on the standard deviation of the measured and calculated nuclide concentrations alone. Tolerance factors that account for the additional uncertainty component due to a limited sample size were not applied in this study to either the actinides or the fission-product uncertainty estimates. Although such tolerance factors will have a minimal impact on the actinides because of the relatively large number of samples available, tolerance factors will increase the fission-product uncertainties. Therefore, the effect of fission-product uncertainties estimated in this report likely underestimate the effect as compared to results based on statistical analyses that include the use of tolerance factors.

The published spent fuel radiochemical assay programs containing results for the fission products important in burnup credit are limited primarily to Calvert Cliffs ATM-104 (assembly D047) and the more recent Takahama-3 measurements. Several other experiments (e.g., KRI) include some fission-product measurements. The experiments containing fission-product data are summarized in Table 4 and were discussed previously in Section 4. The burnup-credit fission-product nuclides with measured data (excluding  $^{103}\text{Rh}$ , which has only one measurement) represent about 80% of the total reactivity worth available from all fission products listed in Table 1.

The margins associated with nuclide uncertainties in calculations using both actinide and fission-product credit were estimated using the bounding method, and the Monte Carlo sampling and S/U methods used previously for the actinide-only calculations. The direct difference approach cannot be applied currently to the fission products because of the limited amount of nuclide validation data. The direct difference method requires a relatively large set of experiments containing a common set of measured nuclides. The Monte Carlo sampling and sensitivity methods, however, do not require such a common data set, and utilize all available measurements from different experiments.

In this study of the fission products, the nuclides  $^{99}\text{Tc}$ ,  $^{103}\text{Rh}$ ,  $^{133}\text{Cs}$ ,  $^{143}\text{Nd}$ ,  $^{145}\text{Nd}$ ,  $^{147}\text{Sm}$ ,  $^{149}\text{Sm}$ ,  $^{150}\text{Sm}$ ,  $^{151}\text{Sm}$ ,  $^{152}\text{Sm}$ ,  $^{151}\text{Eu}$ ,  $^{153}\text{Eu}$ , and  $^{155}\text{Gd}$  were included in the criticality calculations. The one  $^{103}\text{Rh}$  measurement provides an estimate of the calculational bias, but precludes an estimate of the standard deviation since only one measurement is available. For the purposes of this illustrative study, the relative

standard deviation of the calculated  $^{103}\text{Rh}$  concentration was assumed to be nominally  $\pm 30\%$ . The nuclides with no measured data,  $^{95}\text{Mo}$ ,  $^{109}\text{Ag}$ , and  $^{101}\text{Ru}$ , were excluded from the criticality analysis.

The results using a bounding approach for actinide and fission-product burnup credit, calculated with a uniform and an axial-burnup profile, are listed in Table 13. The limiting margins associated with the nuclide variability is almost two times larger than the margins observed for the actinide-only calculations for high-burnup fuel. For calculations with a uniform (flat) axial burnup of 60 GWd/MTU, the relative margin is about  $\pm 8.4\%$ , compared to about  $\pm 4.8\%$  for actinide-only burnup credit. The increase is attributed to the relatively large uncertainty for many of the fission products. For the calculations with an axial-burnup profile and assembly-averaged burnup of 60 GWd/MTU, the relative margin decreases to  $\pm 5.9\%$ , compared to  $\pm 3.8\%$  for actinide-only burnup credit. As discussed previously, these results do not include additional fission-product uncertainty to account for the limited number of fission-product measurements (i.e., tolerance factors). If tolerance factors were applied, the total uncertainty with fission-product credit could be considerably larger than that found in this study.

The results of the Monte Carlo uncertainty sampling calculations performed using the KRONOS code with actinide and fission-product burnup credit are listed in Table 14. The results also indicate that the margin for nuclide uncertainty is larger when fission products are included. However, the increase is observed to be much less than that seen using the bounding method. The maximum relative margin estimated using the Monte Carlo sampling method with actinide and fission-product credit and a uniform axial burnup was  $\pm 3.0\%$ , compared to  $\pm 2.2\%$  when only the actinides are credited. The margins for calculations that use an axial-burnup profile are again observed to be smaller than those for the uniform axial-burnup cases.

The uncertainties estimated using sensitivity methods for actinide and fission-product credit are tabulated in Appendix B. Table B.3 lists the burnup-dependent relative sensitivity coefficients calculated using the SEN35 sequence of SCALE, and Table B.4 lists the relative effect on the  $k_{eff}$  due to the variability in the individual burnup-credit actinide and fission-product nuclides. The aggregate effect is estimated as the root sum square of the individual effects (i.e., independent uncertainties). The values are observed to be in good agreement with the values predicted by the Monte Carlo method. The results obtained by additively combining the individual uncertainties are also listed.

Figure 12 compares the margin predicted using the different uncertainty propagation methods for the uniform axial-burnup case. The results for an axial-burnup profile are illustrated in Figure 13. The margins predicted using the independent best-estimate methods yield nearly identical results for the uniform axial-burnup and axially-varying burnup profiles. The relative margin predicted using best-estimate methods ranges from about  $\pm 1.6\%$  at 10 GWd/MTU to  $\pm 3.2\%$  at 60 GWd/MTU for a fixed initial enrichment of 3.5 wt % and a uniform axial burnup. The maximum relative margin at 60 GWd/MTU decreases from  $\pm 3.2\%$  to about  $\pm 2.0\%$  when the axial-burnup profile is applied.

Table 13 Results of actinide plus fission product bounding criticality calculations

Case	Burnup <sup>b</sup> (GWd/MTU)	Axial profile included	$k_{eff}^a$			Bounding margin	
			Nominal	Best- estimate	Bounding <sup>c</sup>	$\Delta k_{eff}^d$	$\Delta k_{eff}/k_{eff}^e$
1	10	No	1.0207	1.0245	1.0555	0.0310	3.03%
2	20	No	0.9406	0.9438	0.9837	0.0399	4.23%
3	30	No	0.8619	0.8679	0.9145	0.0466	5.37%
4	40	No	0.7945	0.7997	0.8527	0.0530	6.63%
5	50	No	0.7384	0.7430	0.7982	0.0552	7.43%
6	60	No	0.7016	0.7062	0.7645	0.0583	8.26%
7	10	Yes	1.0146	1.0201	1.0513	0.0312	3.06%
8	20	Yes	0.9480	0.9509	0.9858	0.0349	3.67%
9	30	Yes	0.8903	0.8960	0.9327	0.0367	4.10%
10	40	Yes	0.8438	0.8471	0.8895	0.0424	5.01%
11	50	Yes	0.8010	0.8059	0.8486	0.0427	5.30%
12	60	Yes	0.7710	0.774	0.8195	0.0457	5.91%

<sup>a</sup> Standard deviation of all KENO V.a  $k_{eff}$  calculations  $< 10^{-3}$ .

<sup>b</sup> Initial enrichment of 3.5 wt % <sup>235</sup>U.

<sup>c</sup> Calculated using bias and uncertainty adjusted concentrations.

<sup>d</sup> Best-estimate – bounding values.

<sup>e</sup>  $\Delta k_{eff} / k_{eff} \times 100\%$ , where  $k_{eff}$  is the best-estimate  $k_{eff}$  value.

Table 14 Results of Monte Carlo actinide plus fission-product uncertainty calculations

Case	Burnup <sup>b</sup> (GWd/MTU)	Axial profile included	Neutron multiplication factor ( $k_{eff}$ ) <sup>a</sup>		
			Nominal	Best-estimate	KRONOS <sup>c</sup> mean $k_{eff} \pm 2 \sigma$ (%)
1	10	No	1.0198	1.0253	1.0252 $\pm$ 0.0162 (1.58%)
2	20	No	0.9393	0.9457	0.9447 $\pm$ 0.0158 (1.67%)
3	30	No	0.8634	0.8693	0.8689 $\pm$ 0.0194 (2.03%)
4	40	No	0.7967	0.7997	0.8010 $\pm$ 0.0210 (2.42%)
5	50	No	0.7389	0.7430	0.7438 $\pm$ 0.0220 (2.82%)
6	60	No	0.7038	0.7064	0.7078 $\pm$ 0.0110 (3.11%)
7	10	Yes	1.0169	1.0223	1.0205 $\pm$ 0.0156 (1.53%)
8	20	Yes	0.9463	0.9498	0.9511 $\pm$ 0.0152 (1.60%)
9	30	Yes	0.8901	0.8941	0.8951 $\pm$ 0.0150 (1.68%)
10	40	Yes	0.8414	0.8477	0.8470 $\pm$ 0.0150 (1.77%)
11	50	Yes	0.7998	0.8036	0.8042 $\pm$ 0.0150 (1.87%)
12	60	Yes	0.7706	0.7757	0.7756 $\pm$ 0.0152 (1.96%)

<sup>a</sup> Standard deviation of KENO V.a  $k_{eff}$  calculations  $< 10^{-3}$ .

<sup>b</sup> Initial enrichment of 3.5 wt % <sup>235</sup>U.

<sup>c</sup>  $2\sigma$  value is the standard deviation from the distribution of  $k_{eff}$  values.

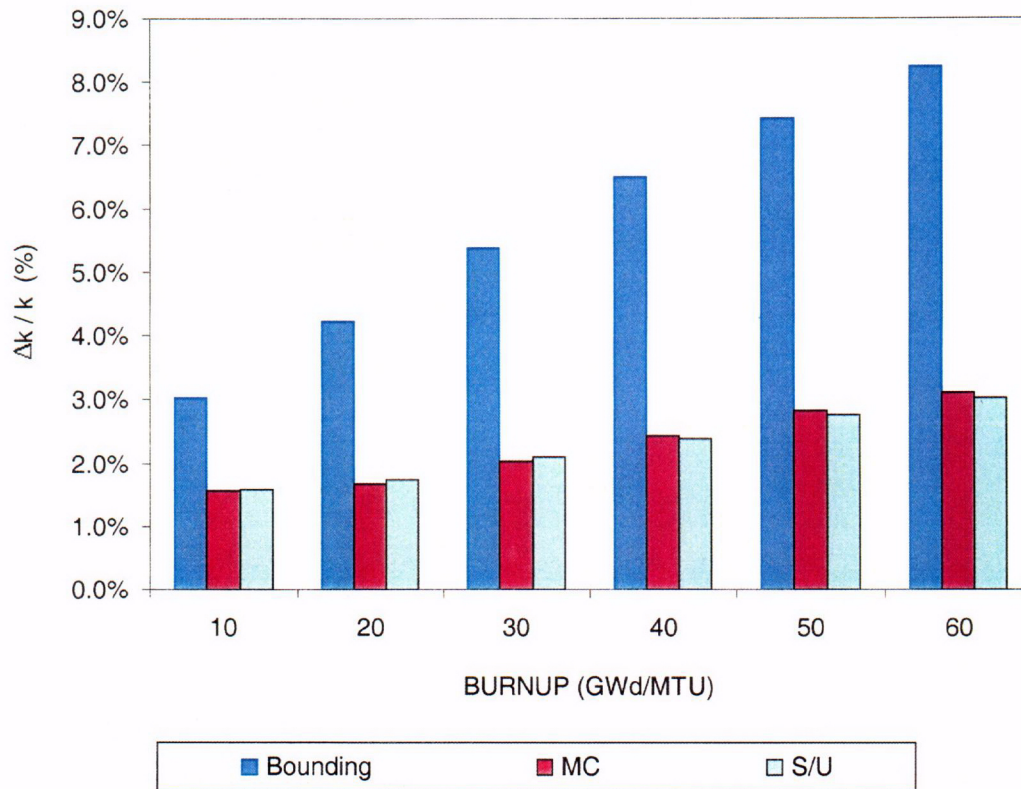


Figure 12 Relative margins for nuclide variability estimated using the limiting bounding method, and best-estimate Monte Carlo (MC) sampling, and sensitivity/uncertainty (S/U) methods for actinide and fission-product burnup credit and a uniform (flat) axial burnup. The criticality calculations were performed using a generic burnup-credit cask and assumed a fixed initial enrichment of 3.5 wt % <sup>235</sup>U.

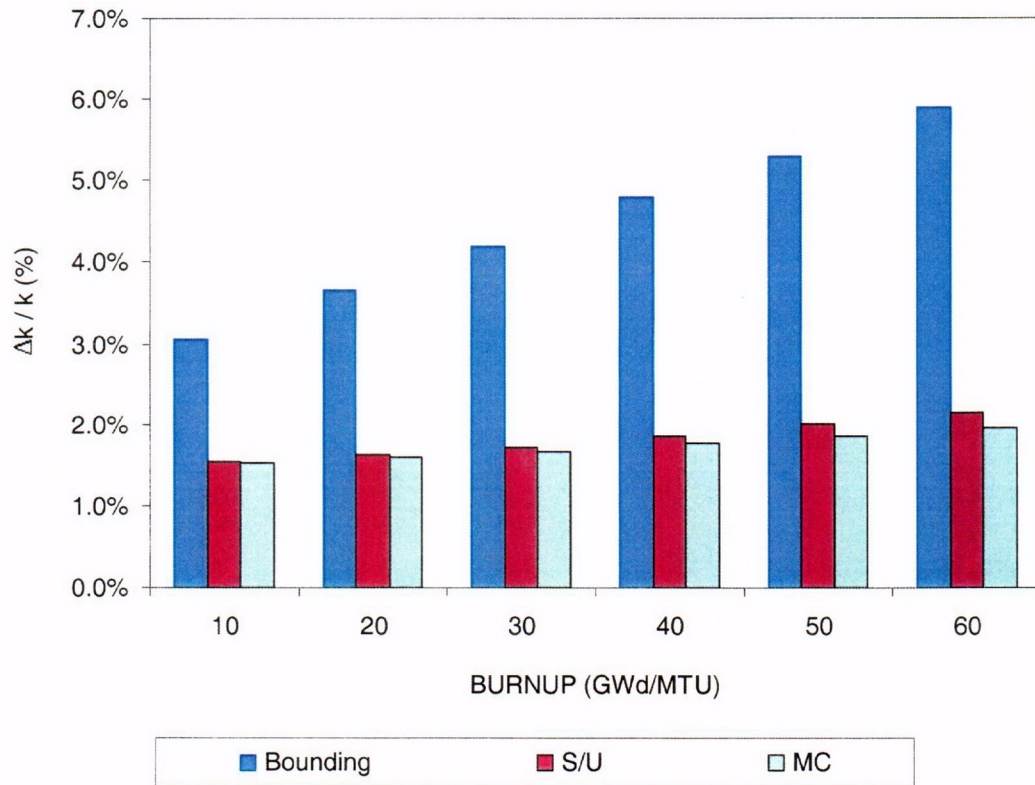


Figure 13 Relative margins for nuclide variability estimated using the limiting bounding method, and best-estimate Monte Carlo (MC) sampling, and sensitivity/uncertainty (S/U) methods for actinide and fission-product burnup credit and an axially-varying burnup profile. The criticality calculations were performed using a generic burnup-credit cask and assumed a fixed initial enrichment of 3.5 wt %  $^{235}\text{U}$ .

## 6 BIAS RESULTS

The analyses, in the preceding section, deal primarily with the evaluation of the subcritical margin to account for the effects of nuclide uncertainties in the criticality calculations. However, in addition to accounting for the uncertainty, the bias must also be considered. Based on the results presented in Section 5, the overall effect of nuclide bias, on average, is observed to be negative (the calculated neutron multiplication factor is underpredicted). The direct difference results suggest an increasingly negative bias trend with increasing burnup. The relative magnitude of the bias effect on the neutron multiplication factor for actinide-only burnup credit is observed to be less than 1% in  $k_{eff}$  over the full range of the experimental data.

The nuclide bias may be estimated directly using the results of the direct difference calculations and applied as an additional subcritical margin in the criticality calculation. Alternatively, the effect of bias may be considered by adjusting the predicted nuclide concentrations based on the average bias observed in the nuclide validation results. That is, the average bias for each nuclide  $i$  is applied to improve the calculated concentration using the relationship:

$$C_i^* = C_i \bar{X}_i$$

where  $C_i^*$  is the bias-adjusted concentration,  $C_i$  is the calculated concentration, and  $(\bar{X})$  is the experiment-to-measured ratio. The  $\bar{X}$  values in Table 5 were derived from the average bias of all samples. There was no attempt in this study to identify potential trends in nuclide bias with the burnup or enrichment of the sample. Such a task would be a significant undertaking, and would be complicated by the limited size of the experimental database. This section evaluates the validity of using average nuclide bias factors, as presented in Table 5, to represent the effect of bias on the neutron multiplication factor over the enrichment and burnup range covered by the experimental data.

### 6.1 ACTINIDE-ONLY BURNUP CREDIT

To estimate the effect of nuclide bias for actinide-only burnup-credit calculations, actinide concentrations predicted by the burnup calculations were applied directly in the criticality calculation. The calculations were then repeated using the calculated concentrations adjusted for the average nuclide bias as presented in Table 5. The effect of the nuclide bias was then quantified as the difference in the  $k_{eff}$  values ( $\Delta k_{eff}$ ).

For the initial bias calculations, the conservatively adjusted nuclide bias factors,  $\bar{X}_i'$ , were applied.

That is, no positive bias was credited in the analysis. The calculations were performed over an enrichment range from 2.4 to 4.5 wt %. For each enrichment, burnup values were selected that were representative of the lower-, mid-, and high-burnup fuel as determined from inventory of discharged PWR assemblies in the U.S. The low- and high-burnup values used in the analysis were 10 GWd/MTU lower and 10 GWd/MTU higher than the average-burnup value, respectively. The range is sufficient to cover the vast majority of discharged fuel.

The results of the actinide-only calculations are listed in Table 15 and illustrated in Figure 14. The predicted margin for the nuclide bias in the table is expressed as the  $\Delta k_{eff}$  value and as  $\Delta k_{eff} / \Delta k_{eff}$ . The relative margin for bias over all evaluated enrichment and burnup combinations is between -0.5 and -1.0%. The margins in Figure 14 are observed to be relatively constant with increasing enrichment. For example, the relative margin is between -0.7 and -0.9% for each enrichment value assuming average (typical) burnup values. In obtaining these results, the burnup was increased as the enrichment increased.

Table 15 Results of nuclide bias calculations for actinide-only burnup credit

Case	Enrichment (wt % <sup>235</sup> U)	Burnup (GWD/MTU)	$k_{eff}^a$		Bias margin	
			Nominal	Bias- corrected	$\Delta k_{eff}^b$	$\Delta k_{eff}/k_{eff}^c$
1	2.4	15	0.9178	0.9231	-0.0053	-0.57%
2	2.4	25	0.8564	0.8635	-0.0071	-0.82%
3	2.4	35	0.8063	0.8133	-0.0070	-0.86%
4	2.8	20	0.9294	0.9348	-0.0054	-0.57%
5	2.8	30	0.8692	0.8751	-0.0059	-0.67%
6	2.8	40	0.8190	0.8249	-0.0059	-0.72%
7	3.2	25	0.9375	0.9423	-0.0048	-0.51%
8	3.2	35	0.8773	0.8834	-0.0062	-0.70%
9	3.2	45	0.8282	0.8341	-0.0058	-0.70%
10	3.6	30	0.9433	0.9478	-0.0046	-0.48%
11	3.6	40	0.8855	0.8922	-0.0067	-0.75%
12	3.6	50	0.8355	0.8411	-0.0056	-0.66%
13	3.9	35	0.9387	0.9437	-0.0050	-0.53%
14	3.9	45	0.8825	0.8891	-0.0066	-0.74%
15	3.9	55	0.8345	0.8417	-0.0072	-0.86%
16	4.2	40	0.9345	0.9394	-0.0049	-0.52%
17	4.2	50	0.8799	0.8858	-0.0059	-0.66%
18	4.2	60	0.8399	0.8457	-0.0058	-0.69%
19	4.5	45	0.9302	0.9346	-0.0043	-0.46%
20	4.5	55	0.8778	0.8837	-0.0060	-0.67%

<sup>a</sup> Standard deviation of all KENO V.a  $k_{eff}$  calculations  $< 10^{-3}$ .

<sup>b</sup> Nominal – bias-corrected values.

<sup>c</sup>  $\Delta k_{eff} / k_{eff} \times 100\%$ , where  $k_{eff}$  is the bias-corrected  $k_{eff}$  value.

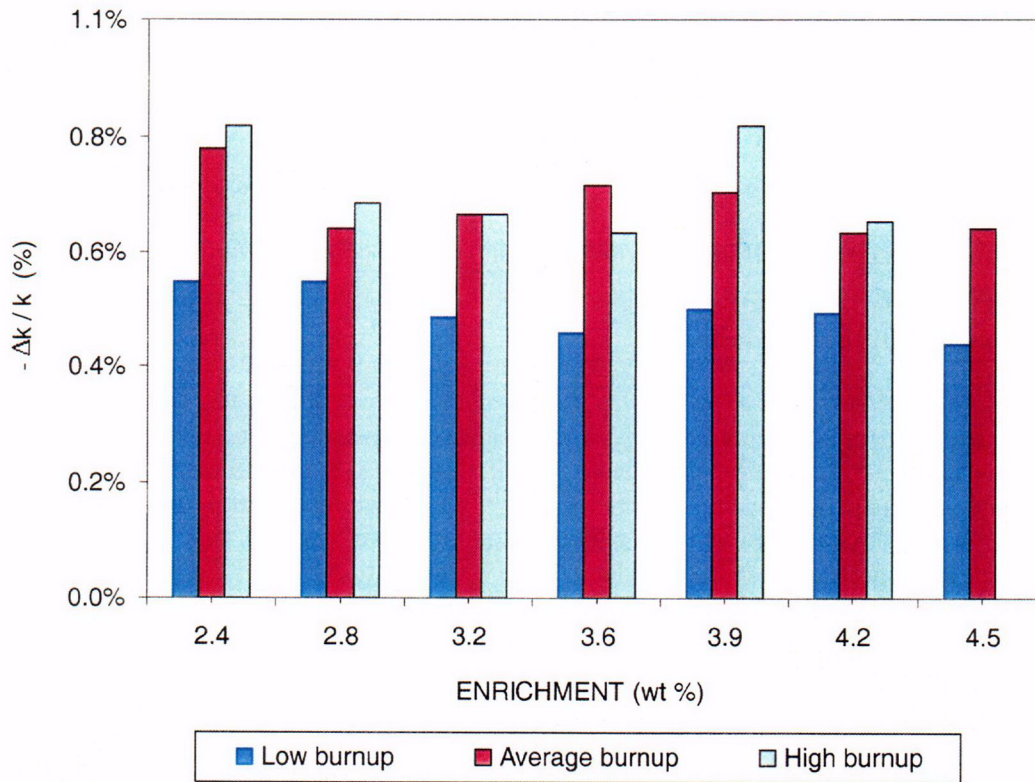


Figure 14 Relative margins for nuclide bias for actinide-only burnup credit. The results were based on bias-adjusted nuclide concentrations that conservatively did not credit positive bias.

In general, the negative bias margin for a fixed enrichment value is seen to increase with burnup. For example, the relative margin estimated for 3.9 wt % fuel increases from about  $-0.5\%$  at 35 GWd/MTU to  $-0.9\%$  at 55 GWd/MTU.

The results obtained by adjusting the individual nuclide concentrations can be compared to the margin predicted using the direct difference calculations presented in Section 5 to provide verification of the approach. The direct difference results provide a realistic measure of the bias that does not assume that individual nuclide bias estimates are constant over the enrichment and burnup range. The bias predicted in the direct difference calculations was assumed to be linear with enrichment and burnup, and was constrained to go to zero at the origin (zero burnup) since there is no calculational bias associated with the use of fresh-fuel compositions. The magnitude of the bias margin is observed to be comparable between the two independent methods. However, the margins in the direct difference method increase with burnup, whereas the bias observed with bias-adjusted nuclide concentrations remains relatively constant with enrichment and burnup. This effect is attributed to the use of a constant average nuclide bias (e.g.,  $\bar{X}_i$  factors) to adjust the calculated concentrations, rather than evaluating the potential burnup and enrichment dependence of the nuclide biases.

As the burnup approaches zero, it is expected that the approach will overpredict the actual bias. At higher-burnup values, the biases predicted by both methods are observed to be in reasonably good agreement. The maximum relative bias estimated for a burnup of 50 GWd/MTU using the direct difference method is  $-0.76\%$ . This can be compared to the results obtained using bias-adjusted nuclide concentrations that range from  $-0.46$  to  $-0.86$  over the burnup interval from 45 to 55 GWd/MTU (value depends on the enrichment value used in the calculation). Extrapolation beyond the burnup range of the experimental data (about 50 GWd/MTU), the direct difference method predicts an increasingly negative bias. However, this is not observed in the results obtained with bias-adjusted nuclide concentrations, a procedure that leads to a relatively constant bias effect.

The bias calculations described were repeated using the unadjusted bias factors ( $\bar{X}$ ) listed in Table 5 that credit positive nuclide bias. These results yielded a net bias effect that was statistically the same as the results obtained using the conservative ( $\bar{X}'$ ) bias values. That is, the  $k_{eff}$  results were the same, within the uncertainty of the KENO V.a criticality calculations. This result is expected since the majority of the burnup-credit nuclide concentrations are negatively biased in terms of the reactivity effect. The exceptions ( $^{236}\text{U}$ ,  $^{238}\text{Pu}$ ,  $^{240}\text{Pu}$ ) exhibit a small positive bias, or have a relatively small effect on the neutron multiplication factor.

## 6.2 ACTINIDE AND FISSION-PRODUCT CREDIT

The effect of nuclide bias was also estimated for calculations involving actinide and fission-product credit. The average fission-product nuclide bias values were obtained from Table 5. Unlike the actinide-only calculations, the results obtained with fission products cannot be independently verified with results from the direct difference method because of the very limited quantity of experimental fission-product assay data that precludes extending the use of the direct difference method to fission products. Nevertheless, the fission-product results obtained using the bias-adjusted nuclide concentrations are included in this section for illustrative purposes only. Fission-product credit is not recommended until such time as the experimental database is expanded to allow adequate nuclide validation.

The results of the actinide and fission product criticality calculations are listed in Table 16 and are illustrated in Figure 15. Again, the margin associated with nuclide bias was expressed as the  $\Delta k_{eff}$  value

Table 16 Effect of nuclide bias for actinide and fission-product burnup credit

Case	Enrichment (wt % <sup>235</sup> U)	Burnup (GWd/MTU)	$k_{eff}^a$		Bias margin	
			Nominal	Bias-corrected	$\Delta k_{eff}^b$	$\Delta k_{eff}/k_{eff}^c$
1	2.4	15	0.8719	0.8788	-0.0069	-0.78%
2	2.4	25	0.7947	0.8026	-0.0079	-0.98%
3	2.4	35	0.7336	0.7427	-0.0092	-1.23%
4	2.8	20	0.8737	0.8812	-0.0075	-0.85%
5	2.8	30	0.8002	0.8085	-0.0083	-1.03%
6	2.8	40	0.7397	0.7485	-0.0087	-1.17%
7	3.2	25	0.8742	0.8823	-0.0081	-0.92%
8	3.2	35	0.8024	0.8119	-0.0095	-1.17%
9	3.2	45	0.7440	0.7532	-0.0092	-1.22%
10	3.6	30	0.8731	0.8820	-0.0089	-1.00%
11	3.6	40	0.8049	0.8151	-0.0103	-1.26%
12	3.6	50	0.7464	0.7560	-0.0096	-1.27%
13	3.9	35	0.8619	0.8721	-0.0102	-1.17%
14	3.9	45	0.7961	0.8065	-0.0104	-1.28%
15	3.9	55	0.7408	0.7516	-0.0108	-1.43%
16	4.2	40	0.8536	0.8624	-0.0088	-1.02%
17	4.2	50	0.7897	0.8004	-0.0107	-1.34%
18	4.2	60	0.7436	0.7548	-0.0111	-1.48%
19	4.5	45	0.8421	0.8530	-0.0109	-1.28%
20	4.5	55	0.7830	0.7928	-0.0098	-1.24%

<sup>a</sup> Standard deviation of all KENO V.a  $k_{eff}$  calculations  $< 10^{-3}$ .

<sup>b</sup> Nominal – bias-corrected values.

<sup>c</sup>  $\Delta k_{eff} / k_{eff} \times 100\%$ , where  $k_{eff}$  is the bias-corrected  $k_{eff}$  value.

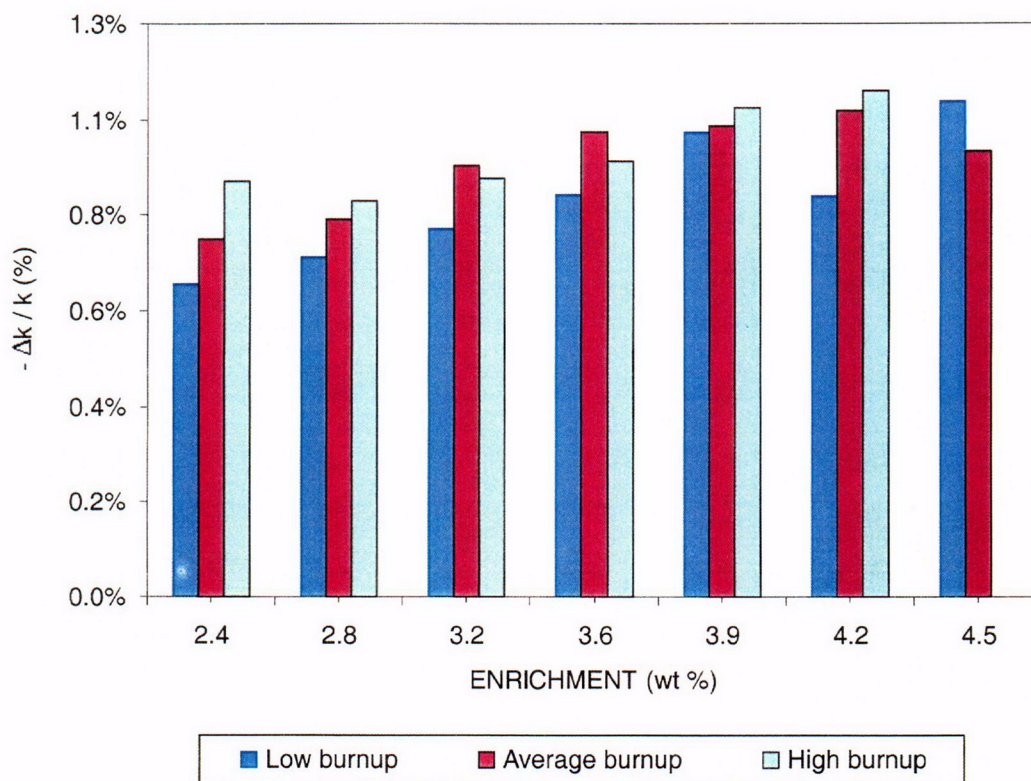


Figure 15 Relative margins for nuclide bias for actinide and fission-product burnup credit. The results were based on bias-adjusted nuclide concentrations that conservatively did not credit positive bias.

and as  $\Delta k_{eff} / \Delta k_{eff}$ . The results indicate that there is a larger negative bias associated with the use of fission products. However, further investigation indicated that the majority of the increase is associated with the use of the conservative nuclide bias factors  $\overline{X}_i$  that do not credit positive bias. When the calculations were repeated using unadjusted nuclide bias factors the net margin for bias was similar to that observed in the actinide-only calculations.

## 7 SUMMARY AND CONCLUSIONS

This report has explored several alternative strategies for propagating the effects of nuclide uncertainty to the predicted neutron multiplication factor,  $k_{eff}$ , in burnup-credit calculations. Section 3 described a conventional bounding method and several different best-estimate methods that can be used to provide more realistic estimates of the margin associated with effects of nuclide uncertainty. Section 4 provided a review of currently available radiochemical assay data for PWR spent fuel, and summarized the results of nuclide validation studies performed using the SCALE code system. In Section 5, the nuclide uncertainties, determined from the comparisons of computed and measured nuclide concentration in Section 4, were used to predict the margin associated with the nuclide uncertainties using the bounding and best-estimate strategies.

The bounding method, while easy to implement and clearly easy to defend as conservative, results in limiting and unrealistically large margins to account for nuclide variability. The method of propagating the effects of nuclide uncertainties in the bounding method overestimates the real importance of nuclide uncertainties on the predicted  $k_{eff}$  and precludes a realistic evaluation of the real subcritical margin.

Several different best-estimate strategies for combining and propagating nuclide uncertainties have been evaluated in this report and compared for a burnup-credit analysis of a prototype burnup-credit rail-type cask. The best-estimate methods enable a more accurate estimate of the effects of nuclide uncertainty by realistically simulating the effects of random variability in the nuclide concentrations.

The effects of nuclide uncertainty were addressed separately (Section 5) from the bias (Section 6) which is a non-random systematic error. However, both components must ultimately be considered in determining an appropriately conservative margin of subcriticality in a criticality calculation. The separate evaluation of the uncertainty and bias in this report enables the criticality analysis to exclude credit for positive nuclide bias (recommended practice in nuclear criticality safety).

For actinide-only burnup credit calculations the margins for nuclide uncertainty predicted using best-estimate methods were about one half the limiting margins predicted using the bounding method. When fission products were included in the analysis the benefits of the best-estimate methods were even larger.

The ISG-8 Rev. 1 guidance recommends a limit on the amount of credit for burnup to 40 GWd/MTU or less, and recommends a loading offset (additional penalty) for fuel with an initial enrichment between 4 and 5 wt %. The recommended limits were based to a large extent on the lack of radiochemical assay data above 40 GWd/MTU and 4 wt % (the majority of enrichments were less than 3.2 wt %) that were available for code validation at the time the guidance was issued. The recent publication and analysis of the Takahama-3 PWR radiochemical assay data significantly extends the range of the validation database. The nuclide validation results performed with the SCALE system using the Takahama-3 data suggest that nuclide uncertainties are comparable to those observed in the lower enrichment and lower-burnup samples. These results suggest that the nuclide uncertainties for SNF exceeding 4 wt % and 40 GWd/MTU are expected to be similar to SNF below these limits. A more quantitative analysis of the uncertainties and trends in the data are provided in Section 5.

The above findings have potentially important implications for the ISG-8 Rev. 1 guidance and may provide a technical basis to support increased utilization of burnup credit for transportation and storage casks.

The margins for nuclide uncertainty presented in this study are intended for illustrative purposes only and cannot be applied directly to other criticality assessments. The cases are given as examples to

demonstrate the potential benefits of using best-estimate uncertainty analysis methods. The results presented in this report are based on a generic rail-type burnup-credit cask and were performed using the SCALE code system and nuclear data libraries. Results for other configurations and code systems must be assessed separately. Also, a more rigorous statistical analysis of the isotopic validation data may be required for safety analysis applications, such as the development and application of tolerance intervals, which were not considered in this study. Nevertheless, the benefits of best-estimate methods illustrated in this report are expected to be similar for other configurations and code systems.

## 8 REFERENCES

1. U.S. Nuclear Regulatory Commission, *Spent Fuel Project Office Interim Staff Guidance – 8, Rev. 1 – Limited Burnup Credit*, U.S. NRC, July 30, 1999.
2. American National Standard, *Nuclear Criticality Safety in Operations with Fissionable Material Outside Reactors*, ANSI/ANS-8.1-1998, 1998.
3. U.S. Department of Energy, *Topical Report on Actinide-Only Burnup Credit for PWR Spent Nuclear Fuel Packages*, DOE/RW-0472, Rev. 2, Office of Civilian Radioactive Waste Management, U.S. Department of Energy, 1998.
4. M. D. DeHart, *Sensitivity and Parametric Evaluations of Significant Aspects of Burnup Credit for PWR Spent Fuel Packages*, ORNL/TM-12973, Lockheed Martin Energy Research Corporation, Oak Ridge National Laboratory, May 1996.
5. M. D. DeHart and O. W. Hermann, *An Extension of the Validation of SCALE (SAS2H) Isotopic Prediction for PWR Spent Fuel*, ORNL/TM-13317, Lockheed Martin Energy Research Corporation, Oak Ridge National Laboratory, September 1996.
6. M. Rahimi, E. Fuentes, D. Lancaster, *Isotopic and Criticality Validation for PWR Actinide-Only Burnup Credit*, DOE/RW-0497, Office of Civilian Radioactive Waste Management, U.S. Department of Energy, May 1997.
7. M. D. DeHart, *A Stochastic Method for Estimating the Effect of Isotopic Uncertainties in Spent Nuclear Fuel*, ORNL/TM-2001/83, UT-Battelle, LLC, Oak Ridge National Laboratory, September 2001.
8. B. T. Rearden and R. L. Childs, “Prototypical Sensitivity and Uncertainty Analysis Codes for Criticality Safety with the SCALE Code System,” in *Proc. of ANS/ENS 2000 International Winter Meeting and Embedded Topical Meetings*, November 12–16, 2000, Washington, DC. *Trans. Am. Nucl. Soc.* **83**, 98–100 (2000).
9. B. L. Broadhead and B. T. Rearden, “Foundations for Sensitivity-Based Criticality Validation Techniques,” in *Proc. of American Nuclear Society ANS/ENS 2000 International Winter Meeting and Embedded Topical Meetings*, November 12–16, 2000, Washington, D.C. *Trans. Am. Nucl. Soc.* **83**, 93–95 (2000).
10. B. L. Broadhead, C. M. Hopper, and C. V. Parks, *Sensitivity and Uncertainty Analyses Applied to Criticality Safety Validation: Illustrative Applications and Initial Guidance*, NUREG/CR-6655, Vol. 2 (ORNL/TM-13692/V2), U.S. Nuclear Regulatory Commission, Oak Ridge National Laboratory, November 1999.
11. C. V. Parks, M. D. DeHart, and J. C. Wagner, *Review and Prioritization of Technical Issues Related to Burnup Credit for LWR Fuel*, NUREG/CR-6665 (ORNL/TM-1999/303), U.S. Nuclear Regulatory Commission, Oak Ridge National Laboratory, February 2000.
12. O. W. Hermann, S. M. Bowman, M. C. Brady, and C. V. Parks, *Validation of the SCALE System PWR Spent Fuel Isotopic Composition Analyses*, ORNL/TM-12667, Lockheed Martin Energy Research Corporation, Oak Ridge National Laboratory, March 1995.
13. Y. Nakahara, K. Suyama, and T. Suzaki, *Technical Development on Burnup Credit for Spent LWR Fuels*, Japan Atomic Energy Research Institute, Tokai Research Institute, JAERI-Tech 2000-071, October 2000 (Japanese).

14. C. E. Sanders and I. C. Gauld, *Isotopic Analysis of High-Burnup PWR Spent Fuel Samples from the Takahama-3 Reactor*, ORNL/TM-2001/259, UT-Battelle, LLC, Oak Ridge National Laboratory, 2002.
15. O. W. Hermann, M. D. DeHart, and B. D. Murphy, *Evaluation of Measured LWR Spent Fuel Composition Data for Use in Code Validation*, ORNL/M-6121, Lockheed Martin Energy Research Corporation, Oak Ridge National Laboratory, February 1998.
16. S. R. Bierman and R. J. Talbert, *Benchmark Data for Validating Irradiated Fuel Compositions Used in Criticality Calculations*, Pacific Northwest Laboratory, PNL-10045 (UC-722), October 1994.
17. M. C. Brady-Raap, *Compilation of Radiochemical Analyses of Spent Nuclear Fuel Samples*, Pacific Northwest National Laboratory, PNNL-13677, September 2001.
18. O. W. Hermann and C. V. Parks, "SAS2H: A Coupled One-Dimensional Depletion and Shielding Analysis Module," Vol. I, Section S2 of *SCALE: A Modular Code System for Performing Standardized Computer Analyses for Licensing Evaluation*, NUREG/CR-0200, Rev. 6 (ORNL/NUREG/CSD-2/R6), Vols. I, II, and III, May 2000. Available from Radiation Safety Information Computational Center at Oak Ridge National Laboratory as CCC-545.
19. O. W. Hermann and R. M. Westfall, "ORIGEN-S: SCALE System Module to Calculate Fuel Depletion, Actinide Transmutation, Fission Product Buildup and Decay, and Associated Radiation Source Terms," Vol. II, Section F7 of *SCALE: A Modular Code System for Performing Standardized Computer Analyses for Licensing Evaluation*, NUREG/CR-0200, Rev. 6 (ORNL/NUREG/CSD-2/R6), Vols. I, II, and III, May 2000. Available from Radiation Safety Information Computational Center at Oak Ridge National Laboratory as CCC-545.
20. W. C. Jordan and S. M. Bowman, "SCALE Cross Section Libraries," Vol. III, Section M4 of *SCALE: A Modular Code System for Performing Standardized Computer Analyses for Licensing Evaluation*, NUREG/CR-0200, Rev. 6 (ORNL/NUREG/CSD-2/R6), Vols. I, II, and III, May 2000. Available from Radiation Safety Information Computational Center at Oak Ridge National Laboratory as CCC-545.
21. R. J. Guenter, D. E. Blahnik, T. K. Campell, U. P. Jenquin, J. E. Mendel, and J. C. K. Thornhill, *Characterization of Spent Fuel Approved Testing Material – ATM-106*, Pacific Northwest Laboratory, PNL-5109-106 (UC-70), October 1988.
22. H. R. Dyer and C. V. Parks, *Recommendations for Preparing the Criticality Safety Evaluation of Transportation Packages*, NUREG/CR-5661 (ORNL/TM-11936), U.S. Nuclear Regulatory Commission, Oak Ridge National Laboratory, April 1997.
23. RW-859 Nuclear Fuel Data, Energy Information Administration, December 2000.
24. J. C. Wagner, *Computational Benchmark for Estimation of Reactivity Margin from Fission Products and Minor Actinides in PWR Burnup Credit*, NUREG/CR-6747 (ORNL/TM-2001/306), U.S. Nuclear Regulatory Commission, Oak Ridge National Laboratory, October 2001.
25. I. C. Gauld and S. M. Bowman, *STARBUCS: A Prototypic SCALE Control Module for Automated Criticality Safety Analyses Using Burnup Credit*, NUREG/CR-6748 (ORNL/TM-2001/33), U.S. Nuclear Regulatory Commission, Oak Ridge National Laboratory, October 2001.
26. S. M. Bowman and L. C. Leal, "ORIGEN-ARP: Automatic Rapid Process for Spent Fuel Depletion, Decay, And Source Term Analysis," Vol. I, Section D1 of *SCALE: A Modular Code System for Performing Standardized Computer Analyses for Licensing Evaluation*, NUREG/CR-0200, Rev. 6 (ORNL/NUREG/CSD-2/R6), Vols. I, II, and III, May 2000. Available from Radiation Safety Information Computational Center at Oak Ridge National Laboratory as CCC-545.

27. L. M. Petrie and N. F. Landers, "KENO V.a: An Improved Monte Carlo Criticality Program with Supergrouping," Vol. II, Section F11 of *SCALE: A Modular Code System for Performing Standardized Computer Analyses for Licensing Evaluation*, NUREG/CR-0200, Rev. 6 (ORNL/NUREG/CSD-2/R6), Vols. I, II, and III, May 2000. Available from Radiation Safety Information Computational Center at Oak Ridge National Laboratory as CCC-545.
28. *Summary Report of Commercial Reactor Critical Analyses Performed for the Disposal Criticality Analysis Methodology*, Office of Civilian Radioactive Waste Management System, U.S. Department of Energy, Yucca Mountain Site Characterization Project Office, B-01717-5705-00075, Rev. 1, August 1998.

**APPENDIX A**

**SPENT FUEL ISOTOPIC ASSAY  
VALIDATION RESULTS**

Table A.1 Experimental actinide assay results

Data	Reactor	Assembly	Sample ID	Fuel (g/cm <sup>3</sup> )	Enr. (wt%)	Burnup (GWd/t)	Experimental concentrations (mg/g U initial)											
							<sup>234</sup> U	<sup>235</sup> U	<sup>236</sup> U	<sup>238</sup> U	<sup>237</sup> Np	<sup>238</sup> Pu	<sup>239</sup> Pu	<sup>240</sup> Pu	<sup>241</sup> Pu	<sup>242</sup> Pu	<sup>241</sup> Am	<sup>243</sup> Am
1	Trino Vercelles	509-104	M11-7	10.079	3.897	12.042	—	26.620	2.736	951.30	—	—	4.5860	0.7165	0.3475	0.0314	—	—
2	Trino Vercelles	509-032	E11-4	10.079	3.13	15.377	—	17.280	2.834	955.80	—	—	5.2660	1.1180	0.6140	0.0864	—	—
3	Trino Vercelles	509-032	E11-7	10.079	3.13	15.898	—	16.610	2.739	955.80	—	—	5.2340	1.1370	0.6180	0.0949	—	—
4	Trino Vercelles	509-032	E11-9	10.079	3.13	11.529	—	20.170	2.502	959.50	—	—	4.4180	0.7750	0.3690	0.0380	—	—
5	Trino Vercelles	509-069	E11-1	10.079	3.13	12.859	—	19.460	2.453	958.70	—	0.0250	4.5800	0.8400	0.4000	0.0460	0.0844**	—
6	Trino Vercelles	509-069	E11-2	10.079	3.13	20.602	—	14.360	3.317	951.80	—	0.0805	5.7550	1.5200	0.8850	0.1720	0.1748**	0.0239
7	Trino Vercelles	509-069	E11-4	10.079	3.13	23.718	—	12.480	3.610	949.30	—	0.1090	5.8950	1.7550	1.0300	0.2435	0.2089**	0.0453
8	Trino Vercelles	509-069	E11-7	10.079	3.13	24.304	—	12.350	3.638	949.20	—	0.1170	6.0700	1.8250	1.0600	0.2575	0.3011**	0.0458
9	Trino Vercelles	509-069	E5-4	10.079	3.13	23.867	—	12.910	3.520	949.20	—	0.1170	5.9500	1.7600	1.0500	0.2400	0.2222**	—
10	Trino Vercelles	509-069	E5-7	10.079	3.13	24.548	—	12.210	3.540	948.30	—	0.1160	5.9800	1.7850	1.0550	0.2540	0.2444**	0.0462
11	Trino Vercelles	509-069	L11-4	10.079	3.13	23.928	—	12.820	3.753	948.50	—	0.1060	6.0600	1.7900	1.0500	0.2470	—	0.0445
12	Trino Vercelles	509-069	L11-7	10.079	3.13	24.362	—	12.250	3.465	948.20	—	0.1160	5.9950	1.8100	1.0550	0.2590	0.2033**	0.0425
13	Trino Vercelles	509-069	L5-4	10.079	3.13	24.33	—	12.970	3.471	948.60	—	0.1100	6.0600	1.7700	1.0600	0.2440	0.2222**	—
14	Trino Vercelles	509-069	L5-7	10.079	3.13	24.313	—	12.310	3.569	947.20	—	0.1140	5.9700	1.7900	1.0600	0.2500	0.2444**	—
15	Turkey Point	D01	G9	10.235	2.556	30.72	0.1321	5.865	3.254	950.20	—	0.1365	4.8380	2.2660	1.0610	0.5020	—	—
16	Turkey Point	D01	G10	10.235	2.556	30.51	0.1321	5.676	3.255	950.60	—	0.1360	4.8400	2.2940	1.0680	0.5248	—	—
17	Turkey Point	D01	H9	10.235	2.556	31.56	0.1225	5.584	3.174	949.50	—	0.1426	4.9300	2.2950	1.1040	0.5477	—	—
18	Turkey Point	D04	G9	10.235	2.556	31.26	0.1131	5.509	3.156	949.90	—	0.1382	4.9410	2.3200	1.1240	0.5428	—	—
19	Turkey Point	D04	G10	10.235	2.556	31.31	0.1320	5.662	3.252	949.80	—	0.1372	4.7880	2.2780	1.0720	0.5235	—	—

Table A.1 (continued)

Data	Reactor	Assembly	Sample ID	Fuel (g/cm <sup>3</sup> )	Enr. (wt%)	Burnup (GWd/t)	Experimental concentrations (mg/g U initial)											
							<sup>234</sup> U	<sup>235</sup> U	<sup>236</sup> U	<sup>238</sup> U	<sup>237</sup> Np	<sup>238</sup> Pu	<sup>239</sup> Pu	<sup>240</sup> Pu	<sup>241</sup> Pu	<sup>242</sup> Pu	<sup>241</sup> Am	<sup>243</sup> Am
20	Calvert Cliffs ATM-104	D047	MKP109-P	10.045	3.04	44.34	0.1361	4.016	4.187	935.90	0.5310	0.3052	4.9433	2.8852	1.1572	0.9530	0.4334	—
21	Calvert Cliffs ATM-104	D047	MKP109-LL	10.045	3.04	27.35	0.1815	9.610	3.563	955.87	0.3041	0.1146	4.8378	1.9503	0.7726	0.3279	0.2832	—
22	Calvert Cliffs ATM-104	D047	MKP109-CC	10.045	3.04	37.12	0.1588	5.866	4.005	944.75	0.4039	0.2144	4.9433	2.5403	1.0245	0.6535	0.3904	—
23	Calvert Cliffs ATM-103	D101	MLA098-P	10.045	2.72	33.17	0.1361	5.423	3.699	955.53	0.3879	0.1683	4.7504	2.3951	0.9218	0.6211	0.3970	—
24	Calvert Cliffs ATM-103	D101	MLA098-JJ	10.045	2.72	18.68	0.1588	11.629	2.836	970.16	0.1980	0.0550	4.4758	1.4103	0.5153	0.1582	0.2207	—
25	Calvert Cliffs ATM-103	D101	MLA098-BB	10.045	2.72	26.62	0.1373	7.874	3.392	968.69	0.3396	0.1099	4.8241	2.0036	0.7740	0.3745	0.3279	—
26	Calvert Cliffs ATM-106	BT03	NBD107-Q	10.036	2.45	46.46	0.0850	1.595	3.449	938.51	0.4281	0.3224	4.2727	2.9487	1.0054	1.3263	0.7212	—
27	Calvert Cliffs ATM-106	BT03	NBD107-MM	10.036	2.45	31.4	0.1736	4.379	3.245	958.25	0.2962	0.1618	4.3272	2.3451	0.8237	0.6198	0.3904	—
28	Calvert Cliffs ATM-106	BT03	NBD107-GG	10.036	2.45	37.27	0.1441	3.075	3.438	957.34	0.3638	0.2209	4.3510	2.6333	0.9224	0.8796	0.4830	—
29	H.B. Robinson	B05	N-9C-D	9.944	2.561	31.66	—	5.514	3.404	955.30	0.3778	0.1475	4.7651	2.4053	0.7851	—	—	—
30	H.B. Robinson	B05	N-9C-J	9.944	2.561	28.47	—	7.012	3.199	946.22	0.3449	0.1293	4.9807	2.2351	0.7726	—	—	—
31	H.B. Robinson	B05	N-9B-N	9.944	2.561	23.81	—	8.180	3.109	960.97	0.2950	0.0789	4.5609	1.8947	0.5718	—	—	—
32	H.B. Robinson	B05	N-9B-S	9.944	2.561	16.02	—	12.140	2.485	960.97	0.1759	0.0321	4.1298	1.2367	0.3449	—	—	—
33	Obrigheim	170	94	9.742	3.13	25.93	—	10.950	3.590	949.50*	—	0.0801	4.8050	1.8000	0.9780	0.3120	—	—
34	Obrigheim	172	92	9.742	3.13	26.54	—	10.580	3.620	949.10*	—	0.0889	4.7130	1.8300	0.9780	0.3280	—	—
35	Obrigheim	176	91	9.742	3.13	27.99	—	9.850	3.700	947.90*	—	0.0948	4.9250	1.9200	1.0580	0.3720	—	—
36	Obrigheim	168	86	9.742	3.13	28.4	—	9.680	3.730	947.50*	—	0.1054	5.0130	2.0200	1.1030	0.4070	—	—

Table A.1 (continued)

Data	Reactor	Assembly	Sample ID	Fuel (g/cm <sup>3</sup> )	Enr. (wt%)	Burnup (GWd/t)	Experimental concentrations (mg/g U initial)											
							<sup>234</sup> U	<sup>235</sup> U	<sup>236</sup> U	<sup>238</sup> U	<sup>237</sup> Np	<sup>238</sup> Pu	<sup>239</sup> Pu	<sup>240</sup> Pu	<sup>241</sup> Pu	<sup>242</sup> Pu	<sup>241</sup> Am	<sup>243</sup> Am
37	Obrigheim	171	89	9.742	3.13	29.04	—	9.580	3.750	947.00*	—	0.1013	4.9570	2.0000	1.1070	0.4050	—	—
38	Obrigheim	176	90	9.742	3.13	29.52	—	9.180	3.810	946.60*	—	0.1071	4.9430	2.0400	1.1280	0.4380	—	—
39	Takahama-3	NT3G23	SF95-1	10.412	4.11	14.3	0.2987	26.740	2.672	949.90	—	0.0172	4.2270	0.7802	0.3690	0.0379	0.0138	0.0027
40	Takahama-3	NT3G23	SF95-2	10.412	4.11	24.35	0.2850	19.270	4.024	942.40	—	0.0710	5.6550	1.5390	0.9578	0.1844	0.0234	0.0229
41	Takahama-3	NT3G23	SF95-3	10.412	4.11	35.42	0.1873	13.260	4.911	933.80	—	0.1539	6.1940	2.1860	1.4860	0.4516	0.0331	0.0805
42	Takahama-3	NT3G23	SF95-4	10.412	4.11	36.69	0.1870	12.300	4.999	933.50	—	0.1588	6.0050	2.2070	1.4660	0.4803	0.0235	0.0847
43	Takahama-3	NT3G23	SF95-5	10.412	4.11	30.4	0.2829	15.440	4.566	938.80	—	0.1020	5.6350	1.8210	1.1530	0.2976	0.0284	0.0440
44	Takahama-3	NT3G24	SF97-2	10.412	4.11	30.73	0.2348	15.710	4.560	937.70	0.4034	0.1250	5.9280	1.8710	1.2350	0.3152	0.0402	0.0513
45	Takahama-3	NT3G24	SF97-3	10.412	4.11	42.16	0.2010	10.300	5.312	928.20	0.5845	0.2581	6.2170	2.4710	1.6890	0.6517	0.0491	0.1410
46	Takahama-3	NT3G24	SF97-4	10.412	4.11	47.03	0.1872	8.179	5.528	924.60	0.6604	0.3199	6.0370	2.6680	1.7700	0.8246	0.0531	0.1924
47	Takahama-3	NT3G24	SF97-5	10.412	4.11	47.25	0.1865	7.932	5.532	924.70	0.6701	0.3188	5.9760	2.6480	1.7540	0.8341	0.0533	0.1935
48	Takahama-3	NT3G24	SF97-6	10.412	4.11	40.79	0.2057	10.160	5.272	931.00	0.5570	0.2175	5.6770	2.3260	1.4940	0.5977	0.0430	0.1170
49	Yankee Rowe	E6-C-F6	T-175	10.18	3.4	15.95	0.1550	19.800	2.880	949.00	—	0.0473	5.9500	1.1200	0.6630	0.0803	—	—
50	Yankee Rowe	E6-C-F6	T-177	10.18	3.4	30.39	0.1420	12.600	4.080	937.00	—	0.1760	7.8700	2.1200	1.5400	0.3460	—	—
51	Yankee Rowe	E6-C-F6	T-179	10.18	3.4	31.33	0.1190	11.900	4.150	935.00	—	0.2140	8.0100	2.2600	1.6400	0.3980	—	—
52	Yankee Rowe	E6-C-F6	T-180	10.18	3.4	20.19	0.1440	17.200	3.300	936.00	—	0.0791	6.6000	1.4400	0.9150	0.1450	—	—
53	Yankee Rowe	E6-SE-C2	T-187	10.18	3.4	32.03	0.1140	11.800	4.180	935.00	—	0.2220	7.9800	2.3700	1.6700	0.4220	—	—

Table A.1 (continued)

Data	Reactor	Assembly	Sample ID	Fuel (g/cm <sup>3</sup> )	Enr. (wt%)	Burnup (GWd/t)	Experimental concentrations (mg/g U initial)											
							<sup>234</sup> U	<sup>235</sup> U	<sup>236</sup> U	<sup>238</sup> U	<sup>237</sup> Np	<sup>238</sup> Pu	<sup>239</sup> Pu	<sup>240</sup> Pu	<sup>241</sup> Pu	<sup>242</sup> Pu	<sup>241</sup> Am	<sup>243</sup> Am
54	Yankee Rowe	E6-SE-C2	T-188	10.18	3.4	31.41	0.1150	11.900	4.090	936.00	—	0.2110	7.6800	2.2700	1.5800	0.4000	—	—
55	Yankee Rowe	E6-SE-E4	T-185	10.18	3.4	35.97	0.1180	9.780	4.450	933.00	—	0.2470	6.9500	2.5700	1.6800	0.5520	—	—
56	Yankee Rowe	E6-SE-E4	T-186	10.18	3.4	35.26	0.1200	9.840	4.440	934.00	—	0.2400	6.8200	2.4800	1.6200	0.5290	—	—

\* Obrigheim <sup>238</sup>U data are calculated.

\*\* Trino Vercellese <sup>241</sup>Am data (only) correspond to 4 years cooling.

Table A.2 Actinide validation results

Data	Reactor	Assembly	Sample ID	Fuel (g/cm <sup>3</sup> )	Enr. (wt%)	Burnup (GWd/t)	Calculated to experimental ratio (C/E)											
							<sup>234</sup> U	<sup>235</sup> U	<sup>236</sup> U	<sup>238</sup> U	<sup>237</sup> Np	<sup>238</sup> Pu	<sup>239</sup> Pu	<sup>240</sup> Pu	<sup>241</sup> Pu	<sup>242</sup> Pu	<sup>241</sup> Am	<sup>243</sup> Am
1	Trino Vercelles	509-104	M11-7	10.079	3.897	12.042	—	1.012	0.894	1.001	—	—	0.938	0.949	0.888	0.876	—	—
2	Trino Vercelles	509-032	E11-4	10.079	3.13	15.377	—	1.032	0.921	1.001	—	—	0.954	0.986	0.961	0.971	—	—
3	Trino Vercelles	509-032	E11-7	10.079	3.13	15.898	—	1.047	0.975	1.000	—	—	0.960	0.994	0.981	0.948	—	—
4	Trino Vercelles	509-032	E11-9	10.079	3.13	11.529	—	1.012	0.854	1.000	—	—	0.958	0.976	0.923	0.935	—	—
5	Trino Vercelles	509-069	E11-1	10.079	3.13	12.859	—	1.001	0.944	1.000	—	0.876	0.991	1.054	1.014	1.060	1.253	—
6	Trino Vercelles	509-069	E11-2	10.079	3.13	20.602	—	1.016	0.949	1.000	—	0.842	0.974	1.001	0.968	1.008	1.256	1.035
7	Trino Vercelles	509-069	E11-4	10.079	3.13	23.718	—	1.033	0.944	1.000	—	0.847	0.992	0.993	0.996	1.001	1.244	0.878
8	Trino Vercelles	509-069	E11-7	10.079	3.13	24.304	—	1.010	0.950	1.000	—	0.814	0.955	0.966	0.976	0.992	0.868	0.918
9	Trino Vercelles	509-069	E5-4	10.079	3.13	23.867	—	0.993	0.971	1.000	—	0.800	0.985	0.996	0.985	1.031	1.178	—
10	Trino Vercelles	509-069	E5-7	10.079	3.13	24.548	—	1.011	0.981	1.001	—	0.840	0.972	0.997	0.993	1.030	1.082	0.941
11	Trino Vercelles	509-069	L11-4	10.079	3.13	23.928	—	0.998	0.912	1.001	—	0.888	0.967	0.982	0.988	1.008	—	0.922
12	Trino Vercelles	509-069	L11-7	10.079	3.13	24.362	—	1.015	0.999	1.001	—	0.825	0.968	0.976	0.984	0.991	1.289	0.997
13	Trino Vercelles	509-069	L5-4	10.079	3.13	24.33	—	0.971	0.995	1.000	—	0.889	0.972	1.009	0.999	1.062	1.205	—
14	Trino Vercelles	509-069	L5-7	10.079	3.13	24.313	—	1.013	0.969	1.002	—	0.836	0.971	0.985	0.977	1.022	1.070	—
15	Turkey Point	D01	G9	10.235	2.556	30.72	1.016	0.946	1.028	0.999	—	1.018	1.029	0.997	1.040	1.120	—	—
16	Turkey Point	D01	G10	10.235	2.556	30.51	1.020	0.989	1.026	0.999	—	1.008	1.027	0.980	1.028	1.056	—	—
17	Turkey Point	D01	H9	10.235	2.556	31.56	1.079	0.947	1.063	0.999	—	1.030	1.012	1.003	1.022	1.086	—	—

Table A.2 (continued)

Data	Reactor	Assembly	Sample ID	Fuel (g/cm <sup>3</sup> )	Enr. (wt%)	Burnup (GWd/t)	Calculated to experimental ratio (C/E)											
							<sup>234</sup> U	<sup>235</sup> U	<sup>236</sup> U	<sup>238</sup> U	<sup>237</sup> Np	<sup>238</sup> Pu	<sup>239</sup> Pu	<sup>240</sup> Pu	<sup>241</sup> Pu	<sup>242</sup> Pu	<sup>241</sup> Am	<sup>243</sup> Am
18	Turkey Point	D04	G9	10.235	2.556	31.26	1.175	0.977	1.066	0.999	—	1.042	1.009	0.986	0.996	1.074	—	—
19	Turkey Point	D04	G10	10.235	2.556	31.31	1.006	0.947	1.035	0.999	—	1.053	1.041	1.005	1.046	1.118	—	—
20	Calvert Cliffs ATM-104	D047	MKP109-P	10.045	3.04	44.34	1.012	0.905	1.017	0.999	1.075	0.944	1.009	0.955	0.980	1.026	0.895	—
21	Calvert Cliffs ATM-104	D047	MKP109-LL	10.045	3.04	27.35	0.984	0.946	1.029	0.994	1.061	0.905	0.979	0.979	0.977	1.035	0.948	—
22	Calvert Cliffs ATM-104	D047	MKP109-CC	10.045	3.04	37.12	0.967	0.913	1.028	0.997	1.159	0.935	0.987	0.962	0.970	1.046	0.887	—
23	Calvert Cliffs ATM-103	D101	MLA098-P	10.045	2.72	33.17	1.044	0.980	0.986	0.991	1.059	0.932	1.019	0.967	0.999	0.993	0.967	—
24	Calvert Cliffs ATM-103	D101	MLA098-JJ	10.045	2.72	18.68	1.126	0.986	0.991	0.989	0.985	0.765	0.961	0.971	0.930	0.959	0.920	—
25	Calvert Cliffs ATM-103	D101	MLA098-BB	10.045	2.72	26.62	1.147	0.958	0.994	0.984	0.918	0.871	0.966	0.966	0.959	0.997	0.951	—
26	Calvert Cliffs ATM-106	BT03	NBD107-Q	10.036	2.45	46.46	1.251	1.005	1.002	0.997	1.216	0.943	1.024	0.978	0.966	0.962	0.609	—
27	Calvert Cliffs ATM-106	BT03	NBD107-MM	10.036	2.45	31.4	0.761	1.000	1.016	0.992	1.195	0.957	0.995	0.988	0.938	0.981	0.945	—
28	Calvert Cliffs ATM-106	BT03	NBD107-GG	10.036	2.45	37.27	0.839	0.958	0.995	0.987	1.166	0.957	0.993	0.978	0.937	0.979	0.835	—
29	H.B. Robinson	B05	N-9C-D	9.944	2.561	31.66	—	1.042	0.995	0.992	1.063	0.964	1.081	1.004	1.026	—	—	—
30	H.B. Robinson	B05	N-9C-J	9.944	2.561	28.47	—	0.958	1.021	1.005	1.025	0.878	1.012	0.995	0.945	—	—	—
31	H.B. Robinson	B05	N-9B-N	9.944	2.561	23.81	—	1.016	0.977	0.994	0.943	0.940	1.048	0.998	0.995	—	—	—
32	H.B. Robinson	B05	N-9B-S	9.944	2.561	16.02	—	1.008	0.982	1.001	0.938	0.937	1.043	1.023	0.993	—	—	—
33	Obrigheim	170	94	9.742	3.13	25.93	—	0.972	1.009	1.001	—	1.139	1.024	0.996	0.896	0.965	—	—

Table A.2 (continued)

Data	Reactor	Assembly	Sample ID	Fuel (g/cm <sup>3</sup> )	Enr. (wt%)	Burnup (GWd/t)	Calculated to experimental ratio (C/E)											
							<sup>234</sup> U	<sup>235</sup> U	<sup>236</sup> U	<sup>238</sup> U	<sup>237</sup> Np	<sup>238</sup> Pu	<sup>239</sup> Pu	<sup>240</sup> Pu	<sup>241</sup> Pu	<sup>242</sup> Pu	<sup>241</sup> Am	<sup>243</sup> Am
34	Obrigheim	172	92	9.742	3.13	26.54	—	0.977	1.013	1.000	—	1.108	1.049	1.008	0.915	0.964	—	—
35	Obrigheim	176	91	9.742	3.13	27.99	—	0.979	1.017	1.001	—	1.162	1.013	1.005	0.895	0.971	—	—
36	Obrigheim	168	86	9.742	3.13	28.4	—	0.978	1.015	1.001	—	1.076	0.999	0.966	0.873	0.921	—	—
37	Obrigheim	171	89	9.742	3.13	29.04	—	0.958	1.020	1.001	—	1.178	1.014	0.995	0.891	0.977	—	—
38	Obrigheim	176	90	9.742	3.13	29.52	—	0.977	1.012	1.001	—	1.160	1.020	0.990	0.889	0.937	—	—
39	Takahama-3	NT3G23	SF95-1	10.412	4.11	14.3	1.103	1.000	1.001	1.000	—	0.970	1.044	1.035	1.021	1.075	0.878	1.170
40	Takahama-3	NT3G23	SF95-2	10.412	4.11	24.35	0.998	1.002	0.982	1.000	—	0.886	0.991	0.999	0.940	0.988	1.180	1.118
41	Takahama-3	NT3G23	SF95-3	10.412	4.11	35.42	1.279	0.979	1.000	1.000	—	0.992	0.987	1.013	0.947	1.010	1.179	1.167
42	Takahama-3	NT3G23	SF95-4	10.412	4.11	36.69	1.265	0.978	1.000	1.000	—	0.990	0.981	1.014	0.950	1.018	1.613	1.187
43	Takahama-3	NT3G23	SF95-5	10.412	4.11	30.4	0.929	0.980	0.992	1.000	—	0.954	0.992	1.021	0.958	1.030	1.129	1.154
44	Takahama-3	NT3G24	SF97-2	10.412	4.11	30.73	1.099	0.985	0.999	1.000	1.019	0.928	1.010	1.051	0.961	1.022	1.285	1.129
45	Takahama-3	NT3G24	SF97-3	10.412	4.11	42.16	1.066	0.975	0.997	1.000	1.053	0.925	1.010	1.049	0.961	1.015	1.271	1.139
46	Takahama-3	NT3G24	SF97-4	10.412	4.11	47.03	1.060	0.965	0.995	1.000	1.032	0.904	1.001	1.034	0.954	1.007	1.140	1.122
47	Takahama-3	NT3G24	SF97-5	10.412	4.11	47.25	1.066	0.950	0.996	1.001	1.001	0.883	0.980	1.028	0.931	1.001	1.089	1.103
48	Takahama-3	NT3G24	SF97-6	10.412	4.11	40.79	1.081	0.977	0.994	1.000	1.008	0.933	1.021	1.048	0.972	1.017	1.309	1.156
49	Yankee Rowe	E6-C-F6	T-175	10.18	3.4	15.95	0.997	0.993	0.993	1.004	—	0.792	0.931	0.973	0.883	0.996	—	—
50	Yankee Rowe	E6-C-F6	T-177	10.18	3.4	30.39	0.875	0.936	1.008	1.004	—	0.962	0.911	0.998	0.858	1.151	—	—

Table A.2 (continued)

Data	Reactor	Assembly	Sample ID	Fuel (g/cm <sup>3</sup> )	Enr. (wt%)	Burnup (GWd/t)	Calculated to experimental ratio (C/E)											
							<sup>234</sup> U	<sup>235</sup> U	<sup>236</sup> U	<sup>238</sup> U	<sup>237</sup> Np	<sup>238</sup> Pu	<sup>239</sup> Pu	<sup>240</sup> Pu	<sup>241</sup> Pu	<sup>242</sup> Pu	<sup>241</sup> Am	<sup>243</sup> Am
51	Yankee Rowe	E6-C-F6	T-179	10.18	3.4	31.33	1.017	0.948	1.005	1.005	—	0.822	0.892	0.955	0.870	1.063	—	—
52	Yankee Rowe	E6-C-F6	T-180	10.18	3.4	20.19	1.006	0.979	1.005	1.015	—	0.808	0.917	0.972	0.882	1.012	—	—
53	Yankee Rowe	E6-SE-C2	T-187	10.18	3.4	32.03	1.049	0.941	1.006	1.005	—	0.840	0.911	0.934	0.887	1.058	—	—
54	Yankee Rowe	E6-SE-C2	T-188	10.18	3.4	31.41	1.051	0.946	1.020	1.004	—	0.838	0.931	0.953	0.906	1.064	—	—
55	Yankee Rowe	E6-SE-E4	T-185	10.18	3.4	35.97	0.951	0.981	0.989	1.003	—	0.965	1.077	0.945	0.990	1.032	—	—
56	Yankee Rowe	E6-SE-F4	T-186	10.18	3.4	35.26	0.947	0.990	0.984	1.003	—	0.943	1.079	0.958	0.994	1.029	—	—
No. of measurements							32	56	56	56	18	52	56	56	56	52	28	16
Average C/E value							1.040	0.982	0.992	1.000	1.051	0.936	0.992	0.992	0.957	1.013	1.088	1.071
Average E/C value							0.962	1.018	1.008	1.000	0.952	1.068	1.008	1.008	1.045	0.987	0.919	0.934
Standard deviation (of C/E)							0.113	0.030	0.037	0.005	0.086	0.100	0.042	0.028	0.048	0.051	0.204	0.105
Relative Standard deviation (% of C/E)							10.8%	3.1%	3.7%	0.5%	8.2%	10.7%	4.2%	2.8%	5.0%	5.1%	18.8%	9.9%

Table A.3 Experimental fission product assay results

Data	Reactor	Assembly	Sample ID	Enr. (wt%)	Burnup (GWd/t)	Experimental concentrations (mg/g U initial)															
						<sup>95</sup> Mo	<sup>99</sup> Tc	<sup>101</sup> Ru	<sup>103</sup> Rh	<sup>109</sup> Ag	<sup>133</sup> Cs	<sup>143</sup> Nd	<sup>145</sup> Nd	<sup>147</sup> Sm	<sup>149</sup> Sm	<sup>150</sup> Sm	<sup>151</sup> Sm	<sup>152</sup> Sm	<sup>151</sup> Eu	<sup>153</sup> Eu	<sup>155</sup> Gd
20	Calvert Cliffs ATM-104	D047	MKP109-P	3.04	44.34	—	0.8954	—	—	—	1.4069	0.8779	0.8441	0.3081	0.0046	0.3638	0.0107	0.1325	0.0034	0.1622	0.0100
21	Calvert Cliffs ATM-104	D047	MKP109-LL	3.04	27.35	—	0.6361	—	—	—	0.9644	0.7048	0.5786	0.2303	0.0029	0.2089	0.0075	0.0665	0.0018	0.0852	0.0062
22	Calvert Cliffs ATM-104	D047	MKP109-CC	3.04	37.12	—	0.8158	—	—	—	1.2367	0.8298	0.7409	0.2704	0.0019	0.2897	0.0094	0.1096	0.0010	0.1300	0.0074
23	Calvert Cliffs ATM-103	D101	MLA098-P	2.72	33.17	—	0.7495	—	—	—	—	—	—	—	—	—	—	—	—	—	—
24	Calvert Cliffs ATM-103	D101	MLA098-JJ	2.72	18.68	—	0.4689	—	—	—	—	—	—	—	—	—	—	—	—	—	—
25	Calvert Cliffs ATM-103	D101	MLA098-BB	2.72	26.62	—	0.6215	—	—	—	—	—	—	—	—	—	—	—	—	—	—
26	Calvert Cliffs ATM-106	BT03	NBD107-Q	2.45	46.46	—	0.7230	—	—	—	—	—	—	—	—	—	—	—	—	—	—
27	Calvert Cliffs ATM-106	BT03	NBD107-MM	2.45	31.4	—	0.5107	—	—	—	—	—	—	—	—	—	—	—	—	—	—
28	Calvert Cliffs ATM-106	BT03	NBD107-GG	2.45	37.27	—	0.5943	—	0.6516	—	—	0.7174	0.7246	0.2659	0.0022	0.3000	0.0080	0.1210	0.0013	0.1505	0.0070
39	Takahama-3	NT3G23	SF95-1	4.11	14.3	—	—	—	—	—	—	0.4631	0.3328	—	—	—	—	—	—	—	—
40	Takahama-3	NT3G23	SF95-2	4.11	24.35	—	—	—	—	—	—	0.7149	0.5384	—	—	—	—	—	—	—	—
41	Takahama-3	NT3G23	SF95-3	4.11	35.42	—	—	—	—	—	—	0.9299	0.7392	—	—	—	—	—	—	—	—
42	Takahama-3	NT3G23	SF95-4	4.11	36.69	—	—	—	—	—	—	0.9373	0.7598	—	—	—	—	—	—	—	—
43	Takahama-3	NT3G23	SF95-5	4.11	30.4	—	—	—	—	—	—	0.8303	0.6518	—	—	—	—	—	—	—	—
44	Takahama-3	NT3G24	SF97-2	4.11	30.73	—	—	—	—	—	—	0.8307	0.6480	0.2050	0.0040	0.2499	0.0135	0.0955	—	—	—
45	Takahama-3	NT3G24	SF97-3	4.11	42.16	—	—	—	—	—	—	1.0080	0.8387	0.2355	0.0043	0.3599	0.0150	0.1191	—	—	—
46	Takahama-3	NT3G24	SF97-4	4.11	47.03	—	—	—	—	—	—	1.0480	0.9118	0.2468	0.0039	0.4074	0.0149	0.1298	—	—	—
47	Takahama-3	NT3G24	SF97-5	4.11	47.25	—	—	—	—	—	—	1.0490	0.9179	0.2479	0.0038	0.4113	0.0147	0.1319	—	—	—
48	Takahama-3	NT3G24	SF97-6	4.11	40.79	—	—	—	—	—	—	0.9736	0.8247	0.2371	0.0038	0.3409	0.0129	0.1207	—	—	—

Table A.4 Fission product validation results

Data	Reactor	Assembly	Sample ID	Enr. (wt%)	Burnup (GWd/t)	Calculated to experimental ratio (C/E)															
						<sup>95</sup> Mo	<sup>99</sup> Tc	<sup>101</sup> Ru	<sup>103</sup> Rh	<sup>109</sup> Ag	<sup>133</sup> Cs	<sup>143</sup> Nd	<sup>145</sup> Nd	<sup>147</sup> Sm	<sup>149</sup> Sm	<sup>150</sup> Sm	<sup>151</sup> Sm	<sup>152</sup> Sm	<sup>151</sup> Eu	<sup>153</sup> Eu	<sup>155</sup> Gd
20	Calvert Cliffs ATM-104	D047	MKP109-P	3.04	44.34	—	1.123	—	—	—	1.034	0.987	0.994	0.935	0.595	1.062	1.195	1.263	0.639	1.060	0.803
21	Calvert Cliffs ATM-104	D047	MKP109-LL	3.04	27.35	—	1.053	—	—	—	1.016	0.990	1.002	1.075	0.779	1.092	1.347	1.698	0.907	1.062	0.597
22	Calvert Cliffs ATM-104	D047	MKP109-CC	3.04	37.12	—	1.068	—	—	—	1.024	0.976	0.996	1.030	1.337	1.100	1.206	1.334	1.854	1.057	0.831
23	Calvert Cliffs ATM-103	D101	MLA098-P	2.72	33.17	—	1.049	—	—	—	—	—	—	—	—	—	—	—	—	—	—
24	Calvert Cliffs ATM-103	D101	MLA098-JJ	2.72	18.68	—	1.007	—	—	—	—	—	—	—	—	—	—	—	—	—	—
25	Calvert Cliffs ATM-103	D101	MLA098-BB	2.72	26.62	—	1.047	—	—	—	—	—	—	—	—	—	—	—	—	—	—
26	Calvert Cliffs ATM-106	BT03	NBD107-Q	2.45	46.46	—	1.415	—	—	—	—	—	—	—	—	—	—	—	—	—	—
27	Calvert Cliffs ATM-106	BT03	NBD107-MM	2.45	31.4	—	1.458	—	—	—	—	—	—	—	—	—	—	—	—	—	—
28	Calvert Cliffs ATM-106	BT03	NBD107-GG	2.45	37.27	—	1.446	—	0.788	—	—	1.003	0.985	0.995	0.890	1.040	1.251	1.233	0.920	0.963	0.877
39	Takahama-3	NT3G23	SF95-1	4.11	14.3	—	—	—	—	—	—	0.979	1.006	—	—	—	—	—	—	—	—
40	Takahama-3	NT3G23	SF95-2	4.11	24.35	—	—	—	—	—	—	0.975	1.001	—	—	—	—	—	—	—	—
41	Takahama-3	NT3G23	SF95-3	4.11	35.42	—	—	—	—	—	—	0.968	1.000	—	—	—	—	—	—	—	—
42	Takahama-3	NT3G23	SF95-4	4.11	36.69	—	—	—	—	—	—	0.974	1.005	—	—	—	—	—	—	—	—
43	Takahama-3	NT3G23	SF95-5	4.11	30.4	—	—	—	—	—	—	0.977	1.007	—	—	—	—	—	—	—	—
44	Takahama-3	NT3G24	SF97-2	4.11	30.73	—	—	—	—	—	—	1.006	1.015	1.017	0.979	1.071	1.291	1.243	—	—	—
45	Takahama-3	NT3G24	SF97-3	4.11	42.16	—	—	—	—	—	—	1.001	1.011	0.989	1.040	1.069	1.337	1.304	—	—	—
46	Takahama-3	NT3G24	SF97-4	4.11	47.03	—	—	—	—	—	—	1.003	1.014	0.974	1.155	1.064	1.330	1.319	—	—	—
47	Takahama-3	NT3G24	SF97-5	4.11	47.25	—	—	—	—	—	—	0.993	1.013	0.978	1.147	1.055	1.276	1.311	—	—	—

Table A.4 (continued)

Data	Reactor	Assembly	Sample ID	Enr. (wt%)	Burnup (GWd/t)	Calculated to experimental ratio (C/E)															
						<sup>95</sup> Mo	<sup>99</sup> Tc	<sup>101</sup> Ru	<sup>103</sup> Rh	<sup>109</sup> Ag	<sup>133</sup> Cs	<sup>143</sup> Nd	<sup>145</sup> Nd	<sup>147</sup> Sm	<sup>149</sup> Sm	<sup>150</sup> Sm	<sup>151</sup> Sm	<sup>152</sup> Sm	<sup>151</sup> Eu	<sup>153</sup> Eu	<sup>155</sup> Gd
48	Takahama-3	NT3G24	SF97-6	4.11	40.79	—	—	—	—	—	—	1.002	1.011	0.997	1.062	1.078	1.344	1.274	—	—	—
No. of measurements						0	9	0	1	0	3	14	14	9	9	9	9	9	4	4	4
Average C/E value						N/A	1.185	N/A	0.788	N/A	1.025	0.988	1.004	0.999	0.998	1.070	1.286	1.331	1.080	1.036	0.777
Average E/C value							0.844		1.269		0.976	1.012	0.996	1.001	1.002	0.934	0.777	0.751	0.926	0.966	1.287
Standard deviation of C/E							0.194				0.009	0.013	0.009	0.039	0.221	0.018	0.059	0.142	0.532	0.048	0.124
Relative Standard deviation (% of C/E)							16.3%				0.9%	1.3%	0.9%	3.9%	22.1%	1.7%	4.6%	10.7%	49.3%	4.7%	15.9%

**APPENDIX B**

**SENSITIVITY AND UNCERTAINTY  
CALCULATIONS**

Table B.1 Tabulated actinide-only sensitivity coefficients and estimated uncertainties (uniform axial burnup)

Nuclide	Relative std. dev. $1\sigma$ (%)	Sensitivity coefficient <sup>a</sup> , S						Relative uncertainty in $k_{eff}$ ( $2\sigma$ uncertainty interval)					
		10 GWd/t <sup>b</sup>	20 GWd/t	30 GWd/t	40 GWd/t	50 GWd/t	60 GWd/t	10 GWd/t	20 GWd/t	30 GWd/t	40 GWd/t	50 GWd/t	60 GWd/t
<sup>234</sup> U	10.83%	-2.79E-04	-2.54E-04	-2.44E-04	-2.45E-04	-2.58E-04	-2.75E-04	6.04E-05	5.50E-05	5.29E-05	5.30E-05	5.60E-05	5.97E-05
<sup>235</sup> U	3.07%	1.97E-01	1.74E-01	1.49E-01	1.22E-01	9.09E-02	6.75E-02	1.21E-02	1.07E-02	9.13E-03	7.46E-03	5.58E-03	4.14E-03
<sup>236</sup> U	3.72%	-3.04E-03	-4.71E-03	-5.74E-03	-6.26E-03	-6.53E-03	-6.59E-03	2.26E-04	3.51E-04	4.27E-04	4.66E-04	4.86E-04	4.90E-04
<sup>238</sup> U	0.47%	-1.63E-01	-1.63E-01	-1.66E-01	-1.67E-01	-1.68E-01	-1.69E-01	1.53E-03	1.54E-03	1.57E-03	1.57E-03	1.58E-03	1.59E-03
<sup>237</sup> Np	8.21%	-7.42E-04	-2.11E-03	-3.84E-03	-5.64E-03	-7.34E-03	-8.50E-03	1.22E-04	3.47E-04	6.31E-04	9.26E-04	1.21E-03	1.40E-03
<sup>238</sup> Pu	10.68%	-9.48E-05	-6.05E-04	-1.82E-03	-3.80E-03	-6.42E-03	-8.74E-03	2.02E-05	1.29E-04	3.88E-04	8.11E-04	1.37E-03	1.87E-03
<sup>239</sup> Pu	4.21%	5.36E-02	9.60E-02	1.36E-01	1.80E-01	2.20E-01	2.46E-01	4.51E-03	8.08E-03	1.15E-02	1.51E-02	1.85E-02	2.07E-02
<sup>240</sup> Pu	2.78%	-2.22E-02	-4.23E-02	-5.78E-02	-6.98E-02	-7.89E-02	-8.45E-02	1.23E-03	2.35E-03	3.21E-03	3.88E-03	4.39E-03	4.70E-03
<sup>241</sup> Pu	4.97%	4.24E-03	1.74E-02	3.60E-02	5.68E-02	7.69E-02	9.06E-02	4.21E-04	1.73E-03	3.58E-03	5.65E-03	7.64E-03	9.01E-03
<sup>242</sup> Pu	5.08%	-1.33E-04	-9.81E-04	-2.58E-03	-4.45E-03	-6.28E-03	-7.63E-03	1.35E-05	9.96E-05	2.62E-04	4.52E-04	6.37E-04	7.75E-04
<sup>241</sup> Am	18.76%	-1.32E-03	-4.68E-03	-8.43E-03	-1.14E-02	-1.35E-02	-1.47E-02	4.95E-04	1.76E-03	3.16E-03	4.26E-03	5.06E-03	5.52E-03
<sup>243</sup> Am	9.85%	-9.88E-06	-1.60E-04	-6.69E-04	-1.64E-03	-2.99E-03	-4.24E-03	1.95E-06	3.14E-05	1.32E-04	3.24E-04	5.89E-04	8.36E-04
								Total relative uncertainty (%)					
Root sum square								1.31%	1.39%	1.58%	1.88%	2.20%	2.43%
Additive								2.07%	2.72%	3.40%	4.10%	4.71%	5.11%

<sup>a</sup> Sensitivity coefficients assumed an initial enrichment of 3.5 wt%.

<sup>b</sup> GWd/t = GWd/MTU.

Table B.2 Tabulated actinide-only sensitivity coefficients and estimated uncertainties (with axial burnup profile)

Nuclide	Relative std. dev. 1 $\sigma$ (%)	Sensitivity coefficient <sup>a</sup> , S						Relative uncertainty in $k_{eff}$ (2 $\sigma$ uncertainty interval)					
		10 GWd/t <sup>b</sup>	20 GWd/t	30 GWd/t	40 GWd/t	50 GWd/t	60 GWd/t	10 GWd/t	20 GWd/t	30 GWd/t	40 GWd/t	50 GWd/t	60 GWd/t
<sup>234</sup> U	10.83%	-2.90E-04	-2.69E-04	-2.49E-04	-2.57E-04	-2.65E-04	-2.63E-04	6.28E-05	5.83E-05	5.39E-05	5.57E-05	5.73E-05	5.70E-05
<sup>235</sup> U	3.07%	2.00E-01	1.82E-01	1.70E-01	1.58E-01	1.38E-01	1.17E-01	1.23E-02	1.12E-02	1.04E-02	9.69E-03	8.47E-03	7.18E-03
<sup>236</sup> U	3.72%	-3.07E-03	-4.30E-03	-4.48E-03	-5.28E-03	-5.85E-03	-6.00E-03	2.28E-04	3.19E-04	3.33E-04	3.93E-04	4.35E-04	4.46E-04
<sup>238</sup> U	0.47%	-1.62E-01	-1.63E-01	-1.60E-01	-1.56E-01	-1.53E-01	-1.50E-01	1.53E-03	1.53E-03	1.51E-03	1.47E-03	1.44E-03	1.41E-03
<sup>237</sup> Np	8.21%	-8.25E-04	-1.91E-03	-2.74E-03	-3.72E-03	-4.78E-03	-5.62E-03	1.36E-04	3.15E-04	4.51E-04	6.12E-04	7.86E-04	9.23E-04
<sup>238</sup> Pu	10.68%	-9.95E-05	-4.73E-04	-9.82E-04	-1.75E-03	-2.79E-03	-4.00E-03	2.13E-05	1.01E-04	2.10E-04	3.73E-04	5.95E-04	8.54E-04
<sup>239</sup> Pu	4.21%	5.66E-02	8.89E-02	1.19E-01	1.34E-01	1.51E-01	1.63E-01	4.76E-03	7.48E-03	1.00E-02	1.13E-02	1.27E-02	1.37E-02
<sup>240</sup> Pu	2.78%	-2.27E-02	-3.77E-02	-4.50E-02	-5.32E-02	-6.12E-02	-6.30E-02	1.26E-03	2.09E-03	2.50E-03	2.96E-03	3.41E-03	3.50E-03
<sup>241</sup> Pu	4.97%	4.57E-03	1.43E-02	2.43E-02	3.27E-02	4.15E-02	5.30E-02	4.55E-04	1.42E-03	2.42E-03	3.26E-03	4.13E-03	5.27E-03
<sup>242</sup> Pu	5.08%	-1.56E-04	-8.13E-04	-1.52E-03	-2.38E-03	-3.34E-03	-4.42E-03	1.58E-05	8.25E-05	1.54E-04	2.42E-04	3.39E-04	4.49E-04
<sup>241</sup> Am	18.76%	-1.56E-03	-4.33E-03	-6.32E-03	-8.43E-03	-1.05E-02	-1.20E-02	5.85E-04	1.63E-03	2.37E-03	3.16E-03	3.93E-03	4.49E-03
<sup>243</sup> Am	9.85%	-1.31E-05	-1.39E-04	-3.73E-04	-7.43E-04	-1.28E-03	-2.02E-03	2.58E-06	2.75E-05	7.36E-05	1.46E-04	2.51E-04	3.98E-04
Total relative uncertainty (%)													
Root sum square								1.33%	1.39%	1.52%	1.59%	1.67%	1.74%
Additive								2.13%	2.63%	3.06%	3.36%	3.65%	3.87%

<sup>a</sup> Sensitivity coefficients assumed an initial enrichment of 3.5 wt %.<sup>b</sup> GWd/t = GWd/MTU.

Table B.3 Tabulated actinide and fission product sensitivity coefficients and estimated uncertainties (uniform axial burnup)

Nuclide	Relative std. dev. $1\sigma$ (%)	Sensitivity coefficient <sup>a</sup> , S						Relative uncertainty in $k_{eff}$ ( $2\sigma$ uncertainty interval)					
		10 GWd/t <sup>b</sup>	20 GWd/t	30 GWd/t	40 GWd/t	50 GWd/t	60 GWd/t	10 GWd/t	20 GWd/t	30 GWd/t	40 GWd/t	50 GWd/t	60 GWd/t
<sup>234</sup> U	10.83%	-2.74E-04	-2.47E-04	-2.17E-04	-2.26E-04	-2.31E-04	-2.45E-04	5.93E-05	5.36E-05	4.70E-05	4.89E-05	5.01E-05	5.31E-05
<sup>235</sup> U	3.07%	2.23E-01	1.94E-01	1.79E-01	1.37E-01	1.03E-01	7.54E-02	1.37E-02	1.19E-02	1.10E-02	8.44E-03	6.31E-03	4.63E-03
<sup>236</sup> U	3.72%	-2.81E-03	-4.39E-03	-4.61E-03	-5.54E-03	-5.62E-03	-5.75E-03	2.09E-04	3.26E-04	3.43E-04	4.12E-04	4.18E-04	4.28E-04
<sup>238</sup> U	0.47%	-1.35E-01	-1.58E-01	-8.58E-02	-1.51E-01	-1.50E-01	-1.72E-01	1.28E-03	1.49E-03	8.08E-04	1.42E-03	1.42E-03	1.62E-03
<sup>237</sup> Np	8.21%	-7.49E-04	-2.14E-03	-3.61E-03	-5.46E-03	-6.97E-03	-8.08E-03	1.23E-04	3.52E-04	5.93E-04	8.97E-04	1.14E-03	1.33E-03
<sup>238</sup> Pu	10.68%	-8.40E-05	-5.32E-04	-1.45E-03	-3.11E-03	-5.09E-03	-6.89E-03	1.79E-05	1.14E-04	3.11E-04	6.65E-04	1.09E-03	1.47E-03
<sup>239</sup> Pu	4.21%	6.25E-02	1.10E-01	1.70E-01	2.09E-01	2.56E-01	2.84E-01	5.26E-03	9.23E-03	1.43E-02	1.76E-02	2.16E-02	2.39E-02
<sup>240</sup> Pu	2.78%	-2.12E-02	-4.07E-02	-5.18E-02	-6.41E-02	-7.14E-02	-7.68E-02	1.18E-03	2.26E-03	2.88E-03	3.56E-03	3.97E-03	4.27E-03
<sup>241</sup> Pu	4.97%	4.56E-03	1.85E-02	4.11E-02	6.18E-02	8.37E-02	9.79E-02	4.54E-04	1.84E-03	4.09E-03	6.15E-03	8.33E-03	9.74E-03
<sup>242</sup> Pu	5.08%	-1.31E-04	-9.86E-04	-2.41E-03	-4.33E-03	-6.08E-03	-7.44E-03	1.33E-05	1.00E-04	2.45E-04	4.40E-04	6.17E-04	7.55E-04
<sup>241</sup> Am	18.76%	-1.39E-03	-4.93E-03	-8.28E-03	-1.14E-02	-1.33E-02	-1.45E-02	5.20E-04	1.85E-03	3.11E-03	4.29E-03	5.00E-03	5.44E-03
<sup>243</sup> Am	9.85%	-1.01E-05	-1.65E-04	-6.44E-04	-1.63E-03	-2.93E-03	-4.18E-03	2.00E-06	3.26E-05	1.27E-04	3.21E-04	5.77E-04	8.23E-04
<sup>99</sup> Tc	16.33%	-1.37E-03	-2.62E-03	-3.47E-03	-4.67E-03	-5.51E-03	-6.23E-03	4.48E-04	8.55E-04	1.13E-03	1.53E-03	1.80E-03	2.03E-03
<sup>103</sup> Rh	30.00%	-3.57E-03	-6.87E-03	-9.24E-03	-1.20E-02	-1.39E-02	-1.53E-02	2.14E-03	4.12E-03	5.54E-03	7.19E-03	8.32E-03	9.15E-03
<sup>133</sup> Cs	0.88%	-1.74E-03	-3.34E-03	-4.46E-03	-5.98E-03	-7.05E-03	-7.94E-03	3.07E-05	5.88E-05	7.85E-05	1.05E-04	1.24E-04	1.40E-04
<sup>143</sup> Nd	1.34%	-5.18E-03	-9.79E-03	-1.27E-02	-1.65E-02	-1.85E-02	-1.99E-02	1.39E-04	2.62E-04	3.41E-04	4.42E-04	4.96E-04	5.34E-04
<sup>145</sup> Nd	0.86%	-9.13E-04	-1.80E-03	-2.34E-03	-3.28E-03	-3.90E-03	-4.48E-03	1.57E-05	3.09E-05	4.02E-05	5.63E-05	6.70E-05	7.69E-05

Table B.3 (continued)

Nuclide	Relative std. dev. 1 $\sigma$ (%)	Sensitivity coefficient <sup>a</sup> , S						Relative uncertainty in $k_{eff}$ (2 $\sigma$ uncertainty interval)					
		10 GWd/t <sup>b</sup>	20 GWd/t	30 GWd/t	40 GWd/t	50 GWd/t	60 GWd/t	10 GWd/t	20 GWd/t	30 GWd/t	40 GWd/t	50 GWd/t	60 GWd/t
<sup>147</sup> Sm	3.93%	-8.54E-04	-1.49E-03	-1.77E-03	-2.17E-03	-2.32E-03	-2.45E-03	6.72E-05	1.17E-04	1.40E-04	1.71E-04	1.83E-04	1.93E-04
<sup>149</sup> Sm	22.12%	-1.21E-02	-1.45E-02	-1.52E-02	-1.66E-02	-1.70E-02	-1.73E-02	5.36E-03	6.42E-03	6.74E-03	7.35E-03	7.51E-03	7.67E-03
<sup>150</sup> Sm	1.71%	-5.36E-04	-1.24E-03	-1.87E-03	-2.75E-03	-3.47E-03	-4.09E-03	1.83E-05	4.24E-05	6.38E-05	9.41E-05	1.19E-04	1.40E-04
<sup>151</sup> Sm	4.57%	-4.92E-03	-6.82E-03	-8.16E-03	-1.01E-02	-1.14E-02	-1.25E-02	4.50E-04	6.23E-04	7.46E-04	9.20E-04	1.04E-03	1.14E-03
<sup>151</sup> Eu	49.26%	-1.58E-04	-2.15E-04	-2.54E-04	-3.09E-04	-3.48E-04	-3.80E-04	1.56E-04	2.12E-04	2.50E-04	3.04E-04	3.43E-04	3.75E-04
<sup>152</sup> Sm	10.66%	-1.09E-03	-2.28E-03	-3.05E-03	-4.18E-03	-4.94E-03	-5.52E-03	2.32E-04	4.87E-04	6.50E-04	8.92E-04	1.05E-03	1.18E-03
<sup>153</sup> Eu	4.67%	-4.76E-04	-1.37E-03	-2.39E-03	-3.73E-03	-4.94E-03	-5.92E-03	4.45E-05	1.28E-04	2.23E-04	3.49E-04	4.61E-04	5.53E-04
<sup>155</sup> Gd	15.94%	-8.90E-04	-2.36E-03	-4.59E-03	-7.92E-03	-1.13E-02	-1.41E-02	2.84E-04	7.52E-04	1.46E-03	2.53E-03	3.61E-03	4.50E-03
Total relative uncertainty (%)													
Root sum square								1.59%	1.74%	2.10%	2.39%	2.77%	3.02%
Additive								3.22%	4.37%	5.52%	6.62%	7.56%	8.21%

<sup>a</sup> Sensitivity coefficients assumed an initial enrichment of 3.5 wt %.

<sup>b</sup> GWd/t = GWd/MTU.

Table B.4 Tabulated actinide plus fission product sensitivity coefficients and estimated uncertainties (with axial burnup profile)

Nuclide	Relative std. dev. $1\sigma$ (%)	Sensitivity coefficient <sup>a</sup> , S						Relative uncertainty in $k_{eff}$ ( $2\sigma$ uncertainty interval)					
		10 GWd/t <sup>b</sup>	20 GWd/t	30 GWd/t	40 GWd/t	50 GWd/t	60 GWd/t	10 GWd/t	20 GWd/t	30 GWd/t	40 GWd/t	50 GWd/t	60 GWd/t
<sup>234</sup> U	10.83%	-2.80E-04	-2.58E-04	-2.45E-04	-2.36E-04	-2.32E-04	-2.31E-04	6.06E-05	5.58E-05	5.31E-05	5.11E-05	5.03E-05	5.01E-05
<sup>235</sup> U	3.07%	2.18E-01	2.06E-01	1.92E-01	1.81E-01	1.66E-01	1.55E-01	1.34E-02	1.27E-02	1.18E-02	1.11E-02	1.02E-02	9.54E-03
<sup>236</sup> U	3.72%	-2.78E-03	-3.69E-03	-4.29E-03	-4.62E-03	-4.89E-03	-4.99E-03	2.07E-04	2.74E-04	3.19E-04	3.44E-04	3.63E-04	3.71E-04
<sup>238</sup> U	0.47%	-1.56E-01	-1.49E-01	-1.46E-01	-1.41E-01	-1.39E-01	-1.36E-01	1.47E-03	1.41E-03	1.37E-03	1.33E-03	1.31E-03	1.28E-03
<sup>237</sup> Np	8.21%	-7.28E-04	-1.50E-03	-2.34E-03	-3.11E-03	-3.93E-03	-4.49E-03	1.20E-04	2.46E-04	3.85E-04	5.11E-04	6.46E-04	7.37E-04
<sup>238</sup> Pu	10.68%	-8.26E-05	-3.20E-04	-7.38E-04	-1.28E-03	-2.01E-03	-2.64E-03	1.76E-05	6.84E-05	1.58E-04	2.74E-04	4.30E-04	5.63E-04
<sup>239</sup> Pu	4.21%	5.82E-02	8.87E-02	1.14E-01	1.40E-01	1.65E-01	1.84E-01	4.90E-03	7.47E-03	9.61E-03	1.18E-02	1.39E-02	1.55E-02
<sup>240</sup> Pu	2.78%	-2.05E-02	-3.19E-02	-4.10E-02	-4.73E-02	-5.33E-02	-5.74E-02	1.14E-03	1.78E-03	2.28E-03	2.63E-03	2.96E-03	3.19E-03
<sup>241</sup> Pu	4.97%	4.26E-03	1.21E-02	2.14E-02	3.12E-02	4.17E-02	5.13E-02	4.24E-04	1.20E-03	2.13E-03	3.11E-03	4.15E-03	5.10E-03
<sup>242</sup> Pu	5.08%	-1.30E-04	-5.75E-04	-1.24E-03	-1.95E-03	-2.74E-03	-3.43E-03	1.32E-05	5.84E-05	1.26E-04	1.98E-04	2.78E-04	3.48E-04
<sup>241</sup> Am	18.76%	-1.34E-03	-3.33E-03	-5.43E-03	-7.19E-03	-8.91E-03	-1.03E-02	5.03E-04	1.25E-03	2.04E-03	2.70E-03	3.34E-03	3.86E-03
<sup>243</sup> Am	9.85%	-1.05E-05	-8.71E-05	-2.70E-04	-5.40E-04	-9.25E-04	-1.33E-03	2.07E-06	1.72E-05	5.31E-05	1.06E-04	1.82E-04	2.61E-04
<sup>99</sup> Tc	16.33%	-1.34E-03	-2.06E-03	-2.69E-03	-3.20E-03	-3.70E-03	-4.01E-03	4.39E-04	6.73E-04	8.80E-04	1.04E-03	1.21E-03	1.31E-03
<sup>103</sup> Rh	30.00%	-3.49E-03	-5.35E-03	-7.00E-03	-8.27E-03	-9.53E-03	-1.04E-02	2.09E-03	3.21E-03	4.20E-03	4.96E-03	5.72E-03	6.25E-03
<sup>133</sup> Cs	0.88%	-1.71E-03	-2.63E-03	-3.45E-03	-4.10E-03	-4.75E-03	-5.19E-03	3.01E-05	4.62E-05	6.07E-05	7.21E-05	8.36E-05	9.14E-05
<sup>143</sup> Nd	1.34%	-5.09E-03	-7.77E-03	-1.01E-02	-1.19E-02	-1.36E-02	-1.46E-02	1.37E-04	2.08E-04	2.71E-04	3.19E-04	3.65E-04	3.91E-04
<sup>145</sup> Nd	0.86%	-9.05E-04	-1.40E-03	-1.86E-03	-2.22E-03	-2.59E-03	-2.86E-03	1.56E-05	2.41E-05	3.19E-05	3.82E-05	4.45E-05	4.90E-05

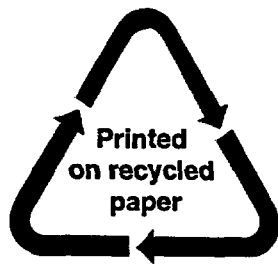
Table B.4 (continued)

Nuclide	Relative std. dev. 1 $\sigma$ (%)	Sensitivity coefficient <sup>a</sup> , S						Relative uncertainty in $k_{eff}$ (2 $\sigma$ uncertainty interval)					
		10 GWd/t <sup>b</sup>	20 GWd/t	30 GWd/t	40 GWd/t	50 GWd/t	60 GWd/t	10 GWd/t	20 GWd/t	30 GWd/t	40 GWd/t	50 GWd/t	60 GWd/t
<sup>147</sup> Sm	3.93%	-8.43E-04	-1.22E-03	-1.53E-03	-1.74E-03	-1.94E-03	-2.08E-03	6.63E-05	9.60E-05	1.20E-04	1.37E-04	1.52E-04	1.64E-04
<sup>149</sup> Sm	22.12%	-1.20E-02	-1.23E-02	-1.26E-02	-1.26E-02	-1.26E-02	-1.19E-02	5.31E-03	5.45E-03	5.59E-03	5.57E-03	5.60E-03	5.28E-03
<sup>150</sup> Sm	1.71%	-5.27E-04	-9.17E-04	-1.30E-03	-1.63E-03	-1.98E-03	-2.33E-03	1.80E-05	3.13E-05	4.46E-05	5.58E-05	6.76E-05	7.98E-05
<sup>151</sup> Sm	4.57%	-4.87E-03	-5.97E-03	-6.97E-03	-7.72E-03	-8.51E-03	-9.50E-03	4.45E-04	5.46E-04	6.37E-04	7.06E-04	7.78E-04	8.69E-04
<sup>151</sup> Eu	49.26%	-1.56E-04	-1.91E-04	-2.22E-04	-2.44E-04	-2.67E-04	-2.97E-04	1.54E-04	1.89E-04	2.18E-04	2.40E-04	2.63E-04	2.93E-04
<sup>152</sup> Sm	10.66%	-1.07E-03	-1.76E-03	-2.36E-03	-2.84E-03	-3.29E-03	-3.66E-03	2.29E-04	3.76E-04	5.03E-04	6.05E-04	7.02E-04	7.80E-04
<sup>153</sup> Eu	4.67%	-4.64E-04	-9.56E-04	-1.52E-03	-2.05E-03	-2.64E-03	-3.14E-03	4.33E-05	8.94E-05	1.42E-04	1.92E-04	2.47E-04	2.93E-04
<sup>155</sup> Gd	15.94%	-8.79E-04	-1.68E-03	-2.77E-03	-3.95E-03	-5.38E-03	-6.54E-03	2.80E-04	5.34E-04	8.83E-04	1.26E-03	1.71E-03	2.08E-03
								Total relative uncertainty (%)					
Root sum square								1.55%	1.63%	1.73%	1.86%	2.02%	2.14%
Additive								3.15%	3.80%	4.39%	4.93%	5.47%	5.87%

<sup>a</sup> Sensitivity coefficients assumed an initial enrichment of 3.5 wt %.

<sup>b</sup> GWd/t = GWd/MTU.

NRC FORM 335 (2-89) NRCM 1102 3201, 3202	U.S. NUCLEAR REGULATORY COMMISSION	1. REPORT NUMBER (Assigned by NRC, Add Vol., Supp., Rev., and Addendum Numbers, if any.)
<b>BIBLIOGRAPHIC DATA SHEET</b> <i>( See instructions on the reverse)</i>		NUREG/CR-6811 ORNL/TM-2001/257
2. TITLE AND SUBTITLE  Strategies for Application of Isotopic Uncertainties in Burnup Credit	3. DATE REPORT PUBLISHED	
	MONTH June	YEAR 2003
	4. FIN OR GRANT NUMBER W6479	
5. AUTHOR(S)  I. C. Gauld	6. TYPE OF REPORT  Technical	
	7. PERIOD COVERED <i>(Inclusive Dates)</i>	
8. PERFORMING ORGANIZATION — NAME AND ADDRESS <i>(If NRC, provide Division, Office or Region, U.S. Nuclear Regulatory Commission, and mailing address; if contractor, provide name and mailing address.)</i> Oak Ridge National Laboratory Managed by UT-Battelle, LLC Oak Ridge, TN 37831-6370		
9. SPONSORING ORGANIZATION — NAME AND ADDRESS <i>(If NRC, type "Same as above"; if contractor, provide NRC Division, Office or Region, U.S. Regulatory Commission, and mailing address.)</i> Division of Systems Analysis and Regulatory Effectiveness Office of Nuclear Regulatory Research U.S. Nuclear Regulatory Commission Washington, DC 20555-0001		
10. SUPPLEMENTARY NOTES R. Y. Lee, NRC Project Manager		
11. ABSTRACT <i>(200 words or less)</i>  Uncertainties in the predicted nuclide concentrations in spent nuclear fuel represent a major source of uncertainty in criticality calculations that use burnup credit. The methods used to propagate the uncertainties in the calculated concentrations to the uncertainty in the predicted neutron multiplication factor ( $k_{eff}$ ) of the system can have a significant effect on the overall uncertainty in the safety margin in criticality calculations, and ultimately affect the potential capacity of spent fuel casks. This report surveys several different best estimate strategies for considering the effects of nuclide uncertainties in burnup credit analyses, and compares the results with conventional bounding methods of uncertainty propagation for a prototypical burnup credit cask design. To quantify the comparison, each of the strategies for estimating uncertainty uses a common database of measured spent fuel isotopic assay data for pressurized-light-water reactor fuels and the predicated nuclide concentrations obtained using the current version of the SCALE code system. The experimental database has been significantly expanded to include new high-enrichment and high-burnup spent fuel assay data recently published for a wide range of important burnup credit actinide and fission product nuclides.		
12. KEY WORDS/DESCRIPTORS <i>(List words or phrases that will assist researchers in locating the report.)</i>  Criticality safety, burnup credit, transportation, spent fuel, nuclide inventories, uncertainties, error propagation, isotopic assay data, high burnup spent fuel	13. AVAILABILITY STATEMENT  unlimited	
	14. SECURITY CLASSIFICATION  <i>(This Page)</i> unclassified	
	<i>(This Report)</i> unclassified	
	15. NUMBER OF PAGES	
16. PRICE		



**Federal Recycling Program**

UNITED STATES  
NUCLEAR REGULATORY COMMISSION  
WASHINGTON, DC 20555-0001

---

OFFICIAL BUSINESS